Encapsulation of an integrin-binding protein into PLGA microspheres

Bouissou, Camille

Award date:
2006

Awarding institution:
University of Bath

Encapsulation of an integrin-binding protein into PLGA microspheres

Submitted by

Camille Bouissou

for the degree of Doctor of Philosophy

of the University of Bath

Department of Pharmacy

May 2006

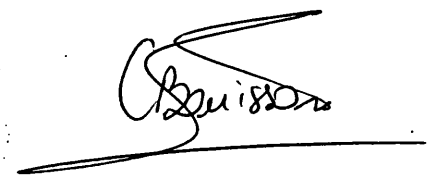

ProQuest LLC
789 East Eisenhower Parkway
P.O. Box 1346
Ann Arbor, MI 48106-1346

Acknowledgements

I have greatly enjoyed the past four years here in Bath and I would like to thank all the people who have contributed in some way to this thesis.

I am particularly indebted to Chris van der Walle and Rob Price, my supervisors, for their support, enthusiasm and inspiration.

A special thanks to my friends in Bath, back home, or wherever they might be at the moment, Francesca, Rachel, Fatima, Benjamin, Anne, Katie and Thanos.

Thank-you to my mother, my father, my sister and my little brother for their never ending support and love.

And lastly, and most importantly, I would like to thank my partner, Nikos, for the attention and effort he put in understanding my work. It was a real pleasure and a real trouble at the same time to answer his questions as he would consistently uncover weak points and mistakes I wouldn't have had the time to resolve. Also, I would like to thank him for his patience, and his expertise in English since without him, this thesis would have never been written correctly in English and as a 'word.doc'.

Scientific publications

The influence of surfactant on PLGA microsphere glass transition and water sorption: remodelling the surface morphology to attenuate the burst release. C. Bouissou, J. J. Rouse, R. Price, C. F. van der Walle, *Pharmaceutical Research* (2006) in press.

Controlled release of the fibronectin central cell binding domain from polymeric microspheres. C. Bouissou, U. Potter, H. Altroff, H. Mardon, C. F. van der Walle *Journal of Controlled Release* (2004) 95(3): 557-566.

Poly(lactic-co-glycolic acid) microspheres. C. Bouissou and C. F. van der Walle; Chapter included to the collective work entitled 'Polymers in Drug Delivery', 2006, CRC Press LLC, in press.

Encapsulation of an integrin-binding protein into PLGA microspheres

Abstract

This thesis examines the encapsulation of an integrin-binding protein (FIII9'-10) in poly(lactic-co-glycolic acid) (PLGA) microspheres fabricated following a water-in-oil-in-water (w/o/w) emulsion solvent evaporation technique. To avoid protein adsorption at the water/oil interface, non-ionic surfactants such as Pluronic F68, Tween 20, Tween 80, Triton X-100 and Igepal CA-630, were individually added to the water phase of the primary emulsion, and compared against model stabilisers such as polyvinyl alcohol (PVA) and bovine serum albumin (BSA).

The backbone integrity and biological activity of FIII9'-10 were examined by sodium dodecyl sulfate polyacrylamide gel (SDS-PAGE) analysis and cell-adhesion assay, respectively. It was found that the β-fold peptide backbone organisation was maintained throughout microencapsulation and that FIII9'-10 promoted cell attachment in a concentration-dependent manner, as desired.

Physical characterisation of the microspheres showed spherical particles of ~100 μm diameter with varying surface morphology, ranging from smooth and highly porous for microspheres made without non-ionic surfactants, to corrugated and scarcely porous for particles fabricated with non-ionic surfactants. These variations were attributed to the molecular interactions between surfactant and drug/PLGA. Examination by dynamic vapour sorption (DVS) and differential scanning calorimetry (DSC) of microspheres made with FIII9'-10 and Triton X-100, selected due to their high encapsulation efficiency (48.2% ±17.2) and their low external porosity, showed that the small Triton X-100 molecules had infiltrated the PLGA matrix thereby creating additional free-volume and decreasing the glass transition temperature (*Tg*) of the polymeric microspheres. The improved capacity for molecular mobility was used to induce surface remodelling of these particles upon exposure to 75% relative humidity. Topographical images of the microspheres prepared with Triton X-100, via atomic force microscopy (AFM) measurements, highlighted the significant reduction in pore depth from 1.57 μm to 0.48 μm suggesting a degree of pore closure. *In vitro* testing confirmed the phenomenon of pore closure as the initial burst release recorded

after 4 hour incubation fell from 91% for untreated microspheres, to 48% for microspheres exposed to 75% relative humidity for 24 hours prior to incubation.

Microencapsulation of a conformationally labile protein was proven successful. Also, the work highlighted that certain non-ionic surfactants should be considered further as prospective stabilisers for the w/o/w emulsion-evaporation technique.

Table of contents

List of abbreviations

ASES	aerosol solvent extraction system
AFM	atomic force microscope
BCA	bicinchoninic acid (protein assay)
BSA	bovine serum albumin
BHK	baby hamster kidney (cell-adhesion assay)
Cp	heat capacity at constant pressure (J/ °C)
CLSM	confocal laser scanning microscope
CCBD	central cell binding domain
DCM	dichloromethane
DVS	dynamic vapour sorption
DMSO	dimethyl sulfoxide
ECM	extracellular matrix
FN	fibronectin
GAS	gas anti-solvent precipitation
ΔH	enthalpy relaxation (J)
HLB	hydrophile/lipophile balance
IPTG	isopropyl-β-D-thiogalactopyranoside
MW	molecular weight (g/mol)
NMP	N-methyl-2-pyrolidone
o/w	oil-in-water single emulsion
PGA	poly glycolic acid
PLA	poly lactic acid
PLLA	poly(L-lactic acid)
PLGA	poly(D,L-lactic-co-glycolic acid)
PE	polyethylene

PEG	polyethylene glycol
mPEG	monomethoxy polyethylene glycol
PVA	polyvinyl alcohol
PBS	phosphate buffered saline
PIN	Phase Inversion Nanoencapsulation
q	heat supplied (J)
RH	relative humidity (%)
RGD	the tripepetide Arg-Gly-Asp named in single letter code
RESS	rapid expansion from supercritical solution
SEM	scanning electron microscope
SDS	sodium dodecyl sulfate
SDS-PAGE	sodium dodecyl sulfate-polyacrylamide gel electrophoresis
TEM	transmission electron microscope
T	Temperature (°C)
Tg	glass transition temperature (°C)
Tc	crystallization temperature (°C)
Tm	melting temperature (°C)
T_a	ageing temperature (°C)
T_K	Kauzmann temperature (°C)
w_A	weight fraction of the monomer A
w/o/w	water-in-oil-in-water double emulsion

List of Figures

Chapter 1

Introduction

1.1 General introduction

The number of protein, peptide and more recently DNA based drugs has been increasing over the past decades. Along with it, the need to develop safe routes of administration has become clearer. However, it is difficult to use these compounds in the context of oral or intravenous administration because of their structural fragility, low bioavailability and short half-life (Johnson & Tracy 1999; Lee 1995). Maintaining constant drug concentrations *in vivo* for an extended period of time is problematic and often resolved via frequent injections of high doses. In the case of patients with type I diabetes, daily injections are required, generally from 1 to 4 times a day. The health care professional reviews blood glucose levels to determine the appropriate type of insulin the person should use. More than one type of insulin may be mixed together in an injection to achieve the best control of blood glucose. Ideally, oral administration would be preferred as it is more acceptable to the patients, it does not require trained personnel, and oral drugs are generally cheaper to manufacture.

In order to avoid the problematic instability of therapeutic compounds, the use of biodegradable and non-biodegradable polymers has been extensively studied. Originally, the objective was to design a controlled-release delivery system for

proteins and peptides (Mathiowitz *et al.* 1997). The resulting product has to conform to the pharmaceutical regulations whereby it must be non-immunogenic, easily reproducible, stable to store, and appropriate for large-scale manufacturing. Suitable polymeric candidates include polyesters well known for their biodegradability and biocompatibility. These include poly lactic acid (PLA), poly glycolic acid (PGA) and especially poly(lactic-co-glycolic acid) (PLGA). PLGA is the main polymer used because it is approved by the Food and Drug Administration (FDA) (Jain 2000). Its low immunogenicity and toxicity, its good mechanical properties and predictable biodegradation kinetics enable its use from microspheres to bone tissue engineering, and other medical applications (Beumer *et al.* 1994).

Among the controlled-release delivery systems studied, one interesting approach has been the encapsulation of bioactive compounds into biodegradable particles of a micron- or nano-scale. The micro- or nanospheres would release the drug entrapped either in a continuous or pulsatile manner according to the therapeutic prerequisites (Cleland 1997). There exist several protocols to manufacture microparticles, yet many of them are only a derivative of the most basic encapsulation method, known as water-in-oil-in-water (w/o/w) double emulsion solvent-evaporation method (Cleland 1997). Although this technique is the most preferred for the encapsulation of hydrophilic proteins, it is not without problems. During microsphere fabrication via the w/o/w system, the primary emulsion (water-in-oil) has been proven to be the most destructive step with respect to protein stability (Blanco & Alonso 1998). On account of this, improved displacement of the protein from the interface by a surfactant would facilitate preservation of the protein's native conformation (van de Weert *et al.* 2000a).

In this study, seven emulsifiers were chosen to enhance the stability of an integrin-binding protein FIII9'-10, the 9^{th} and 10^{th} Fibronectin type III domain pair, encapsulated into PLGA microspheres. The five non-ionic surfactants listed hereafter were selected due to their compatibility with protein structure and emulsion stability: Pluronic F68, Tween 20, Tween 80, Triton X-100 and Igepal CA-630. In addition, bovine serum albumin (BSA) and polyvinyl alcohol (PVA) were used as model reference. Seven different types of microspheres were subsequently produced. Each type of microsphere was first characterised with respect to protein encapsulation efficiency, protein release, protein integrity and protein biological activity. This work was accompanied by a more physico-mechanical oriented study of the polymer with

the aim to dissect and comprehend the underlying molecular interactions between surfactant and drug/PLGA.

These analyses necessitated a thorough understanding of three main points: microsphere engineering, PLGA properties, and protein characteristics. This chapter outlines some of this knowledge, preceded by an overview of pharmaceutical application of biodegradable microparticles. The morphological features and the biodegradation profiles of microspheres are then described, and some essential definitions related to the polymer are presented, with special emphasis on its mechanical stability. Finally, some background information is given on the integrin-binding protein FIII9'-10.

1.2 Pharmaceutical application of PLGA microspheres

The use of biodegradable microspheres for drug delivery is not limited to any specific illness or administration route. An impressive list of encapsulated therapeutic agents already exists and illustrates the great potential of biodegradable microparticles for medical purposes. Antibiotics (Atkins *et al.* 1998), peptides (Li *et al.* 1995), proteins (Yan *et al.* 1994), DNA (Mohamed & van der Walle 2006), antibodies (Homayoun *et al.* 2003), anaesthetics (Le Corre *et al.* 1997), anti-virals (Schlicher *et al.* 1997), anti-hypertension drugs (Sansdrap *et al.* 1999; Yuksel *et al.* 1996), anti-HIV drugs (Akhtar & Lewis 1997), anti-cancer drugs (Lin *et al.* 2005) etc, have been encapsulated and tested as potential commercial products. Studies also extended further with industrial applications orientated towards marine fish culture or veterinary products (Matschke *et al.* 2002; Yang *et al.* 2001). Table 1.1 compiles a selection of drug microencapsulated and examined as candidates for drug delivery.

Drug	Format	Report	Reference
Bromodeoxyuridine	PLGA microspheres	*in vivo* cell labeling efficient labeling at cortical lesion site	Maysinger *et al.*, 1994
5-Fluorouracil	PLGA microspheres	*in vitro* release release for up to 21 days	Boisdron-Celle *et al.*, 1995 and Yeh *et al.*, 2001
5-Fluorouracil	PLGA microspheres	striatal glioma increase in animal survival correlated with release rate	Menei *et al.*, 1996 and Roullin *et al.*, 2003
Iododeoxyuridine	PLGA microspheres	*in vitro* release release over 7–35 days	Reza and Whateley, 1998
Dopamine, norepinephrine	PLGA microspheres	Parkinsonian rat model reduction in rotational behavior for up to 8 weeks	McRae and Dahlstrom, 1994 and McRae *et al.*, 1994
Retinoic acid	PLGA microspheres	*in vitro* release; *in vivo* treatment of vitreoretinopathy model release for up to 40 days; reduction in retinal detachment for up to 40 days	Giordano *et al.*, 1993
Paclitaxel	PLGA microspheres	*in vitro* release release over 60 days	Feng *et al.*, 2000
Paclitaxel	PEG-PLA microspheres	*in vivo* intravenous release higher drug tissue levels than seen with direct injection	Kim *et al.*, 2001
Carboplatin	PLGA microspheres	*in vitro* release release over 22 days	Chen and Lu, 1999
Carboplatin	PLGA microspheres	*in vivo* intracerebral release linear release over 30 days	Chen *et al.*, 1997
Isoniazid	PLGA microspheres	*in vitro* release; *in vivo* subcutaneous release released over 49 days; detectable in plasma for 49 days	Dutt and Khuller, 2001
Estradiol	PLGA microspheres	*in vitro* release release over 40–60 days	Birnbaum *et al.*, 2000
Hormone agonist	PLGA implant	*in vivo* subcutaneous release release over 20–50 days	Heinrich *et al.*, 1991

Table 1.1. List of bioactive compounds encapsulated in PLGA microspheres and studied as potential drug delivery system for medical application (Whittlesey & Shea 2004).

For microparticles fabrication at an industrial scale, equipment needs to be replaced and adapted for controllable, economic and aseptic conditions. An interesting review written by Freitas *et al.* examines some of the technologies available for microsphere preparation, with a particular attention dedicated to droplet formation

(Freitas *et al.* 2005). It is suggested that evolution of the water-in-oil droplets, embryos of the future microspheres, is one of the most critical steps and therefore, extreme caution must be taken at this stage. A variety of apparatus and protocols, such as static-mixing, extrusion through membranes, microfabricated microchannel devices, needles, or dripping using electrostatic forces and ultrasonic jet excitation, are described and reviewed as some may have potential in the industrial environment. Peptide and protein microencapsulation continues to represent a technological challenge in terms of product sterility and scale-up. Nevertheless, some biodegradable drug delivery systems summarised in Table 1.2 are already commercially available.

Applicant	Name of Product	Active Ingredient	Dosage Form
TAP Pharmaceutical Products Inc.	Lupron® Depot	Leuprolide	Microspheres
TAP Pharmaceutical Products Inc.	Enantone® Depot	Leuprolide	Microspheres
Genentech Inc.	Nutropin® Depot	Somatropin	Microspheres
Pharmacia & Upjohn Company	Trelstar® Depot	Triptorelin pamoate	Microspheres
Ipsen and Ferring Pharmaceuticals Company	Decapeptyl®	Triptorelin pamoate	Microspheres
Novartis Pharmaceuticals Corp.	Sandostatin LAR® Depot	Octreotide	Microspheres
Novartis Pharmaceuticals Corp.	Parlodel® Depot	Bromocriptine mesylate	Microspheres
Astra Zeneca Pharmaceuticals LP.	Zoladex®	Goserelin actetate	Rod implant
Atrix Laboratories Inc.	Atridox®	Doxycycline	Gel

Table 1.2. Selection of commercially available drug delivery systems, all using PLGA as a biodegradable carrier.

While the list of candidates for microencapsulation is rather long, the number of bioactive compounds passing all trials in a successful manner is rather small. In effect, studies investigating the encapsulation of model proteins, such as bovine serum albumin (BSA) and lysozyme, have demonstrated the ability to recover the protein intact upon release *in vitro* and *in vivo*. However, the encapsulation of a variety of proteins, peptides or vaccines exhibited different results than those of the model proteins presumably because of their structural stability, and high amphipathicity in the case of BSA. This suggests that protein encapsulation is specific to each new protein loaded, necessitating individual tests and trials (Okumu *et al.* 1997; Sah 1999b).

Further research is necessary in order to better understand and control the mechanisms underlying protein instability, encapsulation efficiency, *in vitro* and *in vivo* release profiles, and degradation. Successful findings in this line of research would extend the use of biodegradable microspheres to a wider range of drugs, applications, and administration routes.

1.3 Microencapsulation techniques

The success of a microencapsulation technique depends primarily on the physicochemical properties of the polymer and the drug. The right method must be selected to ensure the satisfaction of three main criteria:

- The biological activity of the drug must not be altered in order to avoid an immune response.
- The size of the particles has to support the administration route aimed (from nanoparticles for injectable particles, to microns for oral administration or pulmonary delivery).
- The drug release profile must be appropriate to the intended medical application (long term release, pulsatile or delayed release).

Although a number of encapsulation processes have been developed, they all share a similar first step where the drug is dispersed in an organic polymer solution and emulsified. Typical microencapsulation techniques are reviewed below.

1.3.1 Solvent evaporation process

Solvent evaporation is the most frequently used encapsulation technique due to its ease of manipulation, low cost, and rapid completion of microsphere fabrication (Cohen *et al.* 1991; Jeffery *et al.* 1993). The advantage most appreciated remains its suitability for either hydrophobic or hydrophilic drugs by following a single oil-in-water (o/w) emulsion or a double water-in-oil-in-water (w/o/w) emulsion, respectively. In each case, the precipitating polymer confines and encapsulates the drug into the hardening particles during the extraction step.

The single oil-in-water (o/w) emulsification is commonly preferred in the case of lipid-soluble drugs for the reason that the compound is directly added to the oil phase (Jeffery *et al.* 1991). The oil is prepared with polymer and drug dissolved in organic solvent, generally dichloromethane (DCM). The drug is evenly dispersed within the oil phase, and the suspension is emulsified in a large amount of water containing a stabiliser, usually PVA. The emulsion is then left to stir over a sufficient period of time during which solvent is removed by extraction into the continuous aqueous phase and evaporation at the air-liquid interface. The lifetime of the emulsion is generally no more than seconds to minutes, and during this time the polymer precipitates at the solvent front, leading the shell to harden progressively toward the centre of the sphere, and shrinking until the final size of the microspheres is stabilised (Jeyanthi *et al.* 1996; Yang *et al.* 2000). The particles are then collected by filtration or centrifugation, washed, and dried overnight, usually by lyophilisation.

In comparison with the single emulsion, the water-in-oil-in-water (w/o/w) double emulsion is more suitable for water-soluble drugs (Cohen *et al.* 1991). The process is divided in two successive emulsions which are illustrated in Fig. 1.1. The primary water-in-oil emulsion is prepared with an inner aqueous phase, containing the hydrophilic drug occasionally combined with a surfactant, and a continuous oil phase, this being the polymer dissolved in solvent. The two immiscible phases are sonicated or homogenised yielding small aqueous droplets dispersed in oil. The first emulsion is then transferred into a larger volume of water containing a stabiliser, generally PVA, and stirred. The extraction and evaporation of the solvent inducing the solidification of the particles is maintained until completion of solvent removal. Finally, the microspheres are centrifuged, washed, and dried.

Single and double emulsification, do not require elevated or low temperatures unless particular conditions are necessary (Yang *et al.* 2000). Particles can be manufactured at a nano- or micrometer size by regulating the stirring speed of the final emulsion or rate of DCM extraction (De & Robinson 2004). Most importantly, the drug is usually homogeneously distributed throughout the matrix of the microparticles (Yang *et al.* 2001). However, drug loss may be considerable during solvent removal, and more particularly in the case of the double emulsion due to the inevitable exchange flow between the inner and outer water phases (Yang *et al.* 2001). The presence of the inner water droplets in the first emulsion of the water-in-oil-in-water formulation makes coalescence hard to avoid unless surfactants or stabilisers are initially

incorporated to the inner water phase (Capan *et al.* 1999). These difficulties can be significantly reduced in the case of lypophilic drugs since the unnecessary first water phase is withdrawn from the formulation steps. The encapsulation procedures then becomes a solid-in-oil-in-water (s/o/w) where the solid protein is directly dispersed into the oil phase, emulsified and then transferred to the continuous water phase for solvent extraction (Castellanos & Griebenow 2003).

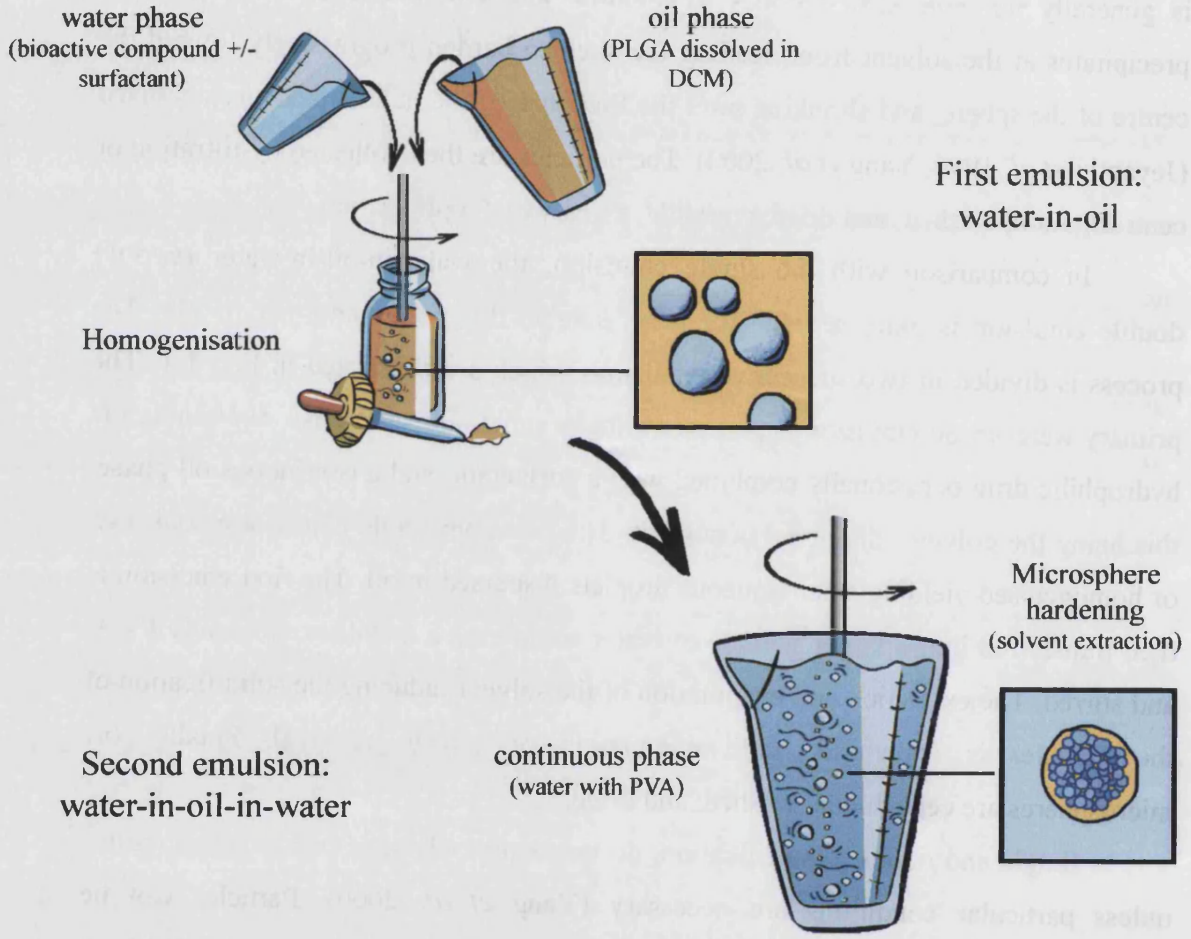

Figure 1.1. Schematic representation of the two process steps in microsphere preparation by double emulsion solvent evaporation technique.

1.3.2 Phase Inversion Nanoencapsulation technique or Coacervation

Coacervation, also called Phase Inversion Nanoencapsulation (PIN), consists of a phase separation process leading to the formation of micro- or nanospheres (Nihant *et al.* 1993). The first stage follows a standard water-in-oil emulsion where the water-soluble or solid drug dispersed in an aqueous phase is stirred into an oil phase composed of the polymer dissolved in DCM. An organic non-solvent, or coacervating agent such as poly(dimethylsiloxane), is then added to the first emulsion and stirred to create a water-in-oil-in-oil emulsion. Although a non-solvent does not permit the solubility of either polymer or drug, it allows for the diffusion of the polymer solvent which brings the polymer to form very soft coacervate droplets entrapping the drug. The physically stabilised coacervate droplets are then transferred to a hardening agent, in fact a second volatile non-solvent such as hexane, heptane or petroleum. This ultimately removes the coacervating agent causing the microspheres to fully harden. Finally, the microspheres are collected, washed and dried.

In this technique, drug loss may occur during phase separation and the formation of coacervate droplets (Nihant *et al.* 1994b). In effect, the polymer must be given enough time to deposit and homogeneously coat the drug particles (Ruiz *et al.* 1990). This depends on the polymer solvent extraction rate, which is regulated by the addition rate of the first non-solvent. Another problem to consider is the sticky consistency of the beads that tends to create agglomerates of coacervate droplets (Thomasin *et al.* 1998). This can be rectified by modifying the stirring rate, temperature, or by incorporating additives. By adjusting process factors such as solvent extraction, addition rate and temperature, a satisfactory result can be achieved and the microparticles can be made to conform to the traditional criteria of micron or nanoscale, uniform drug dispersion, etc. However, residual amounts of DCM and hardening agents are often found in the microspheres (Thomasin *et al.* 1996). Attempts to minimise the presence of potentially harmful residues are being undertaken by investigating the use of supercritical gases instead of non-solvents.

1.3.3 Spray drying method

Spray drying is a very rapid and convenient method, although it requires a fine control of the temperature (Walter *et al.* 2001). Briefly, the drug is mixed with the polymer dissolved in solvent and spray dried through a small nozzle onto liquid nitrogen with an underlying layer of frozen extraction solvent, generally ethanol. By decreasing the temperature to -80°C, the liquid nitrogen disperses and the microparticles are suspended into the cold liquid ethanol allowing the extraction of the polymer solvent. The microspheres are washed again in cold liquid ethanol and collected by filtration which allows for residual solvents to evaporate. Finally, they are dried by lyophilisation.

Spray drying is relatively straight forward but is unfortunately inappropriate for the bioactive compounds which are highly delicate and sensitive to temperature (Fu *et al.* 2001). The technique also requires fine control of inlet and outlet air-temperature and air flow. The latter may cause significant loss of the product due to the adhesion of the soft particles to the inner wall of the spray drier machinery (Chew & Chan 1999). To date, compounds of a variety of sizes and types, such as tetanus and diphteria toxoids (Peyre *et al.* 2003), tetracosactide (Witschi & Doelker 1998), somatostatine analogue (Blanco-Prieto *et al.* 1999) and anticancer drugs (Fu *et al.* 2001; Gavini *et al.* 2004; Lin *et al.* 2005) have been successfully encapsulated via spray-drying, but relatively little information on the effects of the formulation variables is available (Gavini *et al.* 2004).

1.3.4 Precipitation using gases in the supercritical state

Approximately ten years ago, three main processes based on supercritical precipitation emerged. The outline of these techniques remains invariable: the drug is added to an organic phase containing PLGA, and the solvent is then extracted to allow microsphere hardening. All three formula utilize compressed supercritical carbon dioxide (CO_2) fluid to precipitate the organic solution (Eckert *et al.* 1996). However,

each technique is characterised by a particular precipitation mode listed below and illustrated in Fig 1.2:

- precipitation with gaseous anti-solvent (GAS),
- precipitation with a compressed anti-solvent (PCA),
- precipitation by rapid expansion from supercritical solution (RESS).

In the GAS process, the drug-polymeric solution is emulsified and exposed to carbon dioxide in the gaseous, liquid or supercritical state. As carbon dioxide dissolves into the organic solvent, the polymer precipitates into microspheres (Randolph *et al.* 1993).

The process of precipitation with a compressed anti-solvent (PCA) is a semi-continuous mode of fabrication. The organic solution containing the active ingredient is atomized into a continuous flow of supercritical CO_2. As the organic solvent diffuses into the excess CO_2, the atomized droplets harden and the solid microspheres fall in the particle collector. This technique offers the advantage to form microparticles faster, of a smaller particle size, and in a semi-continuous manner. Other processes based on the same principle have been given different names, such as: aerosol solvent extraction system (ASES), supercritical anti-solvent (SA), and solution-enhanced dispersion by supercritical fluids (SEDS) (Bleich *et al.* 1993; Witschi & Doelker 1998).

Finally, in the RESS process, the drug-polymer solution is dissolved in supercritical fluid as anti-solvent and the pressure of the suspension is elevated. The high-pressure solution is atomized through a nozzle into a collection chamber at ambient condition and pressure. Effectively, the process is based on the solubility differences of the polymer in supercritical fluids at high and low pressures, respectively. At ambient pressure, the CO_2 of the fine particles of solute expands rapidly while extracting the organic solvent. Fast polymeric precipitation follows and fine micronized powder of loaded PLGA are collected.

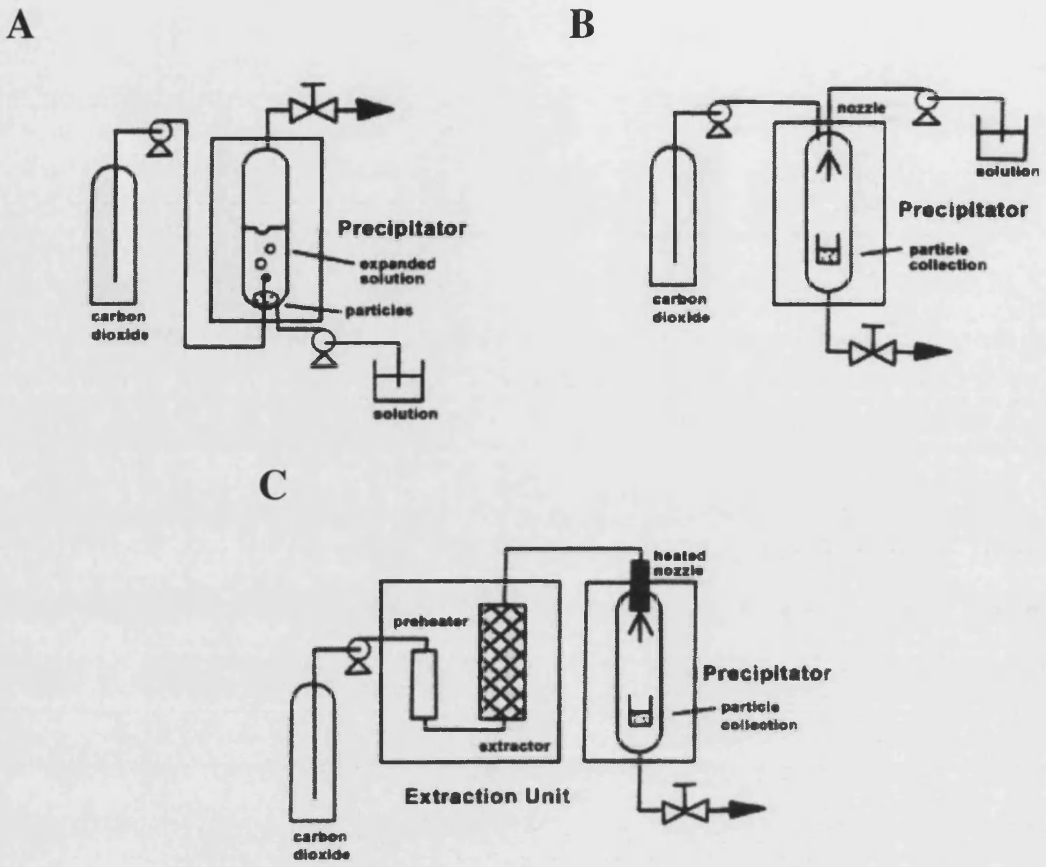

Figure 1.2. Schematic representation of the three main techniques of precipitation using supercritical carbon dioxide: (A) precipitation with gaseous anti-solvent (GAS), (B) precipitation with a compressed anti-solvent (PCA), and (C) precipitation by rapid expansion from supercritical solution (RESS) (Subramaniam et al. 1997).

1.4 Variations of the fabrication techniques

1.4.1 Double-walled microspheres

Double-walled microspheres were developed to circumvent the problem of the initial burst release and also for improved control of drug release profiles (Pekarek *et al.* 1994). Specifically, an external shell acting as rate-limiting barrier is added to the loaded microparticles. Several techniques result in this two-layered structure, one of

them being to simply coat conventional microparticles with a second polymer (Tsung & Burgess 2001). Another method relies on the mechanism of phase-separation of two polymers brought to their critical concentrations, most commonly poly(L-lactic acid) (PLLA) and poly(D,L-lactic-co-glycolic acid) (Mathiowitz & Langer 1989). Under such circumstances, the two polymers combined in organic solvent are immiscible (Dobry & Boyer-Kawenoki 1947). Briefly, the polymers are first dissolved in solvent and mixed before transfer to a continuous aqueous phase. As the solvent progressively evaporates, the concentration of the polymer-polymer droplets increases and ultimately, the polymers phase-separate. The resulting distinct structure of double-walled PLLA/PLGA microspheres is arranged with PLLA as the shell, and PLGA as the core.

Double-walled microspheres demonstrate the advantage of slow release and slow degradation rates which are necessary for extended therapeutic delivery (Lee *et al.* 2002). However, in order to avoid the formation of an external shell which would not control the drug release but only delay the initial burst, extended work is necessary to determine the correct conditions of fabrication of double-walled microspheres. Also, it is important to keep in mind that these encapsulation techniques are not appropriate for small sized microspheres (Liu *et al.* 2004).

1.4.2 Use of grafted-polymer

There have been many attempts to modify the chemical composition of PLGA in order to render it more compatible with specific applications. The chain length and the PLA/PGA ratio are commonly the first variations suggested. A broad range of molecular weight and PLA/PGA fractions are now commercially available. Also, a more hydrophilic (-COOH) uncapped variety of PLGA can be purchased and used for a faster degradation rate, whereas end-capped PLGA generally resists for longer (Friess & Schlapp 2002).

More complicated chemical adjustments have been used to prolong the circulation time of nanoparticles via PEGylation, a conventional method conjugating polyethylene glycol (PEG) to PLGA or PLA (Jeong *et al.* 2000). In addition, PEGylation reduces the detrimental effect of protein adsorption onto the particles (Jeong *et al.* 2000). In a different study led by Pistel *et al.*, PLGA chains were enriched

with additional polymers grafted onto their backbone by melt polymerisation (Pistel *et al.* 2001). Polyvinyl alcohol-grafted-poly(lactic-co-glycolic acid) decreased drug release when long PVA chains were inserted. Oh *et al.* followed a new approach, and obtained a drug release determined by mass erosion of PLGA matrices after conjugating the drug directly to the PLGA chain via ester linkage (Oh *et al.* 1999). The variety of coupling reactions extends further and is in fact limited solely by the therapeutic application of the polymer.

1.4.3 Biodegradable implant formed *in situ*

The biodegradable nature of PLGA has received considerable attention from groups investigating implants which could be injected into the body via a syringe, and would simply be eliminated after progressive biodegradation (Hatefi & Amsden 2002). These polymeric implant systems are formulated to solidify *in situ* upon intramuscular or subcutaneous injection (Lambert & Peck 1995). Briefly, the polymer is dissolved in a biocompatible solvent such as dimethyl sulfoxide (DMSO) or N-methyl-2-pyrolidone (NMP), and mixed with the drug to produce a solution of low viscosity to allow injection through a needle. After injection, the biocompatible solvent is extracted from the solution while the local aqueous environment causes the insoluble polymer to form a gel matrix. As the polymer hardens, the drug begins to diffuse out and is slowly released until complete degradation of the implant.

A variety of active compounds such as LHRH antagonists (Radomsky *et al.* 1993; Ravvarapu *et al.* 2000) and narcotic antagonists (Dunn *et al.* 1996) have already been injected and tested. The ease of application, the ability to localise delivery for a site-specific action and improved patient compliance and comfort support the success of this formulation. However, an initial burst release during the first hours after injection has been repeatedly noticed. The lag between injection and formation of the implant has been verified to be the origin of the burst release (Shively *et al.* 1995).

1.5 Characteristics of microspheres

1.5.1 Morphology of microspheres

During microsphere fabrication, slight changes in the formulation parameters can have radical effects on microsphere morphology (Yang *et al.* 2001). Reproducibility is hard to obtain when working at small scale (milligram), and in order to understand and control the impact of manufacturing processes, a detailed insight in the external and internal morphology is necessary. Physical characterisation aids in comprehending the stresses applied during the preparation of the particles, and determines future medical application (Florence 1997).

External morphology can be defined as microsphere size and shape, external porosity and surface roughness. The inner porosity and pore network determine the internal morphology. Most of the techniques used for the analysis of the microspheres' structure have the advantage of being reliable and easily reproducible (Table 1.3). Therefore, morphology has been more intensively studied than other features of the microspheres, and detailed descriptions are provided in the literature.

External Morphology		Internal Morphology	
Feature	Method	Feature	Method
Overall Shape	Scanning Electron Microscope (SEM)	Overall Shape	SEM and Cryo-SEM
Size	Transmission Electron Microscope (TEM)	Pore Size	TEM
Topography	Atomic Force Microscope (AFM)	Drug distribution	LS Confocal Microscope
Size of the spheres	Light scattering techniques	Pores radius <10 μm	Mercury porosimetry
External porosity	Dye encapsulation	Pores radius in the range of 10-75 μm	Dilatometry

Table 1.3. Commonly used methods to visualize the external and internal features of the microspheres.

1.5.1.1 External morphology of microspheres

Size of the microspheres

Clearly, size is a key factor that affects not only the drug loading and the initial burst release, but also the utility of the particles (Deng *et al.* 1999; Florence 1997; Prabha *et al.* 2002). In a w/o/w emulsion, both the first and second emulsions offer the opportunity to fine-tune the microsphere size. In the primary emulsion, increasing the volume of the aqueous phase leads to larger particles (Jeffery *et al.* 1993). Similarly, certain variations of the oil-phase composition may lead to a more viscous state less easily breakable, thus producing larger spheres. The best known modifications increasing the oil-phase viscosity consist in using a high polymer concentration, a high PLGA molecular weight, or adding gelatine to the oil (Jeffery *et al.* 1993; Mehta *et al.* 1996; Witschi & Doelker 1998; Yang *et al.* 2001). Microparticles are also reported to enlarge slightly when the drug/PLGA ratio increases (Park *et al.* 1995). The addition of non-ionic surfactants within the inner aqueous phase has only a small effect on microsphere size (Rojas *et al.* 1999).

The secondary emulsion also influences microsphere size. Addition of PVA to the external aqueous phase impedes the coalescence of the spheres, and their size reduces significantly as the PVA concentration is increased (Jeffery *et al.* 1993). Also, high stirring speeds improve the breakdown of the first emulsion (Yang *et al.* 2001). Increasing the volume of the continuous aqueous phase leads to larger particles due to rapid solvent extraction (Crotts & Park 1995; Jeffery *et al.* 1993). Temperature also affects particle size: at high temperatures (40°C), solvent evaporation is significantly faster such that the PLGA precipitates nearly instantaneously without shrinking, leading to large particles (Yang *et al.* 2000).

External porosity of the microspheres

The formation of external pores originates from the flow between the inner and outer water phases driven by osmotic pressure. Consequently, porous surfaces are

generally observed when a high volume fraction of aqueous phase is used in the primary emulsion (Crotts & Park 1995; Okumu *et al.* 1997). It was also found that the pore sizes and numbers are higher as the concentration of drug increases (Witschi & Doelker 1998). This could be related to the displacement of the drug from the inner to the continuous water phase which would generate a pore proportional to the drug's size (Sandor *et al.* 2001). When non-ionic surfactant is added to the inner water, the porosity is markedly affected, but the prediction of the resulting porosity is harder (Bouissou *et al.* 2004). The external porosity is an important parameter as it has been reported to regulate the drug release rate as well as the water inflow and outflow during *in vitro* release (Wang *et al.* 2002). It is less clear whether drug entrapment is improved when a nonporous particle is specifically fabricated (Cleland *et al.* 1997; Mehta *et al.* 1996).

Surface roughness

Recently, biodegradable microspheres as drug carriers have been applied to pulmonary delivery (Bivas-Benita *et al.* 2004; Suarez *et al.* 2001). It has been shown that increased surface roughness of particles demonstrate a lower powder cohesiveness (Chew & Chan 2001), and that the surface morphology and roughness of microspheres can be directly modified with the addition of non-ionic surfactants (Bouissou *et al.* 2004). On the other hand, a smooth surface with micropores is easily obtained with PLGA 75/25 (Cohen *et al.* 1991).

1.5.1.2 Internal morphology of microspheres

The internal morphology corresponds to the spherical 'cavities' or 'pores' dispersed throughout the polymeric matrix, and the network of channels linking these pores. Although the cavities materialise during the secondary emulsion while the solvent evaporates, they are thought to originate from the inner water droplets formed during the first emulsion (Schugens *et al.* 1994). Considering that the water droplets also carry the drug, a homogeneous spread is preferred in order to moderate the

phenomenon of initial burst release often reported (Yang *et al.* 2000). An even porosity also improves the draining of the acidic PLGA degradation products which contributes to maintain the internal pH closer to the physiological pH (Kim & Park 2004a). However, there is no clear correlation between the number and size of cavities and the liberation of the polymeric fragments (Crotts *et al.* 1997).

Throughout the w/o/w method, there exist several processes which can substantially influence the internal morphology of the microspheres. During the primary emulsion, the use of a high shearing rate can break the water droplets down to small sizes (Rafati *et al.* 1997). Low viscosity of the oil-phase also facilitates the breakdown of the inner water phase. Consequently, a low volume of oil-phase is often chosen (Yang *et al.* 2001). It is reported that smaller proteins are more homogeneously distributed within the sphere, and the porosity is more consistent than for large proteins of approximately 200 kDa (Sandor *et al.* 2001). The secondary emulsification may also affect the internal porosity (Schugens *et al.* 1994). At low temperatures, the evaporation of the solvent progresses slowly and eventually, the inner water droplets might merge if their stability is too poor (Yang *et al.* 2000). Coalescence also takes place more frequently when the polymeric molecular weight is low (Witschi & Doelker 1998).

1.5.2 Biodegradation of microspheres

1.5.2.1 Description of the biodegradation process

Drug release and biodegradation of microspheres are interdependent (Cleland *et al.* 1997; Lemaire *et al.* 2003). The process of biodegradation of microspheres consists of a random hydrolysis of the ester linkages of the PLGA chain (Gopferich & Langer 1995). There exist two possibilities with respect to the degradation of the polymer that are dependent on the sphere's dimension and the pH of the incubation medium. According to circumstances, the degradation can either be faster than the water uptake, which then dilapidates only the surface (surface erosion), or the water can rapidly penetrate the whole structure before surface erosion begins (bulk erosion) (Burkersroda *et al.* 2002).

In the case of surface erosion, the slow progress of water results in a heterogeneous dispersion through the matrix, as illustrated in Fig. 1.3. Meanwhile, the erosion operates at a constant velocity leading to a reduction in microsphere diameter. In bulk erosion, water is homogeneously distributed within the matrix such that hydrolysis occurs throughout (Batycky *et al.* 1997). The sphere tends to maintain its original size for longer while eroding from within (Deng & Uhrich 2002). It has been determined that in the case of PLGA, extremely large spheres would undergo surface erosion whereas small spheres would bulk-erode (Burkersroda *et al.* 2002).

In drug delivery applications, the requirement for micron sized particles necessitates a better understanding of the bulk erosion mechanism (Desai *et al.* 1997; Prabha *et al.* 2002; Zauner *et al.* 2001). Considering the rapid and extended access of water throughout the particles, it was originally assumed that an immediate loss of mass would be displayed as soon as the chain hydrolysis was triggered. Unexpectedly, a study conducted by Burkersroda *et al.* demonstrated that the mass loss appears somehow delayed despite an instantaneous loss in molecular weight, as seen in Fig. 1.4 (Burkersroda *et al.* 2002). Consequently, the mass loss is not only regulated by the chain scission, but also by a side effect that obstructs the polymeric pieces from leaving the microsphere, thus postponing its starting point. To describe this mechanism more precisely, the following two concepts were introduced: "degradation" which is the microsphere loss in mass, and "erosion" which is the microsphere loss in molecular weight (Gopferich & Langer 1995).

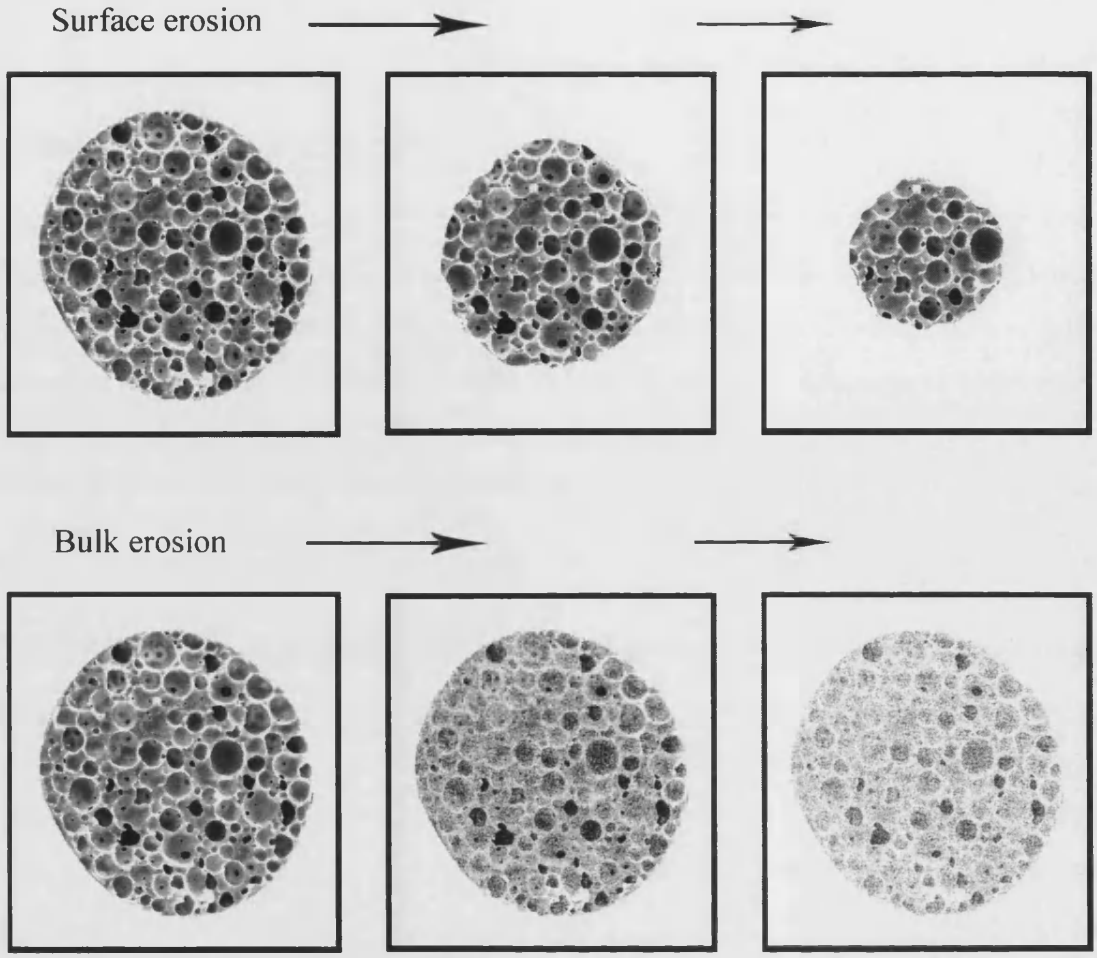

Figure 1.3. Schematic representation of the two modes of microsphere biodegradation. Surface erosion leads to a reduction in the microsphere diameter, whereas bulk erosion deteriorates homogeneously the matrix of the microsphere, even in the centre.

In order to explain the delay in mass loss, the following assumption was proposed. As water infiltrates the sphere, random hydrolysis occurs throughout the structure, segmenting the polymeric chain into various sizes and solubilities. Dissolution of the acidic polymeric segments leads to the expansion of the inner cavities. Due to the accumulation of acidic products in the water, the pH decreases, enhancing the hydrolysation even more. By this stage, the molecular weight of the microsphere has reduced, whereas the mass still remains relatively unchanged. Eventually, diffusion is facilitated by the enlarged cavities and interconnecting channels, driving the chain fragments to the release medium. Only then does the sphere demonstrate a mass loss.

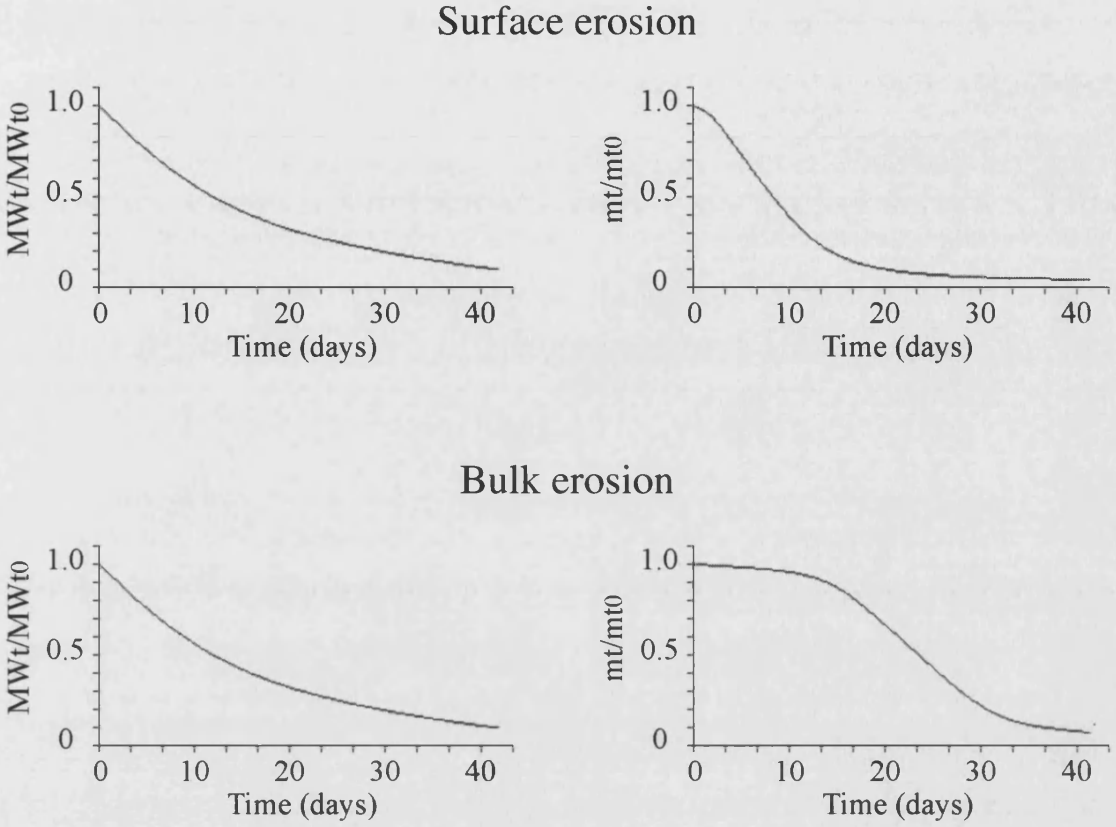

Figure 1.4. Illustration of molecular weight loss (MWt/MWt_0) and mass loss (mt/mt_0) profiles of microspheres undergoing either surface erosion or bulk erosion. The loss is expressed as the ratio of the initial load. Note the delay in mass loss during bulk erosion (Burkersroda et al. 2002; Husmann et al. 2002).

One has to bear in mind that the *in vitro* models may not entirely reflect the complexity of the *in vivo* environment (Blanco-Prieto *et al.* 1999; Johansen *et al.* 2000; Park *et al.* 1995). Traditional protocols of *in vitro* incubation prescribe pre-defined volumes of release medium of phosphate buffer saline (PBS) at pH 7.4 containing a preservative, such as sodium azide, and occasionally a surfactant. In this context, the pH tends to lower faster because of enhanced autocatalysis (Park *et al.* 1995). Even if the buffer is replenished frequently, the enclosed conditions do not allow the rapid removal of the acidic products released by the degradation. In this case, the pH values vary according to the size of the spheres (Fu *et al.* 2000), therefore mass and molecular weight loss data have to be analysed bearing in mind the inaccuracy of the method employed. Similarly, *in vitro* protein release data, which are generally produced by the same method of incubation, do not entirely reflect the situation *in vivo*. Unfortunately,

the complexity of the parameters involved makes it difficult to find an appropriate protocol, although attempts have been made to predict and even control the mechanism.

1.5.2.2 Control and prediction of the degradation profile

The following list summarises the factors that determine the degradation of the polymer:

- the type of polymer
- the type of drug
- the morphology of the matrix
- the diffusion of water
- the polymer degradation products
- the pH
- the osmotic pressure

Two different approaches aiming to control degradation have been employed; namely the modification of the chemical structure of the polymer and the alteration of its mechanical properties. The first approach is based on the regulation of the process of hydrolysis. There are several factors that influence this process:

- the relative stability of the polymer backbone, i.e. the bond half-life at physiological pH and temperature.
- hydrophobicity, which is principally governed by the number of glycolic acid units present in the PLGA chain.
- steric effects, as the alkyl group of the lactic acid units hinders the water access to the ester bonds (Gopferich 1996).
- autocatalysis, as the accumulation of acidic products lowers the pH, thus re-enforcing the attack on the ester linkage.

To control chain hydrolysis, the type of PLGA must be chosen in accordance with the degradation profile desired. For instance, varying the proportion of PLA/PGA or the chain length leads to different degradation speeds (Cleland *et al.* 1997;

Gopferich 1996; Park 1995; Witschi & Doelker 1998). Ester bonds linked with the glycolic acid units (i.e. Glyc/Glyc or Glyc/Lact) have a high hydrolytic reactivity (Park 1995; Shih *et al.* 1996). Therefore, a PLGA with a ratio 75/25 exhibits a longer degradation than a PLGA 50/50 due to a higher number of lactic acid units (Park 1995). For PLGA 50/50 of different molecular weights, the monomer arrangement within the chain dictates the degradation rate (Witschi & Doelker 1998). Similarly, scission at the chain-end is faster than degradation of the internal bonds (Shih *et al.* 1996). Consequently, the direct alteration of the chain backbone has been explored in order to achieve better degradation profiles. In contrast to free COOH-terminal polymer, end-capped polymer with lactic-acid-ethyl-ester delays bulk erosion (Burkersroda *et al.* 2002; Mehta *et al.* 1996). Similarly, the direct conjugation of the polymeric backbone to the drug has been analysed: the drug-PLGA conjugate is processed into microspheres and its extraction is controlled by the polymer degradation (Oh *et al.* 1999; Yoo *et al.* 2000; Yoo *et al.* 1999). Conjugation of the polymeric backbone with PVA also yields different degradation characteristics (Pistel *et al.* 2001). PVA-grafted PLGA induces a lower burst release and a more continuous release profiles.

The second approach aiming to control the biodegradation process is based on the alteration of the mechanical properties of the polymeric chains. The property of most relevance is the mobility of the PLGA chain, which is determined by the glass transition temperature (*Tg*) (Nam & Park 1999). During incubation, the molecular mobility of the polymeric structure eases the infiltration of the water molecules, which in return initiates hydrolysis more rapidly. Elimination of degradation products and shorter PLGA chain length create free volumes. The additional spaces permit even greater hydrolysis, and lead to faster degradation (Ali *et al.* 1993). Therefore, any factor rendering the polymer more plastic is likely to enhance the degradation rate; examples would include plasticizers such as non-ionic surfactants added during fabrication. Alternatively, amorphous PLGA made of more than 30% of PLA undergoes faster degradation than crystalline PLGA comprising less than 30% PLA (crystalline materials retain degradation products mostly due to stiffness) (Ford & Timmins 1989; Park 1995). Also, storage conditions impact on the material characteristics of microspheres (Aso *et al.* 1994; Deng & Uhrich 2002).

Several mathematical models for the prediction of the degradation profile have been proposed (Batycky *et al.* 1997; Göpferich 1997; Gopferich & Langer 1995;

Siepmann & Gopferich 2001; Zhang *et al.* 2003). Ideally, given certain factors such as the size of the sphere, the molecular weight of the polymer and its lifetime, it should be possible to simulate the erosion, and by tuning these parameters to achieve the desired profile. Unfortunately, the difficulty of obtaining reliable mathematical models arises from the multitude of parameters that must be taken into account. So far, no single mathematical model has succeeded in conforming closely to the observed data.

1.5.3 Drug release

The release of any drug from a polymeric device involves the diffusion of the therapeutic compound out of the structure via osmotic pressure (Yang *et al.* 2001). Generally, a fast liberation of drug located nearby the particle surface generates an initial burst release, often thought as problematic. A recent study conducted by Messaritaki *et al.* suggested that the swelling properties were also responsible for the burst release phenomenon (Messaritaki *et al.* 2005). Techniques have been developed to decrease the initial burst through the addition of an external polymeric layer (Lee *et al.* 2002).

The diffusion profile following the burst release is dependent on polymeric transformations occurring prior to and throughout incubation. Such changes include physical plasticization attributed to the effect of moisture during storage, as well as the direct contact with water during incubation. In both cases, the drug release is drastically accelerated in conjunction with the degradation rate (Friess & Schlapp 2002). It was also suggested by Steedam *et al.* that the transition from the glassy state to rubbery state during incubation may alter the drug release profile by changing the internal porous structure (Steendam *et al.* 2001). Kim and Park attempted to control the porosity at a nanometre scale by crystallising PLA/PLGA blend microspheres during solvent evaporation (Kim & Park 2004a). It was found that both PLA and PLA/PLGA microspheres exhibited organised nanoporous crystalline structures during precipitation which allowed a more sustained drug release over time.

1.6 Description of the polymer, poly(lactic-co-glycolic acid)

Poly lactic acid (PLA) was first introduced in 1962 in medical sutures because of its physical integrity and strength. The combination of poly glycolic acid (PGA) monomers with poly lactic acid monomers resulted in poly(lactic-co-glycolic acid) (PLGA). PLGA is biocompatible and approved by the Food and Drug Administration (FDA).

1.6.1 Polymerisation of PLGA

The word 'polymer' originates from the Greek 'poly' for many and 'meros' for parts. By definition, a polymer is a repeat of a basic building block known as monomers. When the same monomer forms the long string of covalently bond units, it is called a homopolymer, whereas a copolymer contains two or more different monomers. The polymerisation of PLGA proceeds by ring-opening linking lactic acid and glycolic acid monomers via ester bonds, as shown in Fig. 1.5. Due to its methyl side group, PLA exists in an optically active form L-PLA as well as in an optically inactive form D,L-PLA. The former is usually preferred for physical and mechanical characteristics that will be later described in section 1.6.2.3. The chain is extended to any desirable length commonly specified by the molecular weight (MW), or by the number of repeat units called degree of polymerisation. The inherent viscosity also characterises the degree of polymerisation as the molecular weight influences solution flowability. By definition, the inherent viscosity is the ratio of the natural logarithm of the relative viscosity to the concentration of the polymer in grams per 100 ml of solvent (therefore, units are dl/g for polymer concentrations in g/dl or %w/v).

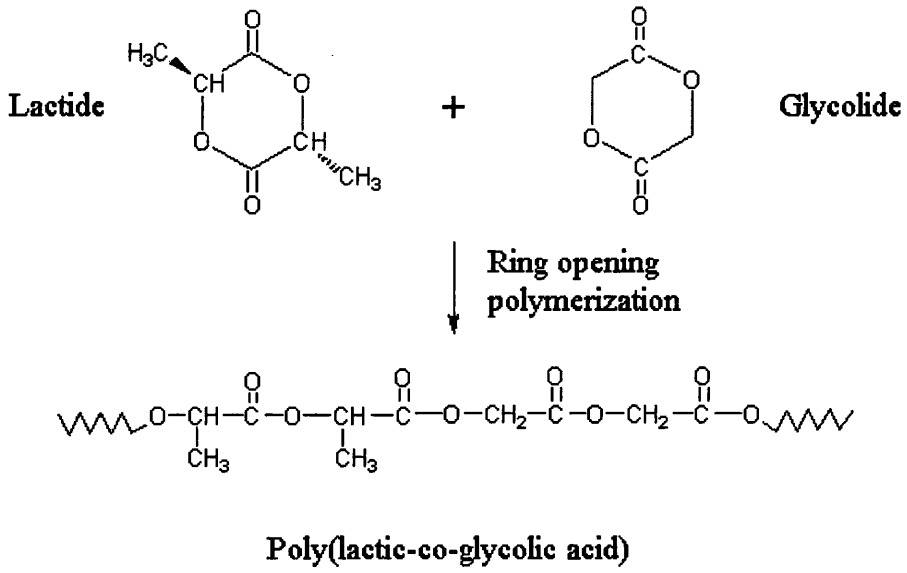

Figure 1.5. Illustration of Lactide and Glycolide monomers linked via ester bonds by ring-opening polymerisation.

1.6.2 Physical and mechanical properties of PLGA

The following section aims to introduce essential notions of physics and thermodynamics that will be used during the discussion of results. The last part will review the mechanical properties acquired by PLGA microspheres made via w/o/w solvent extraction method, and will conclude on the importance of the mechanical parameters for a drug delivery system.

1.6.2.1 Molecular mobility of the polymer chain

The degree of molecular mobility of a polymeric chain depends on the steric nature of the monomers, as well as the enthalpy of the system. There exist two main types of chain motions illustrated in Fig. 1.6. The first refers to main chain reorientation known as primary- or α-relaxation. This consists of long-range segmental motion of groups of 10 to 15 atoms, a phenomenon which occurs when there is enough

space and energy. Secondary- or β-relaxation refers to side group rotations occurring at higher frequencies and shorter times. Obviously, the kinetic energy and space required to move long chain fragments are greater than those necessary for side group rotations. In the case of PLGA, the bulky methyl groups of PLA segments undergo side group rotations, and at high temperatures, as the heat supplies sufficient thermal energy, long-range segmental motions are also initiated (Tice & Cowsar 1984).

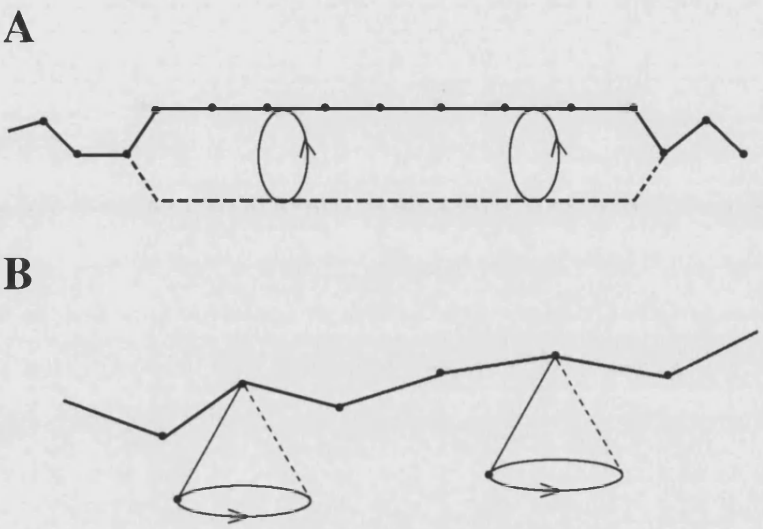

Figure 1.6. Illustration of the α-relaxation or long-range segmental motion (A) and the β-relaxation or side-chain mobility (B) occurring according to the thermal energy provided.

1.6.2.2 From glassy to rubbery state

At high temperatures, amorphous polymers appear fluid and transparent, but as the temperature decreases, they lose their malleability and pliability to become opaque and acquire a hard and brittle texture. Directly inspired from their appearance and consistency, polymers are said to be in a 'rubbery state' at high temperatures, whereas low temperatures bring them into a 'glassy state'. The process, clearly directed by heat, is reversible. In thermodynamic terms, heat is a form of kinetic energy that confers to the polymer the force necessary to initiate movements. In their rubbery state, the characteristic flexible nature of amorphous polymers originates from long-range

segmental motion as explained above. In their glassy state, the kinetic energy is so low that only low amplitude motions, such as side group rotations, are taking place. As the temperature drops, the viscosity increases and eventually, long-range segmental motions grind to a halt. Vitrification occurs, rendering the amorphous material as a glass. In semi-crystalline polymers, only the amorphous regions undergo vitrification.

1.6.2.3 Definition of the glass transition temperature

The glass transition temperature is defined as the temperature at which a rigid or glassy polymer transforms into a softer or rubbery state due to an increase in molecular mobility upon heating (devitrification). The time required for the dynamic conversion to be completed depends on the experimental heating rate as well as the history of the sample. For example, during vitrification, a slow cooling rate contributes in delaying the immobilisation of the polymeric chains while providing more time for cooperative arrangements to take place. Therefore, the slower the cooling rate, the lower the *Tg*.

The glass transition is most commonly visualised via Differential Scanning Calorimetry (DSC) as shown in Fig. 1.7, and it is observed as a relatively abrupt change in heat capacity. The temperature of the *Tg* is defined as the temperature corresponding to the point of inflection of the heating curve (Hodge 1994). Measurements of the glass transition not only give an insight on the thermodynamic capacities of polymers, but they also contain information about structural differences between or within samples.

Only amorphous polymers exhibit a glass transition phenomenon, regardless of their full or partial amorphous composition. The *Tg* of PLGA depends on the respective mechanical characteristics of PLA and PGA. It is known that D-PLA and L-PLA are semi-crystalline because of high uniformity in their polymeric chain hindering molecular flexibility, while D,L-PLA is amorphous due to irregularities in its chain structure (Tice & Cowsar 1984). On the contrary, PGA lacking the methyl side group of PLA is highly crystalline (Ford & Timmins 1989). The ensuing PLA/PGA combination allows the production of a wide variety of copolymers with specific mechanical states resulting from: the nature of the assembled molecules, the PLA/PGA

ratio and the degree of polymerisation. The glass transition temperature of the copolymer can be calculated from the Gordon-Taylor equation (1.1) (Hancock & Zografi 1994):

$$Tg = \frac{w_A Tg_A + kw_B Tg_B}{w_A + kw_B} \qquad 1.1$$

w_A, w_B: weight fraction of the monomers A and B

Tg_A, Tg_B : Tg of the homopolymers A and B

k: the free volume ratio of the two components under any given condition

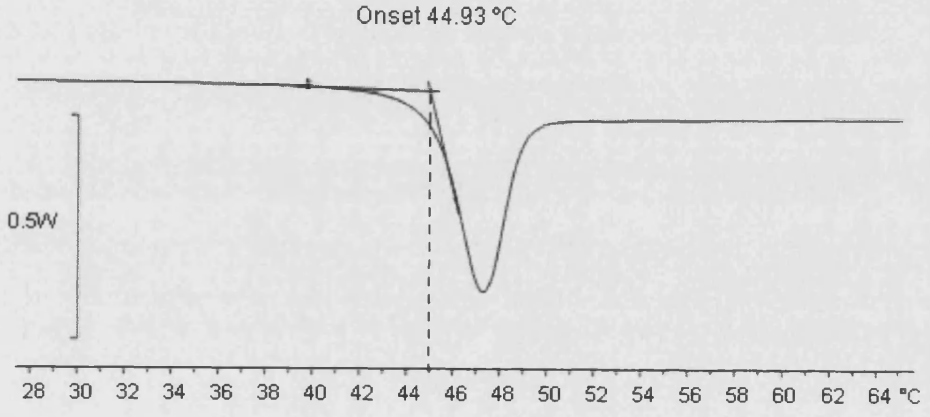

Figure 1.7. Determination of the glass transition temperature of PLGA by following the point of inflection of the DSC curve. Note the change of the baseline indicating a glass transition event and not a melting or crystallising event.

1.6.2.4 Heat capacity

At constant pressure, the heat capacity is the amount of heat required to change the temperature of a substance by 1°C. It is determined by the following equation (1.2):

$$Cp = \frac{q}{T_t - T_0} \qquad 1.2$$

Cp: heat capacity at constant pressure (J/°C)

q: heat supplied (J)

$T_t - T_0$: difference between the temperature at time 't' and the initial temperature (°C or Kelvin)

The heat capacity can be visualised in Fig. 1.8 by plotting the heat flow against temperature. The heat flow is defined by the temperature supplied per unit time. On the basis of a DSC experiment model, the heat flow corresponds to the heat provided to the sample in order to align with the temperature applied to the reference pan. As the temperature rises, there is an increase in heat capacity reflecting the greater capacity of the polymer to absorb heat as it transforms from the glass to the rubber state. While heat is being taken up, an endothermic slope illustrates the physical evolution taking place over a temperature range with no sudden events. This type of change in heat capacity differentiates the glass transition from the phenomenon of melting or freezing where latent heat is involved, as described more in depth in the next section.

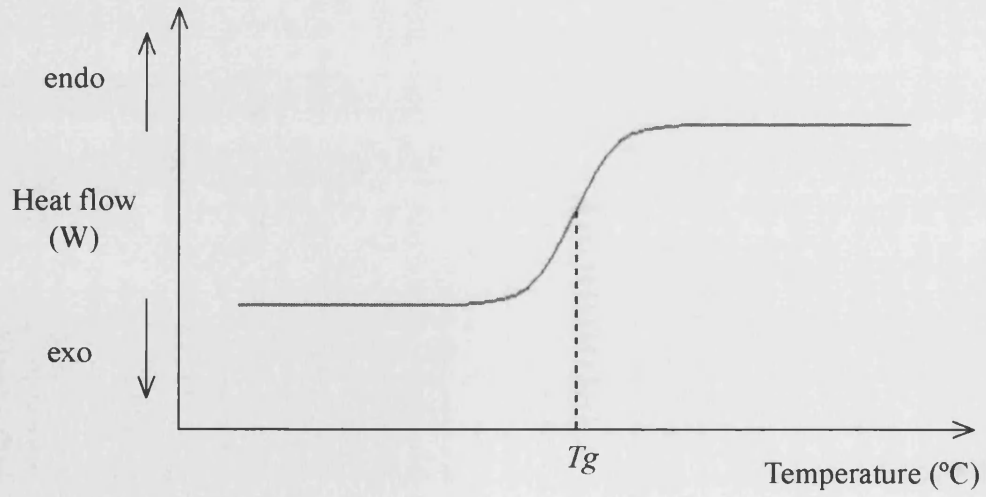

Figure 1.8. Illustration of the change in heat flow over increasing temperature. The endothermic slope indicates that the sample exhibits a higher capacity for absorbing heat.

1.6.2.5 Crystallisation and melting of semi-amorphous polymers

In order to distinguish the glass transition phenomenon from crystallisation and melting, a brief definition of these two processes is given here. For semi-crystalline polymers, as the temperature rises above the glass transition temperature, an exothermic peak is recorded where the polymeric chains fall into crystalline arrangements. This temperature is called the crystallisation temperature, *Tc*, and it is measured at the apex of the peak. By further increasing the temperature, eventually the crystal liquefies and an endothermic peak is observed at the melting transition, *Tm* (e.g.: *Tm* of PGA highly crystalline ~ 230°C; *Tm* of L-PLA semi crystalline ~ 175°C). Crystallisation followed by melting is not always typical of all semi-crystalline polymers.

Crystallisation and melting are characterised by heat emitted and absorbed, respectively. In each case the heat capacity returns to its initial value once the transitions completed (the baseline stays constant before and after the event). This particular feature is known as latent heat of crystallising and melting, and is referred to as a first order transition. In contrast, during the glass transition the material does not recover its initial heat capacity after completion of the transfer. As no latent heat is exhibited, it is called a second order transition. Figure 1.9 illustrates a complete thermograph where glass transition, crystallisation and melting are traced in succession.

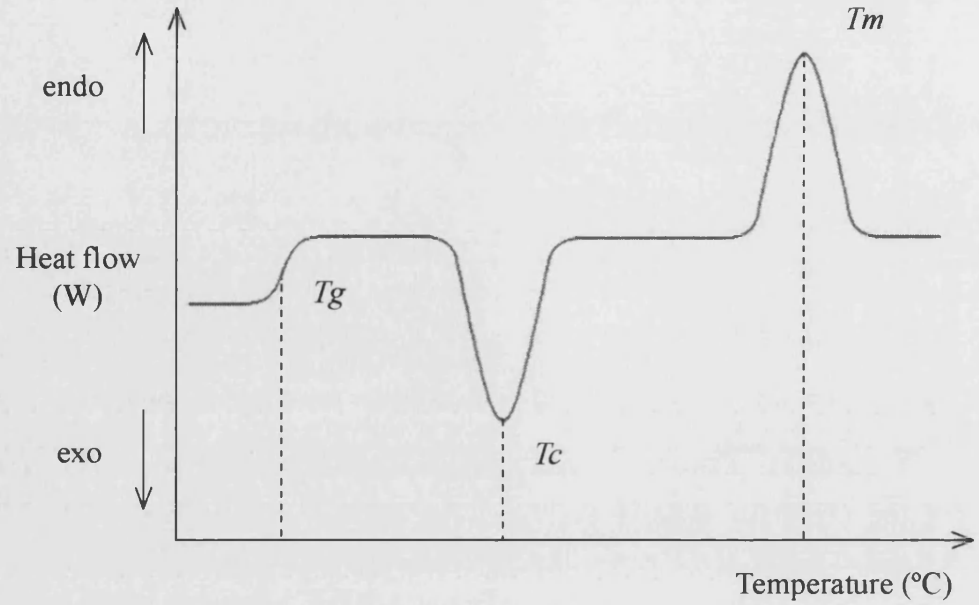

Figure 1.9. Illustration of an entire DSC thermograph representing the thermal transitions of a semi-crystalline sample over heating. The first transformation consists of the glass transition, followed by crystallisation and melting.

1.6.2.6 Enthalpy relaxation

At all states, amorphous materials tend towards equilibrium through molecular rearrangements. The polymeric structures are said to relax. The completion of the molecular relaxation also depends on the environmental temperature and *Tg* as illustrated in Fig. 1.10. At high temperatures, enough kinetic energy is provided to bring the chain segments to equilibrium in a short time (stage 1 in Fig. 1.10). As the temperature decreases, chain mobility is reduced, and more time is required for the sample to return to equilibrium (stage 2). Eventually, the cooperative rearrangements become so slow that there is not sufficient time for the sample to relax (stage 3). At this point, the experimental cooling rate is faster than the relaxation time of the sample and the glassy state is reached.

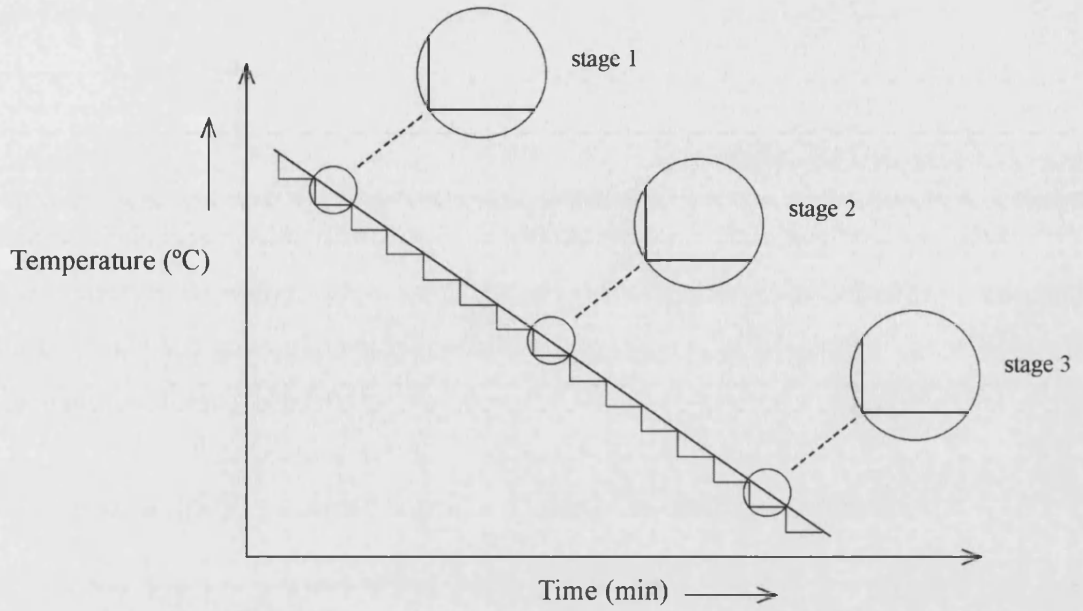

Figure 1.10. Illustration of the time necessary for molecular rearrangements or internal relaxation to be completed in order to equilibrate with the environment.

By definition, the enthalpy relaxation is the heat content of a chemical system returning to equilibrium through changes in atomic arrangement. It is important to note that these molecular rearrangements are dependent on the initial atomic conformation of the polymeric network, which can be evaluated with the study of physical ageing described in the next section. Often, the relaxation time is predicted using mathematical models (Hodge 1994; Shamblin *et al.* 1999), and the maximum enthalpy recovery which corresponds to equilibrium is calculated from the following equation (1.3):

$$\Delta H_{\infty} = (Tg - T)\Delta Cp \qquad 1.3$$

$\Delta H\infty$: maximum enthalpy relaxation (J)

Tg: glass transition temperature (°C)

T: experimental temperature (°C)

ΔCp: change in heat capacity at the glass transition (J/ °C)

1.6.2.7 Physical ageing

The term 'physical ageing' was introduced to distinguish mechanical effects from those produced by degradation or polymorphic changes. Ageing characterizes the impact of time, temperature and environmental conditions on the material when stored below its *Tg*. The phenomenon of physical ageing is observed as a peak superimposed on the glass transition (the enthalpy relaxation peak or overheating peak).

A glassy amorphous polymer in non-equilibrium below its *Tg* will undergo side group rotation. With time, a gradual broadening of the overheating peak is observed, concomitant with an increase in the *Tg* (Fig. 1.11). The progressive reduction of side chain mobility is the result of a gain in matrix density due to loss of intermolecular space. Lowering the storage temperature increases the enthalpy relaxation due to slower molecular motions, and therefore a longer time is necessary for the structure to fully relax (Bailey *et al.* 2002; Hancock *et al.* 1995; Van den Mooter *et al.* 1999). The storage temperature is often referred to as ageing temperature or T_a. As T_a decreases, the molecular mobility diminishes considerably and the relaxation process slows down until eventually a temperature where molecular motion is insignificant is reached. In order to attain such inactivity, it is necessary to cool the material at least 50°C below its *Tg*, a limit also known as the Kauzmann temperature or T_K (Kauzmann 1948). There is a paucity of research dedicated to identifying the stability of drug-loaded PLGA microspheres despite its necessity during storage. Mathematical models have been developed to predict and fit experimental DSC traces (Andreozzi *et al.* 2003; Cowie & Ferguson 1986).

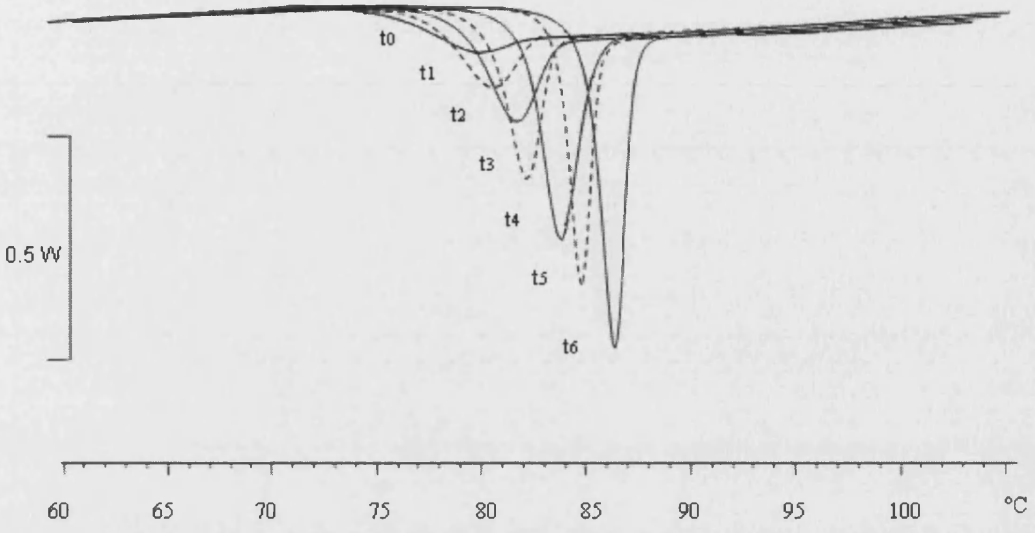

Figure 1.11. Illustration of the molecular relaxation of a polymer subjected to different periods of physical ageing under constant temperature.

Technically, the ageing potential of a glassy polymer is revealed by comparing the first heating peak with the one successive to "quench cooling", a method of cooling so rapidly that molecular relaxation is minimal. The difference between the curves superimposed is often referred to as 'overshoot' or the 'overheating' peak, and its area represents the enthalpy relaxation (Fig. 1.12). Modulated DSC was recently proved to be capable of isolating the glass transition from the enthalpy relaxation signal without quench cooling the sample (Royall *et al.* 1998; Royall *et al.* 1999). In this case, the glass transition is represented by a reversing signal describing a kinetic event, whereas a non-reversing heat flow is associated with the relaxation endotherm of the sample.

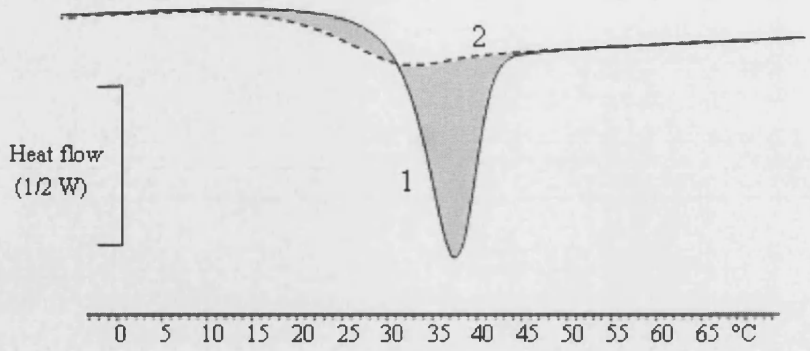

Figure 1.12. Determination of the Enthalpy Relaxation of blank microspheres made with low molecular weight PLGA and aged for 3 months at 4°C with silica gel (1: first heat run; 2: second heat run immediately after quench cooling).

The enthalpy relaxation corresponds to the following equation (1.4):

$$\Delta H = \int_{T_1}^{T_2} (c_1(T) - c_2(T))dT \qquad 1.4$$

ΔH: enthalpy relaxation (J)

c_1, c_2: heat capacity of the first and second heat runs (J/ °C)

T: experimental temperature (°C)

1.6.2.8 Free volume

As explained above, the phenomenon of physical ageing corresponds to a structural recovery. Therefore the spatial arrangement of the polymeric chains imposes a considerable constraint on ageing progress. The entanglement of the polymer chains results in a web of a density relative to their length: the longer the chains, the denser the network. The mesh is constantly left with spaces in between the chains that are waiting to be filled. These volumes are ideal interstices for small chain segments to

rotate and move relatively freely. The local rearrangements yield structures that are successively removed from their previous configuration.

During physical ageing, these spaces are preferentially occupied first. It is suggested that the initial rapid relaxation often observed results from relaxing molecules revolving in these so-called 'free volumes' (Lamarre & Sung 1983). Subsequently, the densification of the matrix shifts the glass transition temperature of the polymer towards higher values as shown in the previous Fig. 1.11.

1.6.2.9 The mechanical properties of PLGA microspheres

Only a few studies have focused on the mechanical progression of PLGA under processing. There are two main systems affecting the copolymer's *Tg* during microsphere fabrication: the inevitable manufacturing stresses such as solvent removal, and supplementary strains, for example due to the additional use of emulsifiers.

During solvent extraction, the polymer precipitates and the microspheres harden rapidly. In doing so, the polymeric chains are effectively immobilised without time for equilibrium to be achieved (Li *et al.* 1995). By varying the speed of the solvent extraction, the molecular arrangement as well as the relaxation point of the polymeric chains will be set in different configurations as illustrated in the previous Fig 1.10. The particles are then collected and dried. Unfortunately, the removal of water is hard to complete and residual amounts of water often lower the *Tg* of the material since water acts as a plasticizer (Passerini & Craig 2001).

Plasticizers are small molecules soluble in the polymer that ease its chain mobility and lower its *Tg*. The emulsifiers or surfactants added to the primary emulsion often operate as plasticizers or anti-plasticizers. Some organic materials, such as triethyl citrate or acetyltributyl citrate, have already been identified as plasticizers when integrated in PLGA films (Kranz *et al.* 2000). Modifying the amount of stabiliser added to the solution may lead to immiscibility when too high concentrations or too large molecules are used (Jeong *et al.* 2000). In this case, thermal analysis reveals two distinct peaks, one belonging to the emulsifier and the other to the polymer, whereas only one peak is seen when the blend between the polymer and the emulsifier is homogeneous. It is also important to note that the temperature corresponding to the

glass transition of PLGA microspheres reflects the history of the sample which can not be ignored and should be optimized (Yang *et al.* 2000).

During storage, the hygroscopic nature of PLGA facilitates water adsorption. PLGA hydration operates at a rate which is dependant on the water-vapour/copolymer affinity, and continues until limitation or saturation is reached (Oksanen & Zografi 1993). Meanwhile, a significant redistribution of the free-volume occurs within the PLGA matrix and increases the chain mobility, thereby lowering the *Tg* (Hancock & Zografi 1994). When finally PLGA microspheres are placed *in vitro* conditions, chain mobility is drastically accelerated with direct exposure to water and elevated temperature. In addition, water uptake swells the PLGA matrix, which may undergo main-chain relaxation (Sharp *et al.* 2001). As a result, hydrolysis increases as water molecules enter more easily in contact with ester linkages (Deng & Uhrich 2002). Degradation products together with the drug are evacuated more rapidly, although in a different manner for amorphous and crystalline regions (Pistner *et al.* 1993). It would be advantageous to be able to control the formulation parameters in order to meet the physical stability required for a drug delivery system. The importance of achieving such a result is not only related to degradation and drug release, but also to the material stability during storage.

1.7 Description of the 9th-10th Fibronectin type III domain pair, FIII9'-10

1.7.1 Introduction

The cells defining a tissue are physically maintained via a mechanical support called the extracellular matrix (ECM). Although the molecular composition of the ECM varies from one cell type to another, polysaccharides and glycoproteins comprise the majority. These macromolecules provide physical scaffolding and are also involved in cell signalling via adhesive recognition sequences (Campbell & Reece 1947). These signals orchestrate mechanisms such as cell adhesion, migration, polarisation, proliferation and differentiation; in summary, a variety of activities involved in

embryogenesis, tumour metastasis, angiogenesis, haemostasis as well as other biological processes. Cell adherence is one of the most extensively studied ECM activities, and the majority of the adhesive proteins interacting with cell-surface receptors have now been identified: collagen, thrombospondin, fibrin, fibronectin, laminin and vitronectin (Kreis & Vale 1999).

Fibronectin (FN) participates directly in the cell-cell contact by binding to ubiquitous cell surface membrane proteins called integrins (Clark & Brugge 1995; Stenman & Vaheri 1978). Integrins span the membrane to bind to the cytoskeleton and are involved in inside-out signalling (Giancotti & Ruoslahti 1999; Kreis & Vale 1999). The key adhesive site in fibronectin is composed of a tri-peptide segment, Arg-Gly-Asp, referred to as RGD in single letter code (Pierschbacher & Ruoslahti 1984). It is important to note that fibronectin does not hold the monopoly on RGD which in fact occurs in numerous ECM proteins as the ligand for several receptors of the integrin family (Ruoslahti 1996). Table 1.4 summarises a list of a few ECM proteins and their adhesive sites, among which RGD is visibly the most frequent.

ECM proteins	Adhesive recognition sequences
FN	RGD, DRVPHSRN, LDV, REDV, IDAPS, KLDAPT, PRARI
Laminin	RGD, LRE, YIGSR, PDSGR, RYVVLPR, LGTIPG, IKVAV, RNIAEII
Fibrinogen	RGD, HHLGGAKQAGDV
Thrombospondin	RGD, VTXG, WSXW
Vitronectin	RGD
Collagen type VI	RGD

Table 1.4. Some ECM proteins and their adhesive sites.

1.7.2 Structure and function of fibronectin

The fibronectin gene is composed of approximately 50 exons which can essentially be separated into three groups according to their notable structural homology (Mosesson & Amrani 1980). These three groups of repetitive homologous domains are known as type I, II and III (FNI, FNII and FNIII) (Skorstengaard *et al.* 1984). Their translation results in a polypeptide compiling approximately 2100-2400 amino acids (220-250 kDa). Two FN molecules oriented in an anti-parallel manner are

united via C-terminal disulphide bonds (An *et al.* 1992). The flexibility among the two subunits enables FN to regulate the accessibility of various binding sites by changing conformation (Johnson *et al.* 1999).

In each subunit, FNI, FNII and FNIII compose more than 90% of the total peptides as shown in Fig. 1.13. Among the three types of module, the FNIII10th domain has been identified with the highest cell adhesion activity (Ruoslahti 1996). This discovery led to more substantial characterisation of adjacent FNIII10 segments, distinguishing the central cell binding domain (CCBD) located on the domains FIII8, 9 and 10. The architecture of the FIII10 domain consists of a protruding loop on the β-strand which holds the RGD site (Leahy *et al.* 1996). The FIII9 domain greatly enhances $\alpha_5\beta_1$ integrin binding via the "synergy site", located and separated from the RGD site by 35 Å (Fig. 1.14) (Nagai *et al.* 1991). The FIII8 side domain facilitates cell adhesion, but it only has a moderate influence (Altroff *et al.* 2001). The $\alpha_5\beta_1$ integrin binding activity of FIII9-10 depends on the maintenance of the secondary and tertiary structure of the FIII9-10 pair (Altroff *et al.* 2003). The positioning of the synergy site relative to RGD is therefore critical for $\alpha_5\beta_1$ integrin binding.

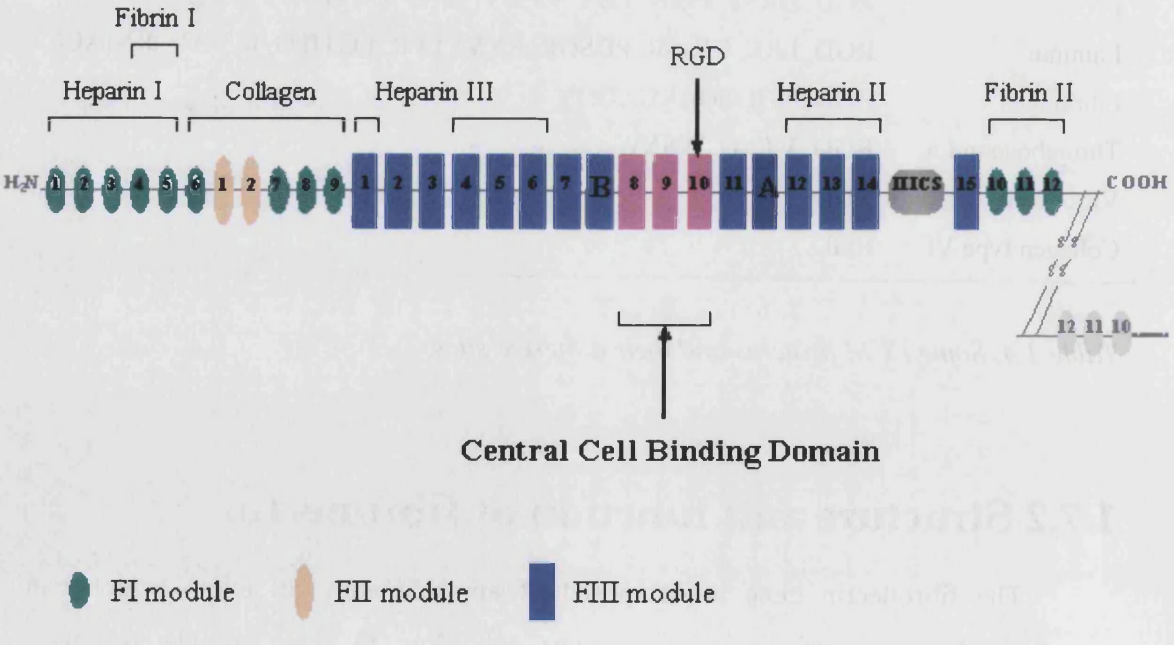

Figure 1.13. Modular organisation and functional regions of a fibronectin monomer. The domains reported to have an activity are distinctively designated and labelled with the name of their associated receptor. The minimal active sequence of the recognition

site of the CCBD is indicated above the 10th domain of FIII of which it belongs to (RGD) (Altroff 1999).

It should be added that the role of fibronectin has been extended beyond integrin binding to include: heparin, fibrin and collagen binding domains, and matrix assembly regions. Figure 1.13 illustrates the domains of the FI, FII, and FIII modules allocated to these functional regions. Although knowledge of some of these binding sites is today considerably detailed, the most essential and best understood site remains the CCBD.

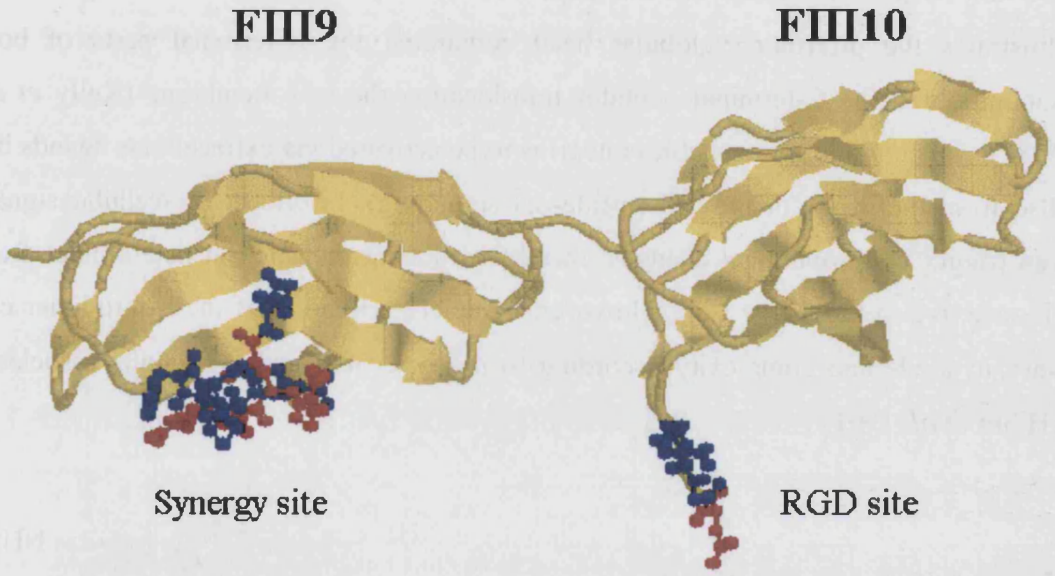

Figure 1.14. Topology of functionally important protruding loops within the FIII9-10 pair.

The variety of functional sites highlights the importance of the role of fibronectin over other ECM molecules. Overall, the protein orchestrates the establishment and maintenance of tissues through the control of cell positioning and cell growth. In the first case, the spatial arrangement of the cell-matrix necessitates a fine regulation of the adhesion of cells to fibronectin and their orientation or even mobility when the need arises (Johnson *et al.* 1992). In the latter case, as the anchorage of normal cells is compulsory in order to initiate their proliferation, the key role of fibronectin is easily understandable (Kubo *et al.* 1987). Moreover, close examination

of the cell-fibronectin activity has shown that the protein is also involved in modulating cell differentiation (Adams & Watt 1989). However, it is important to remember that in all aspects of cell growth and positioning, integrin receptors play a role equally important to fibronectin. The characteristics of adhesion receptors are described in the following section.

1.7.3 General features of integrin receptors

Integrins are heterodimeric glycoproteins composed of α and β subunits which are non-covalently bonded but interdependent (Humphries *et al.* 2003). Figure 1.15 illustrates the protruding globular head containing the N-terminal parts of both subunits, and the C-terminal peptides translocating the cell membrane (Kelly *et al.* 1987). This configuration enables integrins to be activated via extracellular ligands but also from the inside of the cell (inside-out signalling). In effect, intracellular signals can trigger conformational changes, thereby switching the integrin heterodimer from the inactive to the active state. However, complete activation of the heterodimer can vary in mode and complexity according to the type of α and β subunits associated (Hibbs *et al.* 1991).

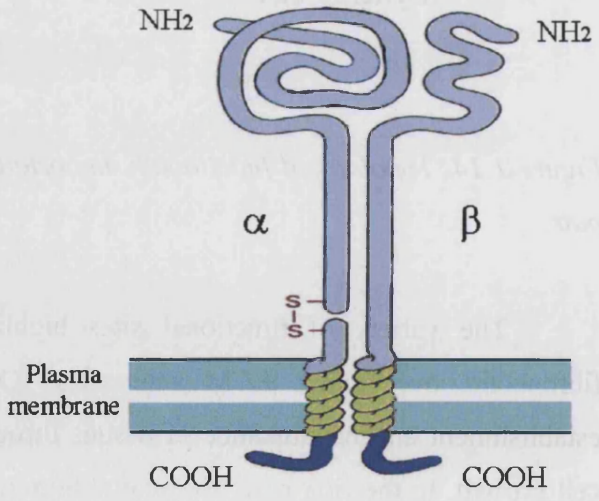

Figure 1.15. Schematic drawing of a typical integrin heterodimer. Both α and β are transmembrane glycoproteins and cell surface expression depends on heterodimer formation (Altroff 1999).

Eighteen α and eight β subunits have been listed in mammals so far (Beckerle 2001). Mutational analyses show that a greater conservation of the β subunits is necessary to ensure normal activity, whereas α subunits tolerate highly divergent

sequences (Laflamme *et al.* 1994). The different active combinations of the α and the β subunits allow a wide variety of recognition of extracellular ligands (Table 1.5). Among the different α/β heterodimers, eleven have been identified to bind to the CCBD of fibronectin (Fig. 1.16). All integrins bind specific ligands according to cell type and ECM, and are regulated by downstream signalling events. For example, β_1 subunit is kinase regulated and enters a high-affinity form after dephosphorylation (Hannigan *et al.* 1996).

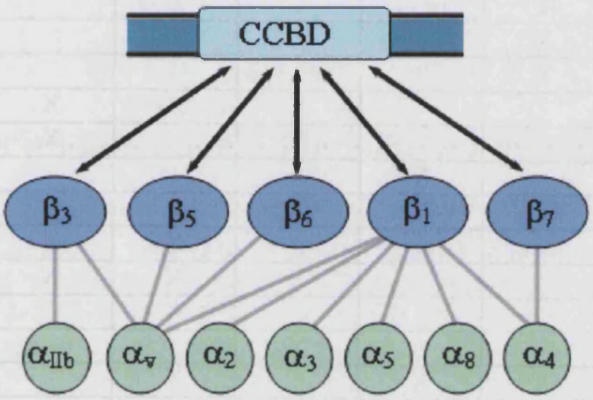

Figure 1.16. Schematic representation of interactions between fibronectin and integrins. Integrin dimers able to recognize the CCBD sequence are formed as indicated with grey lines connecting the subunits. Fibronectin binding by β subunits assembled with all respective α subunits is represented by black arrows (Altroff 1999).

Integrin	Cell-matrix ligands							
	FN	LN	Col	TN	VN	OPN	FBG	TSP
α1β1		X	X					
α2β1		X	X					
α3β1	X	X	X					X
α4β1	X							
α4β7	X							
α5β1	X							
α6β1		X						
α6β4		X						
α7β1	X	X						
α8β1	X	?		X	X	X		
α9β1				X		X		
α10β1			X					
α11β1			X					
αvβ1	X				X			
αvβ3	X			X	X	X	X	X
αvβ5	X				X			
αvβ6	X			X				
αvβ8	X	X	X					
αIIβ3	X						X	X
αDβ2								
αLβ2								
αMβ2							X	
αXβ2							X	
αEβ7								

Table 1.5. Example of ECM ligands and the integrin receptors more or less specific. The diversity of integrin binding interactions offers cells the ability to regulate their affinity and therefore response to the signal. Abbreviations: FN, fibronectin; LN, laminin; Col, collagen; TN, tenascin; VN, vitronectin; OPN, osteopontin; FBG, fibrinogen; TSP, thrombosondin.

1.8 Scope of this thesis

This thesis examines the encapsulation of a mutant 9^{th}-10^{th} type III fibronectin domain pair (FIII9'-10) in biodegradable microspheres using a water-in-oil-in-water double emulsion-evaporation technique. Wild-type FIII9'-10 promotes cell attachment

and spreading on binding to $\alpha_5\beta_1$-integrin receptors which are common to osteoblasts and decidual cells (van der Walle *et al.* 2002). Since $\alpha_5\beta_1$-integrin mediates osteoblast differentiation, angiogenesis, tumorigenesis and embryo implantation, FIII9'-10 has good potential for use in tissue engineering, anti-cancer and implantation therapies (Aplin *et al.* 1999; Cutler & Garcia 2003). For example, the osteocompatibility of PLGA supports the use of FIII9'-10 loaded microspheres injected near osseus wounds to promote bone regeneration. In order to counteract potential protein adsorption during microencapsulation, surfactants or emulsifiers were added individually to the primary water phase. An assortment of five non-ionic surfactants comprising Pluronic F68, Tween 20, Tween 80, Triton X-100 and Igepal CA-630, was selected. The resulting microspheres were compared to particles made with model stabilisers such as PVA and BSA.

Each type of microspheres was evaluated according to its size, morphology, and degradation. The encapsulation efficiency, release profile, and biological integrity characterised with respect to the protein are discussed in the first results chapter (Chapter 3). Despite the fact that each formulation conducted to specific external morphologies ranging from highly porous and smooth, to scarcely porous and ridged, all release profiles exhibited an initial burst. In order to build a more accurate picture of the release phenomenon, microsphere internal and external morphologies were visually examined via scanning electron microscope (SEM) and confocal laser scanning microscope (CLSM) prior and during *in vitro* release in Chapter 4. During incubation, marked differences of the particles' surface underlined the importance of the polymeric chain mechanical activity. Subsequently, the potential of PLGA molecular mobility was further investigated in Chapter 5 with the aim of remodelling the surface porosity before incubation and ideally reducing the initial burst. Finally, as the significance of PLGA's thermodynamic properties grew progressively over the course of this research, the last results chapter was dedicated to formulation parameters impacting on the mechanical integrity of PLGA microspheres.

Chapter 2

Materials and Methods

2.1 Materials

2.1.1 Protein related

FIII9'-10 is a 198 amino acid His-tagged β-sandwich domain pair, belonging to the IgG superfamily, and it exists as a monomer (ca. 21.5 kDa, pI 8.1). *Escherichia coli* (*E. coli*) strain DH5α was used for general cloning procedures, and *E. coli* strain BL21 (DE3) pLysS was used for expression of FIII9'-10 gene. *E. coli* strains DH5α and BL21 were maintained on Luria-Bertani Lennox (LB) plates (0.5% NaCl, 0.5% bacto-yeast extract, 1% bacto-tryptone, 1.5% agar) or in LB liquid (0.5% NaCl, 0.5% bacto-yeast extract, 1% bacto-tryptone) and propagated at 37°C. For selection of transformed *E. coli* DH5α, LB media was supplemented with ampicillin (100 μg/ml). For selection of transformed *E. coli* BL21 (DE3) pLysS, LB media was supplemented with ampicillin (100 μg/ml) and chloramphenicol (15 μg/ml). Protein expression in transformed *E. coli* BL21 (DE3) pLysS was achieved by further addition of isopropyl-β-D-thiogalactopyranoside (IPTG) (0.1 μM final concentration).

2.1.2 Microsphere related

BSA (1 mg/ml), Tween 20 (MW: 1128, HLB: 16.7), Tween 80 (MW: 1310, HLB: 15.0), Triton X-100 (MW: 625, HLB: 13.5), and Igepal CA-630 (MW: 603, HLB: 13.0) were all supplied by Sigma-Aldrich Chemical Co. Polyvinyl alcohol (PVA: MW: 30 000), and Pluronic F68 (MW: 8 400, HLB> 24) were obtained from ICN Biomedicals Inc. Poly(lactic-coglycolic acid) (PLGA) copolymer with a 50:50 D,L-Lactide/Glycolide molar ratio was purchased from Purac biochem Netherlands. Low molecular weight PLGA of ~15 000 g/mol had an inherent viscosity of 0.18 dl/g, and high molecular weight PLGA of ~135 000 g/mol had an inherent viscosity of 0.83 dl/g. The water was distilled to 15 $m\Omega/cm^2$. All other chemical and solvents were purchased from Sigma-Aldrich Chemical Co.

2.2 Synthesis and expression of the protein FIII9'-10

2.2.1 Preparation of competent cells

Competent *E. coli* cells were prepared as adapted from Sambrook *et al.* (Sambrook *et al.* 2001). Briefly, a single bacterial colony was picked using a flamed loop from an agar plate and suspended in 100 ml of LB for over night incubation at 37°C while shaking. 1 ml of the over night suspension was transferred to 100 ml of LB and agitated again at 37°C while cell growth was monitored to an OD600 of ~0.4. The solution was then transferred into 50 ml ice-cold tubes, and stored on ice for 10 min before being centrifuged at 4000 ×g for 10 min at 4°C. The supernatant was carefully discarded and the pellet resuspended by gently vortexing in 30 ml of transformation buffer (TB) (10 mM HEPES, 15 mM $CaCl_2$, 250 mM KCl, 55 mM $MnCl_2$). The suspension was placed back on ice for 10 min, centrifuged again at 4100 ×g for 10 min at 4°C, and after removal of the supernatant, the pellet was resuspended gently in 8 ml

of ice-cold TB. Dimethyl sulfoxide (DMSO) was added to a final concentration of 7% w/v, and the solution was stored on ice for 10 min prior to aliquoting and snap-freezing in liquid nitrogen before storage at -80°C.

2.2.2 Transformation of competent cells

100 µl of competent *E. coli* cells were mixed with 1 µl of DNA, and incubated on ice for 10 to 30 min. The cells were heat shocked for 60-90 seconds at 37-42°C, and then transferred back on ice for 2 min. Finally, the cells were plated onto LB agar containing appropriate antibiotics, ampicillin for *E. coli* DH5α and ampicillin with chloramphenicol for *E. coli* BL21 (DE3) pLysS, and incubated at 37°C overnight.

2.2.3 Extraction of the clone by miniprep

Small-scale preparations of plasmid DNA were made using the QIAprep Spin Plasmid Kit (Qiagen, Ltd, UK), following the manufacturer instructions. Briefly, a 5 ml overnight culture of *E. coli* was harvested and resuspended in 250 µl of buffer P1 (Tris-HCl, pH 8.0, containing RNaseA, 4 µg/ml). The cells were then lysed by the addition of 250 µl of buffer P2 (0.2 M NaOH, 1% w/v SDS) and incubated after gentle mixing, for 5 min at room temperature. The lysate was then neutralised in 350 µl of buffer N3 (potassium acetate, pH 4.8), and kept on ice for 5 min; the tube contents were mixed thoroughly and centrifuged at 12000 ×g for 15 min. The supernatant was applied to a QIAprep spin column, and subsequently washed with PE buffer (1 M NaCl, 50 mM Tris-HCl, 15% v/v ethanol, pH 8.5). DNA was eluted from the column with 50 µl of Tris-HCl (pH 8.5) and stored at -20°C. In order to estimate the DNA purity, a 5 µl sample was electrophoresed on a 0.8% w/v agarose gel and visualised by ethidium bromide staining (4 µg/ml). The yield of DNA was measured by UV absorbance at 260 nm using the rule that 1 A_{260} is equivalent to a double stranded DNA concentration of 50 µg/ml. To check the presence of the FIII9'-10 cassette, 0.2 to 1 µg of DNA was mixed with 5 U of each restriction endonuclease (NheI and HindIII, NEB, UK) and 2 µl 10 × reaction buffer (500 mM Tris-HCl pH 7.5, 50 mM $MgCl_2$, 150 mM NaCl) in a total volume of 20 µl following digestion at 37°C for 4 h.

2.2.4 Agarose gel electrophoresis

1 µl of a 5 × loading buffer was added to each 4 µl of DNA sample and loaded onto a 0.8% agarose gel made according to the recommendations of Sambrook *et al.* (Sambrook *et al.* 2001). The preparation was electrophoresed at 5-10 V/cm in 1 × Tris-borate-EDTA (TBE) running buffer (90 mM Tris-borate, 2 mM EDTA). DNA bands were stained with ethidium bromide (0.5 µg/ml), and visualised on an UV transilluminator (ca. 290 nm).

2.2.5 Expression of the protein FIII9'-10

A single transformed colony of *E. coli* BL21 (DE3) pLysS cells was suspended in 100 ml of LB containing 100 µg/ml of ampicillin and 15 µg/ml of chloramphenicol. The suspension was incubated over night at 37°C in a shaking incubator. The following day, 25 ml of the cell culture was diluted into 1 l of LB with antibiotics, and incubated at 37°C with shaking. Cell growth was monitored to an OD_{600} of 0.6 and at this point, protein expression was induced by addition of 1 ml of a 100 mM stock solution of IPTG. Following a further 3 h incubation, shaking, cells were harvested by centrifugation at 5000 ×g for 15 min at 4°C, and the supernatant discarded. The cell pellet was resuspended in 4 ml of lysis buffer (50 mM NaH_2PO_4, 300 mM NaCl, 10 mM imidazole pH 8) per 100 ml of cell culture to which 1 mg/ml lysozyme was added. The cells were allowed to lyse while kept on ice for 30 min. The solution was then clarified by centrifugation at 50000 ×g for 60 min with the supernatant containing the soluble FIII9'-10 filtered before purification.

2.2.6 Protein purification

Purification of the histidine-tagged FIII9'-10 from bacteria cell lysate was conducted using nickel affinity chromatography with the protein eluted via a concentrated imidazole buffer. The preparation of the nickel-immobilised agarose-bead column prior to sample loading involved washing with water and then lysis buffer. The

filtered bacterial lysate sample was then loaded onto the column equilibrated to allow for the protein to bind to its walls. Next, the column was washed with wash buffer (50 mM NaH_2PO_4, 300 mM NaCl, 50 mM imidazole, pH 8) separating immobilised Hist-tagged protein from bacterial lysate contaminants. Immobilised protein was eluted from the column with elution buffer (50 mM NaH_2PO_4, 300 mM NaCl, 250 mM imidazole, pH 8). Eluted fractions containing protein were monitored by (in-line) UV absorption at 280 nm. The homogeneity of the eluted fractions was verified by sodium dodecyl sulfate polyacrylamide gel (SDS-PAGE). The imidazole was removed by dialysis of the pooled fractions in 1 l of PBS at 4°C, stirring for 24 h. The concentration of the dialysed fractions was measured by A_{280} values using a calculated extinction coefficient of 21620 $cm^{-1}M^{-1}$ (Bouissou et al. 2004). The dialysed fractions were then concentrated using an Amicon stirred cell with 10000 MWCO filter, aliquoted and stored at -80°C until needed.

2.6.7 Analysis of proteins by sodium dodecyl sulfate polyacrylamide gel (SDS-PAGE)

Protein analysis by SDS-PAGE was adapted from Laemmli (Laemmli 1970). Protein samples were mixed with 1/3 volume of protein loading buffer (3 × protein loading buffer: 47 mM Tris-HCl, 5% v/v β-mercaptoethanol, 3.4% w/v SDS, 20% w/v sucrose, 0.01% w/v bromophenol blue, pH 6.8), boiled for 5 min and loaded onto gels (5% polyacrylamide stacking layer and 12% polyacrylamide resolving layer) prepared according to Sambrook *et al.* (Sambrook *et al.* 2001), using MiniProteanIII apparatus (BioRad, UK). Gels were placed in 'SDS-buffer' (196 mM glycine, 0.1% SDS, 50 mM Tris-HCl pH 8.3), and run under a continuous amperage of 30 mA per gel, until the dye reached the bottom of the gel. Proteins were visualised by staining the gels with Coomassie brilliant blue (10% v/v acetic acid, 40% v/v methanol, 0.1% w/v Coomassie brilliant blue R-250) for at least 2 h, followed by destaining overnight in destain solution (10% v/v acetic acid, 40% v/v methanol). Broad-range protein molecular weight markers were purchased from Fermentas.

2.3 Preparation and analysis of microspheres

2.3.1 Preparation of the microspheres

A water-in-oil-in-water (w/o/w) double emulsion-evaporation technique was employed. Aqueous solutions containing 0.5% w/v of PVA, BSA at 1mg/ml, or 5% w/v of non-ionic surfactant (Pluronic F68, Tween 20, Tween 80, Triton X-100, Igepal CA-680) were prepared separately. An inner water phase of 90 µl of FIII9'-10 at 20 mg/ml in phosphate buffered saline (PBS), with 5 µl of aqueous solution with surfactant or stabiliser, or PBS (control) were injected into 950 µl of oil phase: dichloromethane (DCM) containing 5% w/v PLGA, and homogenised at 22000 rpm for 15 seconds (IKA Ultra Turrax T18). This primary emulsion was transferred into 40 ml of water containing 0.5% w/v polyvinyl alcohol (PVA), a requirement for microsphere preparation (Rafati *et al.* 1997), and stirred at 500 rpm for 2 h at room temperature (IKA 'Lab Egg' RW11). The solvent was subsequently evaporated and the capsides were allowed to harden. The microspheres were then harvested by centrifugation at 4000 ×g for 1 min, washed three times in distilled water, snap-frozen in liquid nitrogen and finally lyophilised overnight (Micro Modulyo, ThermoSavant). Lyophilised microspheres were kept at 4°C in a sealed container with silica gel. Microspheres referred to as blank capsides used PBS as the inner aqueous phase. The PVA added to the external aqueous for microsphere preparation phase was not taken into account and only the surfactants incorporated in the primary emulsion were evaluated in this thesis.

2.3.2 External morphology analysis

2.3.2.1 Scanning Electron Microscopy (SEM)

Approximately 1-2 mg of lyophilized microspheres were evenly sprinkled onto a carbon adhesive disk mounted to an aluminium stub. Samples were coated with a

thin layer of gold for 3 min in an Edwards Sputter-coater S150B and viewed using a JEOL JSM6310 SEM operating at 10 kV, 20°C and with a vacuum of 10^{-5} Torr.

2.3.2.2 Atomic Force Microscopy (AFM)

Atomic Force Microscopy images were performed using a NanoScope IIIa controller, a multi-mode AFM head (Digitial Instruments, Santa Barbara, CA) and a J-type scanner. Microspheres were mounted to the AFM magnetic stubs by a layer of Tempfix, a thermoplastic adhesive resin. All AFM surface topography images were recorded in TappingMode™ operation. Tetrahederal-tipped silicon etched cantilevers (OTSP, Digitial Instruments, Santa Barbara, CA) with a nominal tip radius of curvature <10 nm and a resonant frequency 200-400 kHz were utilised for imaging. Surfaces analyses of the topographical images were undertaken with the in-built AFM software.

2.3.2.3 Particle size

Microspheres were suspended in distilled water in a small stirring cell of the Malvern Mastersizer X (Malvern Instruments, UK, Ltd), and particle size measured using laser diffraction with a range lens of 300 mm, a laser obscurity between 12 and 25%. The values reported are the volume based distribution, relatively to the mode diameter and standard deviation of the particles.

2.3.3 Internal morphology analysis

2.3.3.1 Confocal laser scanning microscope (CLSM)

FIII9'-10 (1 mg/ml) was fluorescently labelled with fluorescein isothiocyanate-(FITC-) celite (10 mg) by mixing in 0.05 M $NaHCO_3$, pH 8.5 for 2 h. After centrifugation, unbound FITC was removed by eluting the supernatant through a PD10

column (Amersham Bioscience), equilibrated in NaH_2PO_4, pH 6.5. The molar ratio of label:protein was determined as 1:1 (by A_{280} and A_{495} values), and the protein concentration evaluated using the BCA micro-assay. FITC-labelled FIII9'-10 was encapsulated into PLGA microspheres as described above. Briefly, an inner water phase of 95 µl containing FITC-labelled protein at 10 mg/ml without surfactant was added to 950 µl of DCM with PLGA (5% w/v), and homogenised at 22000 rpm for 15 seconds. This primary emulsion was then transferred into 40 ml of water containing 0.5% w/v PVA, and stirred at 500 rpm for 2 h to allow solvent evaporation and PLGA precipitation. Microspheres were washed, harvested, and dried as described above.

Microspheres were mounted on a slide using Vectashield H-1000 (Vector Laboratories, CA, USA) to prevent photobleaching and a coverslip set in place. Visualization by CLSM (Olympus Fluoview 500, Japan) used an ion laser set to λ_{ex} 488 nm and λ_{em} 505 nm. A series of 1 µm equatorial sections were collected for the microsphere (~ 100 µm diam.).

2.3.4 Polymer structure analysis

2.3.4.1 Storage at selected humidity

Approximately 5 mg of lyophilised microspheres were placed into open Eppendorf tubes in a sealed chamber. The relative humidity of the air in the chamber was controlled using saturated salt solutions. The saturated salt solution was prepared by spreading about 3 mm of dry salt in a shallow beaker and adding water to it in order to moisten the salt. The desiccant was selected according to the humidity required. Sodium chloride and potassium nitrate were used here to prepare saturated salt solutions of 75% and 93% relative humidity, respectively (O'Brien 1948).

2.3.4.2 Dynamic Vapour Sorption

Water sorption/desorption studies of the prepared microspheres were conducted with a calibrated DVS-1-system (Surface Measurement Systems Ltd., London, UK).

The glass pan was carefully filled with approximately 10 mg of microspheres and analyzed against an identical empty glass pan as the reference. The relative humidity was set to 0% and was increased in steps of 23.7% up to 95% relative humidity. The change in mass of the microspheres (as a function of the dry mass at 0% relative humidity) was recorded at each incremental step. Equilibrium mass, at each relative humidity, was determined with a dm/dt of 0.001 %/min. Two sorption/desorption cycles were recorded for each sample. Experiments were recorded at 20°C and the microspheres used for analysis from each batch were free flowing, rather than "compacted".

2.3.4.3 Differential Scanning Calorimetry

DSC plots were obtained using dynamic DSC (DSC 822e, Mettler Toledo). Samples were prepared by carefully weighing ~1-2 mg of microspheres into an aluminium pan, which was then hermetically sealed. An empty pin-holed aluminium pan was used as a reference. Both the reference pan and the sample pan were allowed to equilibrate isothermally for 5 min at 0°C. The pans were then heated at a rate of 10°C/min from 0°C to 85°C, quench cooled to -20°C (in order to eliminate any sample history), then heated again to 85°C at 10°C/min. The results were analysed using Mettler STAR software, and onset of transition was reported as the corresponding glass transition temperature (Hodge 1994).

2.3.5 Protein release and encapsulation

2.3.5.1 Alkaline SDS Extraction method

About 7 mg of dried microspheres were weighed and added to 1 ml of 0.1 M NaOH containing 2% w/v sodium dodecyl sulfate (Hora *et al.* 1990). The solution was shaken overnight with an Eppendorf Mixer 5342, Anderman, at room temperature. After 5 min centrifugation at 12000 ×g, the supernatant was used to estimate the protein content using the BCA assay. The reading of the samples was done by BCA

micro-assay versus the supernatant of blank microspheres of the corresponding batch, and always repeated three times.

2.3.5.2 Protein recovery by the DMSO/NaOH/SDS method

Approximately 7 to 8 mg of dried microspheres were weighed and added to 1 ml of dimethyl sulfoxide (DMSO) to dissolve the polymer (Sah 1997). The tubes were occasionally hand shaken over one hour at room temperature. 5 ml of 0.05 M NaOH containing 0.5% w/v sodium dodecyl sulfate were gently mixed with the solution and allowed to stand for 1 h at room temperature. The protein concentration was then determined using aliquots of the clear solution (samples vs. blank microspheres) by BCA micro-assay.

2.3.5.3 *In vitro* protein release

Approximately 10 mg of dried microspheres were weighed into Eppendorf tubes and suspended in 1 ml of PBS at pH 7.4 with 0.02% w/v sodium azide to prevent microbial growth. The tubes were placed horizontally without shaking at 37°C for 8 weeks. At predetermined times points (30 min, 1, 2, 4, 8, 24, and 72 h incubation; then 1 week, 2 weeks, 4 weeks and 8 weeks incubation), the samples were centrifuged for 2 min at 12000 rpm, and the supernatant was replaced with fresh buffer. The microspheres were resuspended by short sonication when necessary and placed again to incubate. The supernatant collected was analysed to determine the protein concentration using the BCA micro-assay. Blank microspheres incubated following the same procedure were used as reference against the test samples.

2.3.5.4 BCA micro-assay

About 25 µl of protein sample was added to 200 µl of bicinchoninic acid (BCA) working solution. The plate was covered and left at 37°C for 30 min. The absorption was read with a 550 nm filter using a 96-well plate reader (Dynatech MR5000).

2.4 Biological characterisation

2.4.1 Cell adhesion

The baby hamster kidney BHK-21 fibroblast cell line as well as the chemicals and buffer solutions were kindly provided by Dr. H. Mardon (Nuffield Dept. of Obstetrics and Gynaecology, Oxford University, Oxford). 5 mg of lyophilised microspheres in 500 µl of PBS were shaken vigorously at 37°C for 3 h. The suspension was centrifuged (12000 ×g, 1 min) and 50 µl of the supernatant retained for analysis of the protein concentration using the BCA micro-assay. The remainder of the supernatant was used to coat a 96-well flat-bottomed plate following a doubling dilution protocol, and incubating the plate overnight at 4°C. The last lane contained PBS only as the control, as shown in Fig. 2.1. Baby hamster kidney (BHK) cells were passaged the day before the assay as required 10^4 cells per well (50 µl). On the day of the assay, the wells were washed three times with PBS, and non-specific cell binding was blocked by addition of 100 µl per well of BSA (10 mg/ml) in PBS for 1 h at 37°C. The wells were washed again and filled with 50 µl of serum-free medium then incubated at 37°C in 5% CO_2 for 30 min.

Meanwhile, the serum-containing medium was aspirated from the tissue culture flask. The cells were washed in warm PBS (10 ml), and then detached from the flask by addition of trypsin (10 ml) for 5 to 10 min. After centrifugation at 1500 ×g for 3 min and aspiration of the trypsin, the cells were washed in warm PBS, resuspended in 5 ml of serum-free medium in a 50 ml Falcon® tube, and finally placed in a 5% CO_2

incubator for 10 min (the lid left loose to facilitate gaseous exchange). The cell suspension was diluted accordingly to obtain a concentration of 2 x 10^5 of cells per ml and 50 µl added to each well in the 96-well plate, pipetting up and down to ensure even distribution. The plate was incubated at 37°C in 5% CO_2 for 1 h. The media was gently removed, the adherent cells washed with 100 µl of warm PBS, and fixed by addition of 100 µl of warm fixative (4% glutaraldehyde, 4% formaldehyde in PBS) for 10 min at room temperature. The fixative was replaced with 100 µl of 0.1% w/v crystal violet and left for 10 min after which the dye was carefully washed off with tap water, and with methanol when necessary. Finally, 200 µl of methanol was added to each well to solubilise the dye and left for 1 h at room temperature; absorption was measured at 570 nm (Dynatec Plate Reader).

	1	2	3	4	5	6	7	8	9	10	11	12
	100	50	25	12.5	6.25	3.13	1.56	0.78	0.39	0.195	0.097	Control
A												
B												

Figure 2.1. Representation of a 96 wells plate to test cell adhesion. The top 4 rows were used to test surfactant A, with surfactant B tested in the bottom 4 rows. In the last column, PBS was used as a negative control. The samples to examine were added to the plate following doubling dilution starting from the column 1.

Chapter 3

Examination of the biological activity of FIII9'-10 encapsulated with non-ionic surfactants

3.1 Introduction

The encapsulation of bioactive compounds remains a fine art where satisfactory drug delivery systems are hard to obtain. The difficulties encountered throughout microsphere formulation are complicated and hard to overcome, mainly due to the technical limitations imposed at the micron- or nanosize scale. Drug loss, emulsion instability, and incomplete or non-existent release are examples of problems being investigated, although priority is commonly given to drug instability (Crotts & Park 1995; Kim & Park 1999; Yang *et al.* 2001). Indeed, the maintenance of the therapeutical agent is the most crucial criteria of drug delivery complexes, failure of which may initiate an unwanted immune response. During the double emulsion solvent evaporation process, the first emulsion has been reported as the most harmful step for the protein conformational stability (van de Weert *et al.* 2000a).

Proteins are surface active compounds. During exposure at the water/organic solvent interface of the primary emulsion, they tend naturally to orientate their hydrophobic regions towards the oily phase (Sah 1999a). The degree of protein movement at the interfacial region is closely related to the characteristics of the protein itself (Middelberg *et al.* 2000). Its electrostatic capacity, spatial conformation and chain flexibility will either limit or favour protein interactions at the water/oil boundary (Hunter *et al.* 1991). These exchanges often result in aggregation as well as adsorption of the bioactive compound (Hunter *et al.* 1990). If the contact is prolonged, partial or complete unfolding of the protein can take place. In some cases, the consequences of these interactions are irreversible, and denatured proteins are liberated from the microspheres (van de Weert *et al.* 2000a). In other cases, aggregates of protein non-covalently bound to the polymeric matrix simply do not diffuse out of the microparticles, causing discontinuous release behaviour (Morlock *et al.* 1997).

The addition of an emulsifier and surfactant into the primary emulsion of PLGA microspheres has been commonly associated with an increase in drug stability as well as high encapsulation efficiency (Yang *et al.* 2001). It is interesting that cyclodextrins have been used to improve protein stability, but no systematic evaluation of alternative emulsifiers to poly vinylalcohol (PVA) has been reported to date (Kang *et al.* 2002). In this study, a series of non-ionic surfactants has been selected as alternatives to PVA for the encapsulation of FIII9'-10 into PLGA microspheres using a w/o/w double emulsion evaporation technique. A total of five different types of surfactants were incorporated separately to the primary emulsion: Pluronic F68, Tween 20, Tween 80, Triton X-100, and Igepal CA-630. The main criterion for the selection of a particular surfactant was in relation to a non-denaturant effect on proteins.

Microspheres were characterised according to their size and their encapsulation efficiency. The effects of the surfactants on the polymeric microspheres were investigated by examination of the external and internal morphology by SEM, and also by verification of the protein location using CLSM. Finally, the peptide backbone integrity of FIII9'-10 was assayed by SDS-PAGE, and the degree of unfolding of FIII9'-10 following emulsification/encapsulation was assessed using a cell-attachment assay.

3.2 Methods

3.2.1 Preparation of the microspheres

Encapsulation of FIII9'-10 was done as described in section 2.3.1 with the help of stabilisers and surfactants added to the water phase of the primary emulsion. Briefly, the first emulsion consists of 90 µl of FIII9'-10 (20 mg/ml) with 5 µl of emulsifier, or surfactant, or water (control) injected into 950 µl of dichloromethane (DCM) with PLGA (5% w/v). The list of surfactants selected to encapsulate FIII9'-10 comprises: Pluronic F68, Tween 20, Tween 80, Triton X-100, and Igepal CA-630. Their main physico-chemical properties are compiled in Table 3.1.

Surfactant	MW (Da)	HLB value	Viscosity (cps) 25°C	Cloud point (°C)
Igepal CA-630	600	13.0	300	63-67
Triton X-100	625	13.5	240	63-67
Tween 80	1310	15.0	400-620	75
Tween 20	1130	16.7	370-430	98
Pluronic F68	~8400	>24	1000	>100

Table 3.1. Main physico-chemical properties of the selected non-ionic surfactants. (MW: molecular weight; HLB value: Hydrophile/lipophile balance value)

3.2.2 Internal structure of embedded microspheres

The preparation of the microspheres for internal morphology analysis was undertaken following the methods of Sandor *et al.* (Sandor *et al.* 2001). Residual water was removed from the samples by incubation in 100% ethanol. Microspheres were subsequently washed from ethanol with osmium tetraoxide (OsO_4) until complete elimination of the alcohol, and embedded in LR White embedding media, a low

viscosity acrylic embedding medium. After 3 days at 30°C, the hard blocks of resin were cut with a glass knife on a Reichert Ultracut-E microtome (Leica, Weim, Austria) until the equatorial region of embedded microspheres was reached. Finally, the cut blocks were imaged by SEM as described in section 2.3.2.1.

3.3 Results and discussion

3.3.1 Effect of non-ionic surfactants on the encapsulation efficiency

Protein loss is known to take place during the secondary emulsion, where osmotic potential between the inner water droplet and the outer water phase of the embryonic microspheres creates a transfer of drug (Yang *et al.* 2001). The addition of surfactant and stabilisers was expected to ameliorate encapsulation efficiency while forming a physical barrier to prevent the escape of the protein. The total fraction of FIII9'-10 remaining in the recovered microspheres was shown to vary noticeably between the surfactants added to the primary emulsion, as shown in Fig. 3.1. In order to evaluate the importance of the variations within each formulation, a one-way analysis of variance was done on all the populations and compiled in Table 3.2. With no added surfactant, large protein losses were observed (~85%), and only slightly bettered on the addition of PVA (75%). Similar losses to the PVA were measured when using Pluronic F68, Tween 20 and Tween 80. The addition of BSA significantly increased encapsulation efficiency (29%), although the presence of BSA, a protein itself, would have raised the corresponding reading in the BCA protein assay, complicating interpretation. The addition of Triton X-100 or Igepal CA-630 significantly increased the encapsulation efficiency to over 50%.

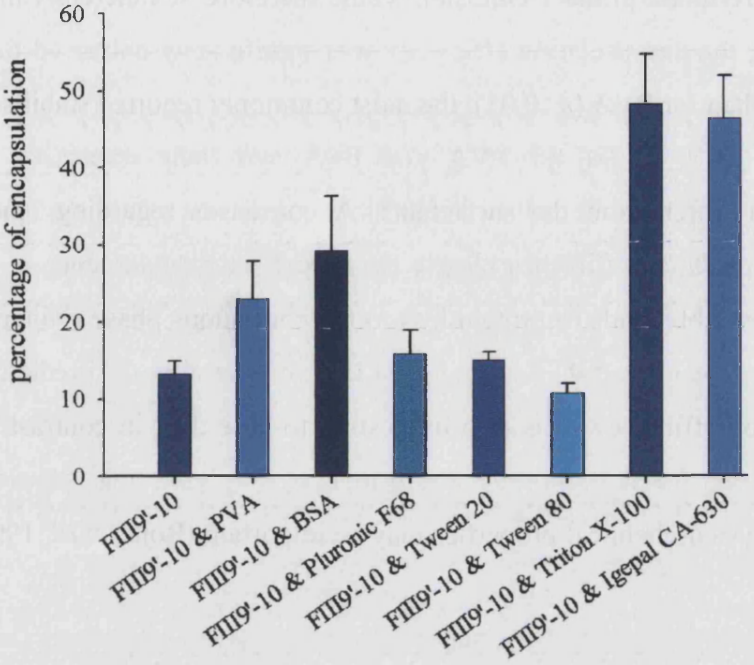

Figure 3.1. Encapsulation efficiencies for FIII9'-10 in PLGA microspheres, expressed as the percentage of the theoretical load (1.8 mg FIII9'-10 per 47.5 mg PLGA). The data represents the mean ± standard error of four independent preparations. The primary emulsion included protein and surfactant as indicated below each bar.

	No surfactant	PVA	BSA	Pluronic F68	Tween 20	Tween 80	Triton X-100
PVA	=						
BSA	#	=					
Pluronic F68	=	=	=				
Tween 20	=	=	#	=			
Tween 80	=	=	#	=	=		
Triton X-100	#	#	#	#	#	#	
Igepal CA-630	#	#	#	#	#	#	=

Table 3.2. Examination of the variations within encapsulation efficiencies of each type of microspheres. The sign '#' indicates when two formulations resulted in significantly different encapsulation efficiencies, whereas the sign '=' implies the contrary.

For the non-ionic surfactants, encapsulation efficiency could be correlated with the low hydrophile/lipophile balance (HLB) values of Triton X-100 and Igepal CA-630. All the surfactants used here have HLB values with the range (13-24) facilitating

o/w emulsion. Their hydrophilicity favours a convex curvature towards the water phase. The resultant primary emulsion would therefore be inherently unstable and yet, despite this, the encapsulation efficiency was significantly enhanced for Triton X-100 and Igepal than for PVA ($p<0.05$), the most commonly reported stabiliser. There are of course no HLB values for PVA and BSA and their respective mechanism of stabilisation differ from the surfactants. A consensus regarding emulsion stability versus encapsulation efficiency clearly must exist since coalescence of the inner water droplets inevitably leads to protein loss to the continuous phase (Nihant *et al.* 1994a), but equally clear is that surfactant HLB values are poor predictive markers of encapsulation efficiency. It is also interesting to note that, in contrast to Rojas *et al.*, the Tween's® did not improve encapsulation, implying that consideration of the protein's physico-chemical properties may be important (Rojas *et al.* 1999).

3.3.2 Size of the microspheres

Particle size was analysed by light scattering using a Malvern Mastersizer X, as detailed in section 2.3.2.3. The microspheres diameters were measured around 90 to 130 μm (Table 3.3). These were similar to previously reported values for w/o/w double emulsion (van de Weert *et al.* 2000c), although these measurements vary widely (Rojas *et al.* 1999; Yang *et al.* 2001). It is interesting to note, that the microspheres with the highest encapsulation efficiency (Triton X-100 and Igepal CA-630) yielded the largest diameter. This suggests that the presence of protein lodged within the matrix may hinder the degree of shrinkage of the polymer.

Microspheres formulations	Mode diameter (μm)
Blank microspheres	97.0 ± 14.2
FIII9'-10 alone	112.9 ± 6.2
FIII9'-10 & PVA	109.3 ± 11.7
FIII9'-10 & BSA	103.2 ± 18.4
FIII9'-10 & Pluronic F68	107.0 ± 5.8
FIII9'-10 & Tween 20	101.8 ± 15.2
FIII9'-10 & Tween 80	92.6 ± 11.5
FIII9'-10 & Triton X-100	125.3 ± 6.3
FIII9'-10 & Igepal CA-630	126.7 ± 12.3

Table 3.3. Measured microsphere diameters and their standard deviation (μm).

3.3.3 Impact on the morphology of the microspheres

Typically, the surface structure for blank microspheres, or microspheres containing FIII9'-10 alone and with PVA or BSA, was smooth and highly porous (Fig. 3.2, A, B, C, and D). The internal view brought further evidence of the porosity created by the even distribution of the small water droplets of the inner aqueous phase (Fig. 3.3). Unexpected and marked differences were observed at the surface of microsphere containing non-ionic surfactants. Inclusion of Pluronic F68 dramatically decreased the size and density of pores (Fig. 3.2, E), while the Tween's® resulted in smooth surfaces (Fig. 3.2, F and G). In addition, Tween 80 exhibited numerous cavities (Fig. 3.2, G), presumably caused by the bursting of water droplets while hardening. A surprising consequence in the use of Triton X-100 and Igepal CA-630 was the appearance of elevated surface ridges (Fig. 3.2, H and I).

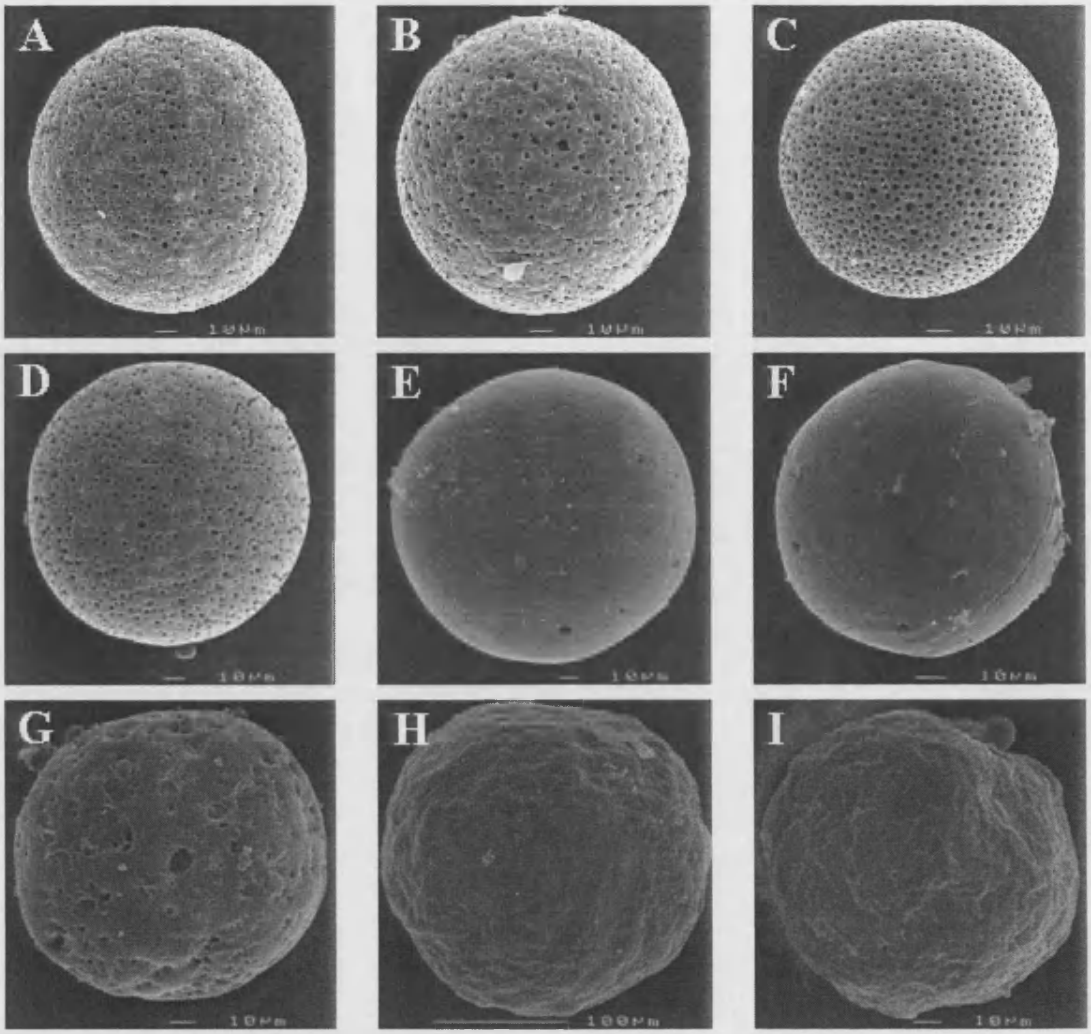

Figure 3.2. Representative SEM micrographs for microspheres encapsulating FIII9'-10 (unless 'blank') and including surfactant in the primary emulsion as indicated. A, 'blank' microsphere; B, no surfactant; C, PVA; D, BSA; E, Pluronic F68; F, Tween 20; G, Tween 80; H, Triton X-100; I, Igepal CA-630 (bar, 10 μm).

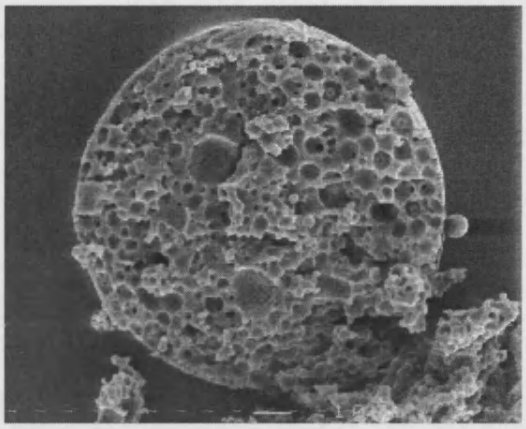

Figure 3.3. View of the internal morphology of a blank microsphere made with PBS as internal aqueous phase revealing numerous internal cavities.

Microspheres acquire their final shape and morphology while hardening during the solvent evaporation process of the secondary emulsion (Jeyanthi *et al.* 1996; Yang *et al.* 2000). Although polymer precipitation depends mostly on solvent extraction, the procedure may also be influenced by interfacial tension caused by the surfactant at the water/oil boundary. A correlation could possibly be established between loss of surface smoothness and porosity, and surfactant HLB value. When the surfactant presented higher affinity towards the water of the inner water droplets (at least HLB >15), it would be expected to weakly affect the hardening of the polymer. As a result, the microspheres would appear smooth and slightly porous. On the contrary, emulsifiers with smaller HLB value (~13) are more hydrophobic and will favour the interaction with the polymer. Under these circumstances, the extraction of the solvent could be constrained by the presence of the emulsifying agent. External morphologies evaluated against the physico-chemical characteristics of each surfactant are compiled in Table 3.4. The images obtained contribute to the support of this argument. In the case of microspheres containing Tween 80, the chaotic surface together with the poor encapsulation efficiency suggests emulsion instability.

Surfactant	HLB value	Viscosity (cps) 25°C	Surface morphology
Igepal CA-630	13.0	300	Ridged, some small pores
Triton X-100	13.5	240	Irregular, some small pores
Tween 80	15.0	400-620	Smooth but with cavities containing small pores
Tween 20	16.7	370-430	Smooth, very few small pores
Pluronic F68	>24	1000	Smooth, some small pores

Table 3.4. FIII9'-10 loaded microsphere surface morphologies compared against selected physico-chemical parameters for the non-ionic surfactants

In summary, an increase in the surface rugosity of the prepared microspheres may be related to decreasing HLB or, less so, to decreasing surfactant viscosity (Table 3.4). Although previous work has related emulsion viscosity to droplet coalescence and internal morphology (Schugens *et al.* 1994), the mechanism behind surface morphology is less clear. The absence of HLB values for PVA and BSA, and their distinct mechanisms for emulsion stabilization, make their comparison to the series of non-ionic surfactants difficult. However, since PVA was universally included during secondary emulsion, it is clear that the surfactant included in the primary emulsion was the determinant of surface morphology. To gain further information about the particles internal morphology, microtome slicing of microspheres was attempted as described by Sandor *et al.* (Sandor *et al.* 2001). Unfortunately, the microspheres proved too fragile, probably a consequence of their much larger size cf. (Sandor *et al.* 2001), and contrast between the polymer and the embedding resin was poor.

3.3.4 Examination of the *in vitro* release profiles

Protein release analysis was covered over eight weeks, with a particular attention for the first hours of incubation where a high release is generally recorded. The results obtained were added over time to obtain a cumulative representation of protein release, as seen in Fig. 3.4. Figure 3.5 presents the cumulative release of FIII9'-

10 based on the actual protein loading shown in Fig. 3.1. In Fig. 3.5, it is important to note that the microspheres made with Tweens®, PVA and Igepal CA-630 release more FIII9'-10 than expected from the encapsulation data. Such discrepancies can sometimes be expected since complete protein extraction is difficult, and protein efficiency protocols often provide underestimate actual values (Sah 1997).

In all cases, a 'burst release' profile for FIII9'-10 from the microspheres was clearly observed in Fig. 3.4 (Wang *et al.* 2002); the magnitude of the primary phase correlating with the respective encapsulation efficiency. Although all microsphere formulations gave rise to a second release phase, only the Pluronic F68 microspheres provided a phase comparable to the magnitude of its burst release (Fig. 3.4). The mechanism of burst release has been shown to occur over a period of microsphere remodelling, before an enclosed 'skin' develops over the surface preventing diffusion out of the internal matrix via surface pores (Wang *et al.* 2002). It was therefore reasoned that burst release from the sparsely porous microspheres in this study would be limited. However, this was not the case.

In order to verify that the majority of FIII9'-10 was not adsorbed on the particles surface and liberated immediately after starting incubation, FITC-labelled FIII9'-10 was encapsulated into microspheres for visualization by CLSM (Fig. 3.6). Imaging over sequential equatorial cross-sections showed FITC-FIII9'-10 coating or depositing within the internal cavities, the structure of which reflected the internal morphology seen by SEM (Fig. 3.3). No fluorescence was seen on the microsphere surface, which suggested that FIII9'-10 was indeed encapsulated entirely within, although no FITC-FIII9'-10 release characteristic was performed. Therefore, the existence of a burst release for lightly porous particles may indicate that the rate of protein release was not limited by surface pores. However, the presence of bright areas indicating high concentrations of labelled protein revealed the random distribution of the drug within the internal cavities. This uneven sharing may have facilitated burst release, if water was freely able to reach the localized areas of high protein content.

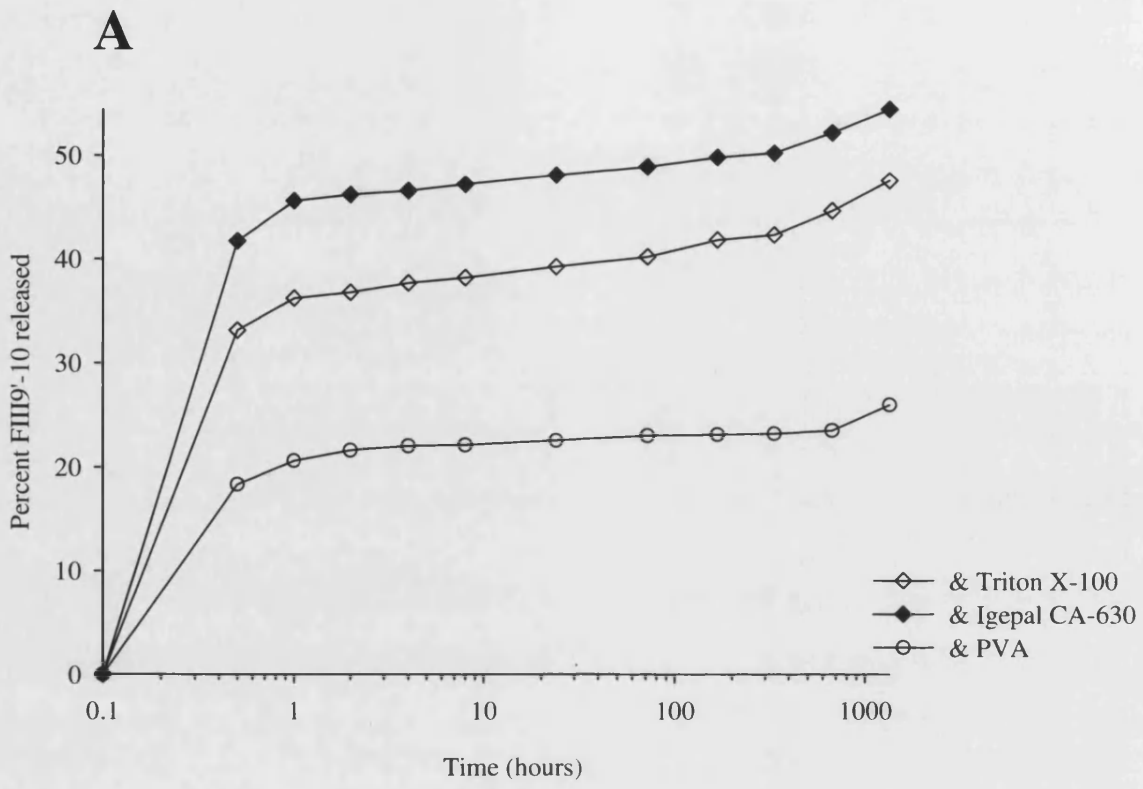
A
Percent FIII9'-10 released
50
40
30
20
10
0
0.1
1
10
100
1000
Time (hours)
& Triton X-100
& Igepal CA-630
& PVA

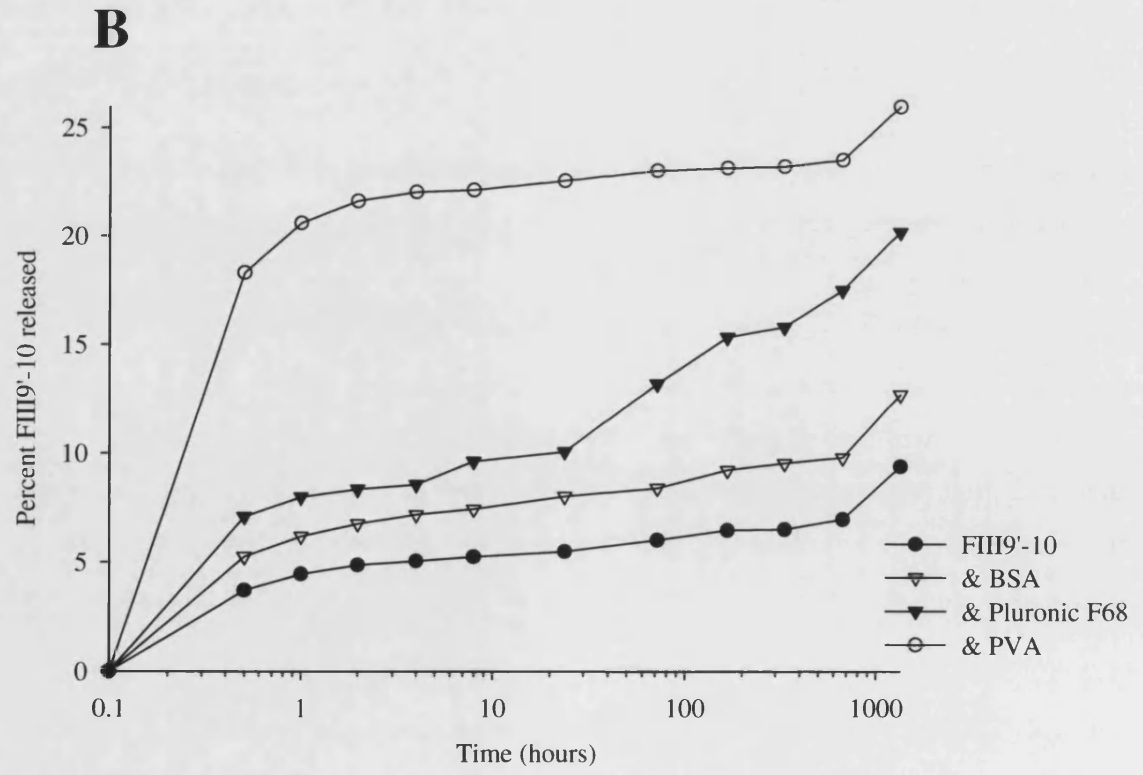
B
Percent FIII9'-10 released
25
20
15
10
5
0
0.1
1
10
100
1000
Time (hours)
FIII9'-10
& BSA
& Pluronic F68
& PVA

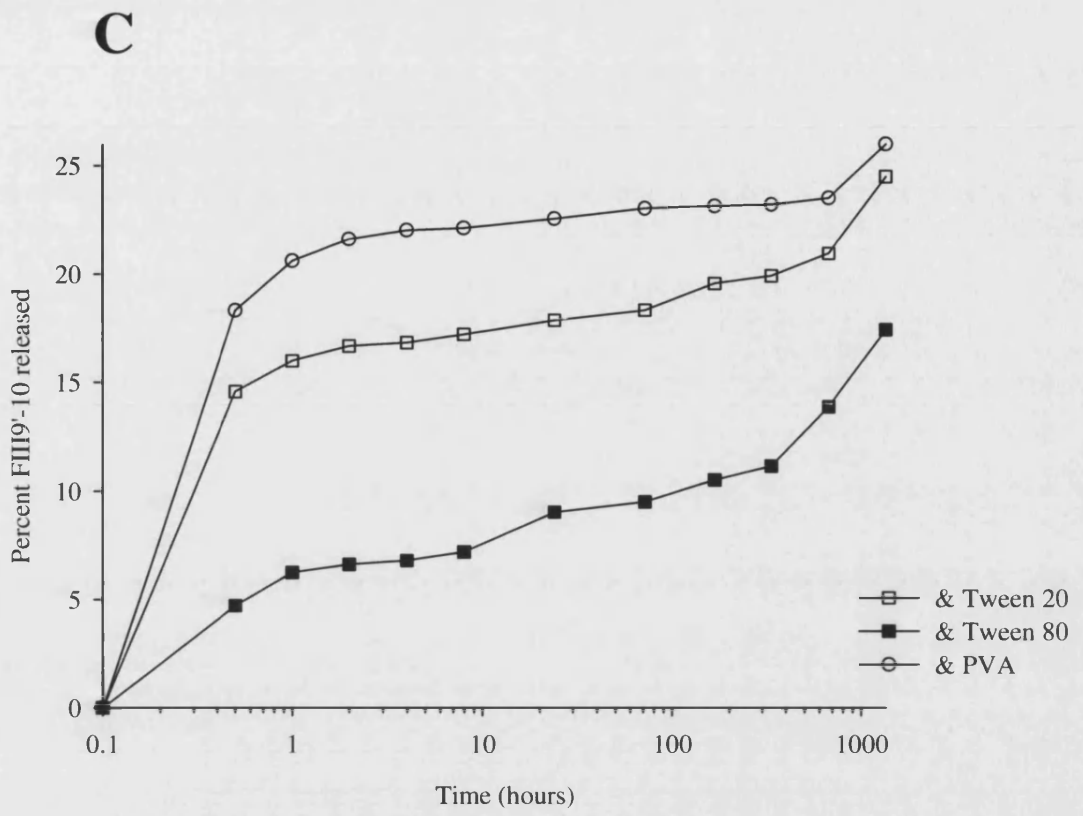

Figure 3.4. Cumulative in vitro release profiles for microspheres fabricated with different stabilisers in the primary emulsion over an 8 week period, expressed as the percentage of the theoretical load. For clarity, the measurements have been separated in three graphs keeping the cumulative release of microspheres made with FIII9'-10 and PVA as the reference between them.

A

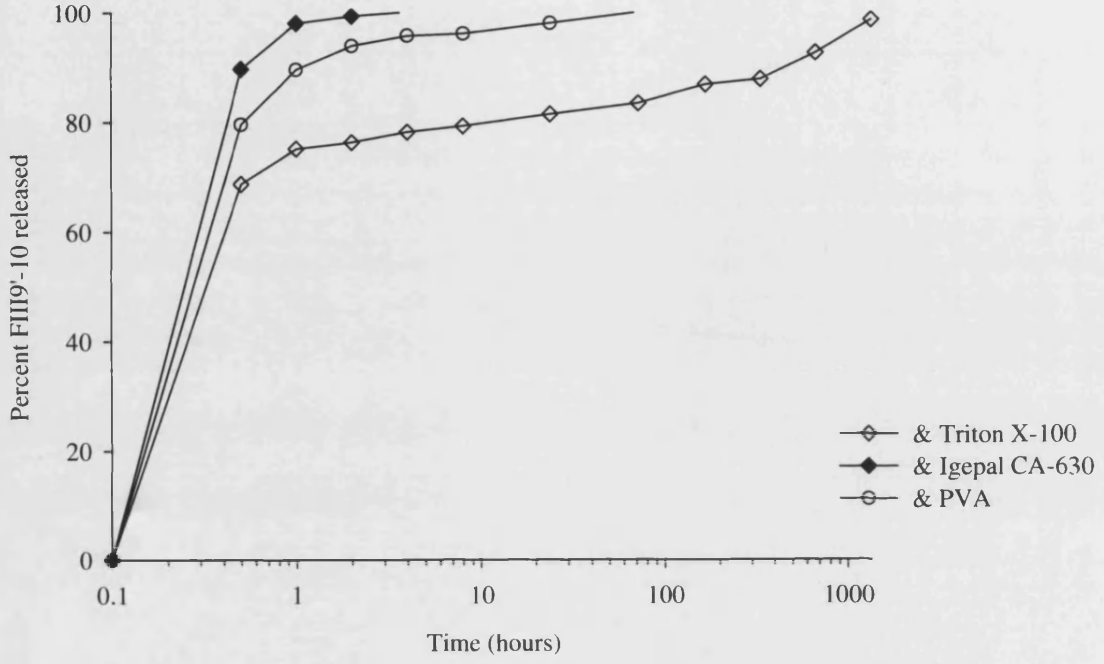
100
80
60
40
20
0
Percent FIII9'-10 released
0.1
1
10
100
1000
Time (hours)
& Triton X-100
& Igepal CA-630
& PVA

B

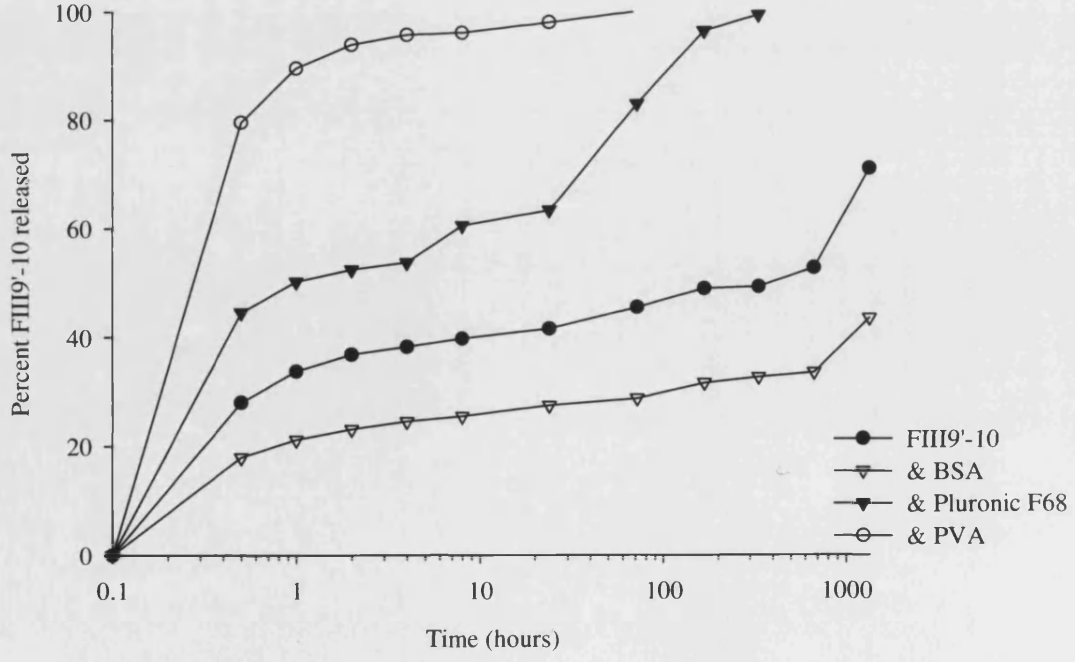
100
80
60
40
20
0
Percent FIII9'-10 released
0.1
1
10
100
1000
Time (hours)
FIII9'-10
& BSA
& Pluronic F68
& PVA

C

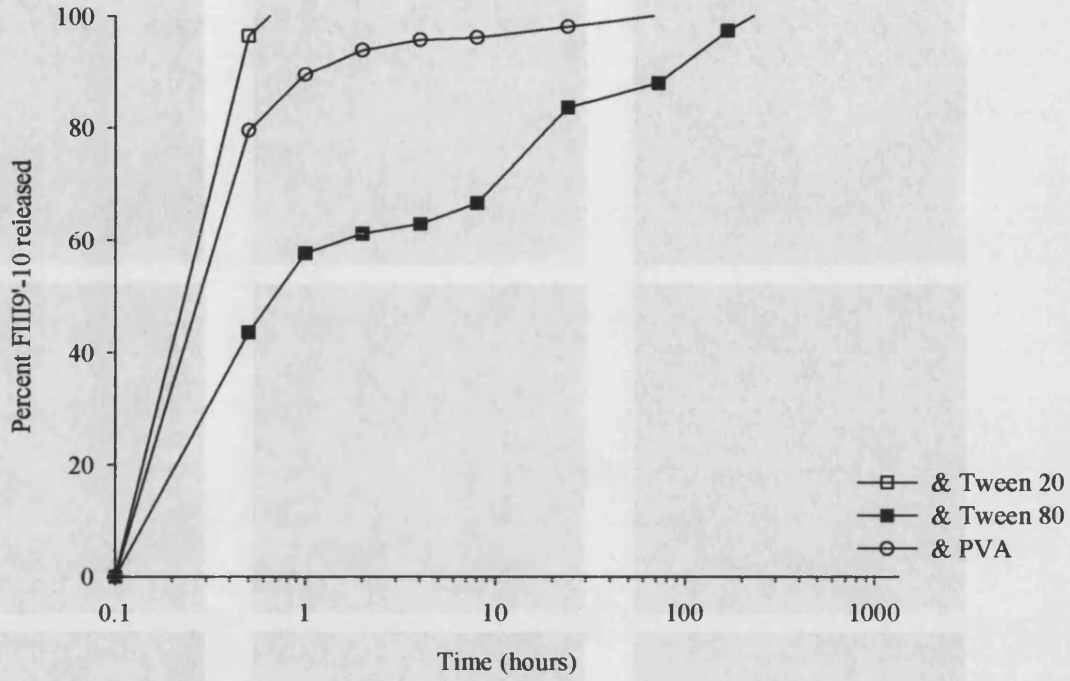

Figure 3.5. Cumulative in vitro release profiles for microspheres fabricated with different stabilisers in the primary emulsion over an 8 week period, expressed as the percentage of the actual protein loading respective to each formulation (encapsulation efficiency).

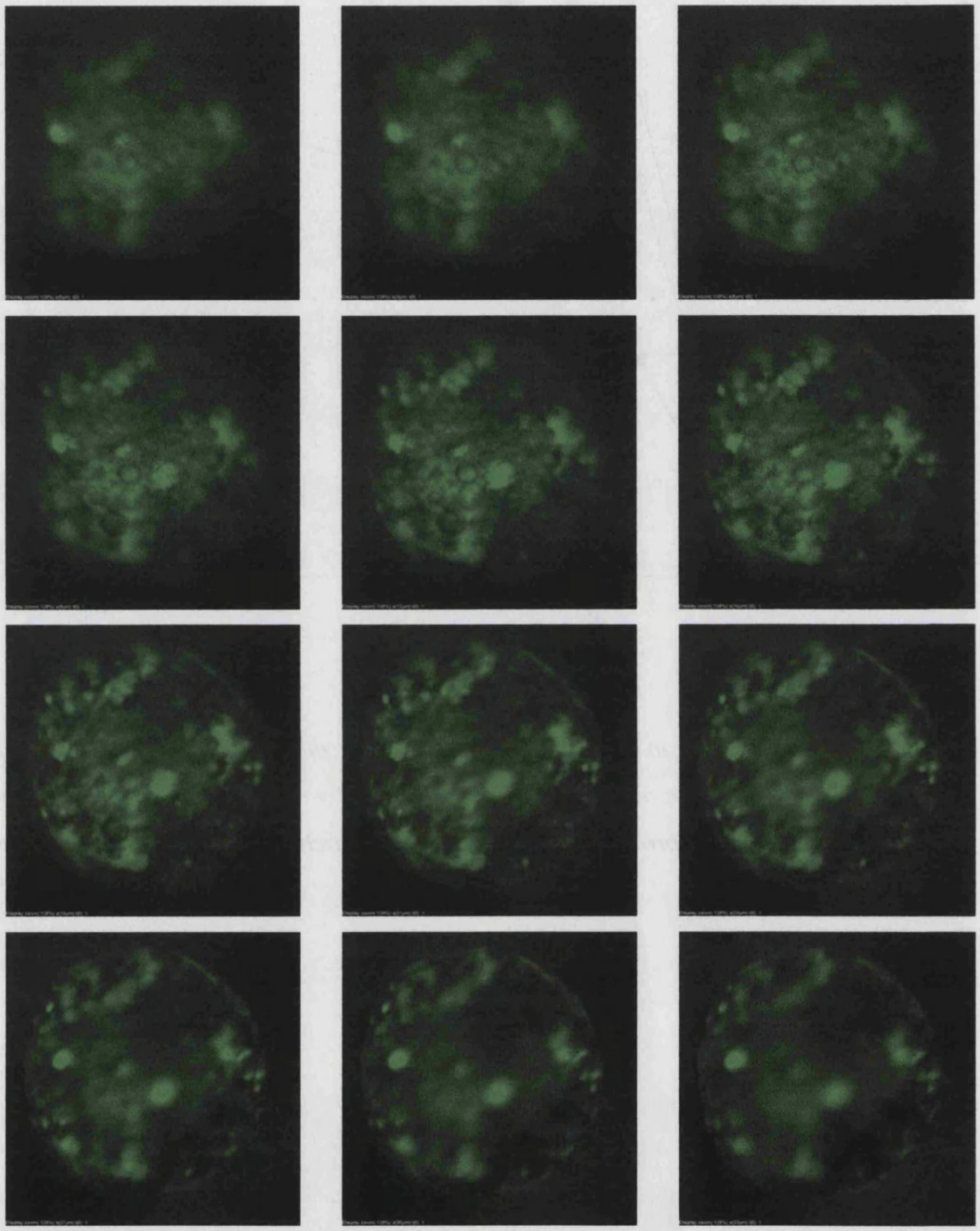

Figure 3.6. Equatorial 'slices' of 1 μm of a PLGA microsphere (~100 μm diameter) encapsulating FITC-labelled FIII9'-10 as imaged by CLSM. Light-shaded areas indicate distribution of FITC- FIII9'-10, showing outlines of, and deposition within, the internal cavities.

3.3.5 Evaluation of the FIII9'-10 biological activity

Samples of protein released after three hours incubation were tested by SDS-PAGE to assess the integrity of the peptide backbone of FIII9'-10. As seen in Fig. 3.7, all bands appeared alongside that for the purified protein and expected MW marker (loading and staining differs between surfactants). These results indicated a consistent preservation of the protein backbone for all non-ionic surfactants, BSA and PVA.

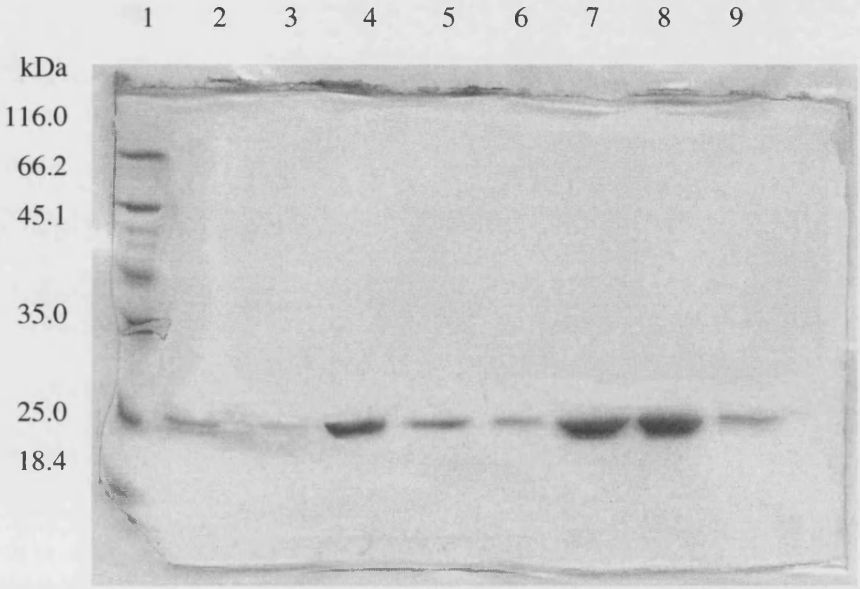

Figure 3.7. SDS-PAGE gel stained with Coomassie blue for FIII9'-10 collected from microspheres during in vitro release. Lane 1, protein marker; lane 2, Ni^{2+}-sepharose purified FIII9'-10. The following lanes describe the surfactant added during FIII9'-10 emulsification: lane 3, PVA; lane 4, BSA; lane 5, Tween 20; lane 6, Tween 80; lane 7, Triton X-100; lane 8, Igepal CA-630; lane 9, Pluronic F68.

However, maintenance of FIII9'-10 conformational integrity is equally important for $\alpha_5\beta_1$ integrin binding. It has been reported that unfolding of the less stable FIII9' domain changes the spatial relationship between RGD and the synergy sites (Van der Walle *et al.* 2002). This disruption has been demonstrated to be critical for binding activity (Altroff *et al.* 2003; Grant *et al.* 1997). To elucidate the stabilizing capacities of surfactants during microencapsulation, the biological activity of the

protein was evaluated by baby hamster kidney (BHK) cell-adhesion assay. The BHK cell attachment test was narrowed to the two most relevant surfactants, Triton X-100 and Igepal CA-630, against PVA, chosen on the basis of high encapsulation efficiencies and promising results (Fig. 3.8). Protein The released was tested after 3 hour incubation at 37°C biological activity This approach circumvented interpretation of data from analytical techniques used to study protein conformational change during emulsion with respect to protein efficacy. The BHK cell-attachment assay has been previously characterized for the elucidation of FIII9'-10 conformational integrity and mutational analysis (Grant *et al.* 1997; Van der Walle *et al.* 2002).

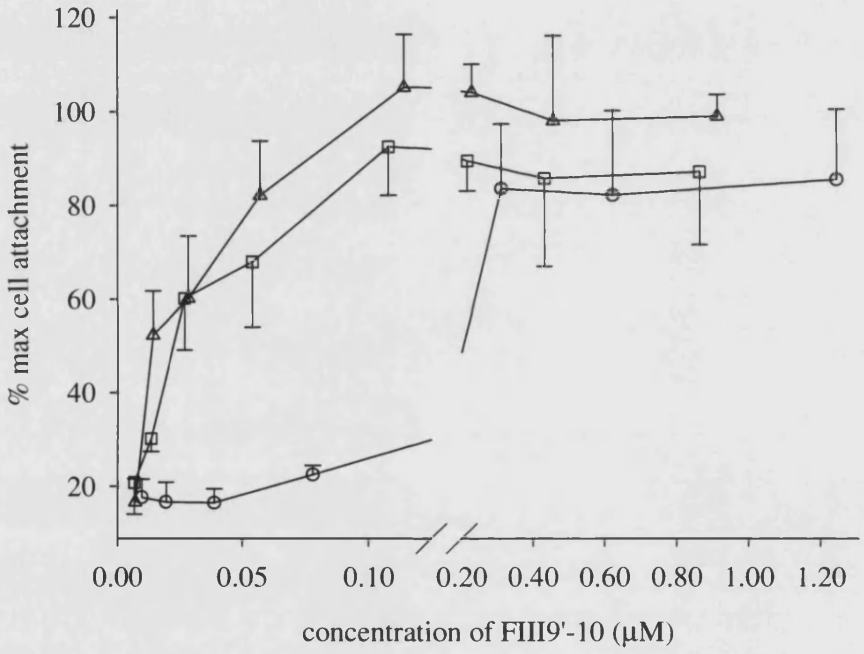

Figure 3.8. BHK fibroblast cell attachment to plastic surfaces coated with FIII9'-10 released after 3 h incubation from microspheres formulated with PVA (circle), Triton X-100 (square) and Igepal CA-630 (triangle), expressed as the percentage of maximal attachment recorded for purified (non-encapsulated) FIII9'-10 at concentrations above 1 μM.

For protein recovered from microspheres fabricated with Triton X-100 and Igepal CA-630, cell adhesion increased in accordance with the protein concentration. Moreover, the cell-attachment percentages were near-equivalent to the cell-adhesion

obtained for purified FIII9'-10 (positive control) (Fig. 3.8). For FIII9'-10 recovered from microspheres fabricated with PVA, the cell-attachment activity dropped unexpectedly to around a third of that for purified FIII9'-10 for concentrations <0.3 μM. The difference in the mean percentage attachment for PVA and Igepal CA-630/Triton X-100 was significant below 0.3 μM ($p<0.05$). The mean for Triton X-100 appeared slightly less than equivalent concentrations of Igepal CA-630, but this difference was not significant ($p>0.05$).

The shift in the curve for PVA, with respect to Triton X-100 and Igepal CA-630, may imply that a greater proportion of the released FIII9'-10 population did not bind the $\alpha_5\beta_1$-integrin with maximal affinity. Possibly, the protein experienced a greater degree of unfolding wherein the spatial organization between the synergy site and RGD site was perturbed. For Triton X-100 and Igepal CA-630, the curves are similar to previously reported attachment data for FIII9-10, with attachment 60–70% of the maximum at 0.05 μM and a plateau above 0.2 μM (Altroff *et al.* 2001). However, for Triton X-100, attachment at concentrations >0.3 μM was 80–90% of the positive control, indicating that a small proportion of the FIII9'-10 population might also have experienced unfolding. In summary, the activity of the FIII9'-10 domain was not or only slightly altered by the manufacturing process for Igepal CA-630 and Triton X-100 respectively, but was lowered for PVA.

3.4 Conclusions

The encapsulation efficiency for FIII9'-10 was increased to 50–60% when using Igepal CA-630 or Triton X-100 in comparison to a rise of 25% for PVA. Unfortunately, the use of HLB as a predictor of protein encapsulation was weak, since any such influence was masked by many other factors, not least the protein itself. However, microsphere morphology did vary in accordance with the HLB values of the surfactants, possibly by alteration of the solvent evaporation process. In particular, microspheres made with Igepal CA-630 and Triton X-100 resembled an 'asteroid' with the appearance of surface ridges. Such surfaces may be useful in the development of microspheres with reduced contact area for improved dispersion and flow.

Low surface porosities did not affect the diffusion of FIII9'-10 from the microspheres' internal pores in a 'burst release', as may have been imagined. FIII9'-10 released from microspheres promoted cell attachment in a concentration-dependent manner. The fact that only Igepal CA-630 and Triton X-100 maintained near-maximal cell attachment indicated that the conformation of the relatively unstable FIII9' domain was preserved. In effect, of the two domains, FIII9' is conformationally more unstable ($\Delta G_{(H2O)}$=7.2 kcal/mol cf. $\Delta G_{(H2O)}$=13.0 kcal/mol for the FIII10 domain (Van der Walle *et al.* 2002)) and would be expected to be involved in any unfolding event imposed on FIII9'-10 in the event of adsorption at the w/o interface during emulsification. However, FIII9'-10 supported a level of cell attachment near-equivalent to the positive control when recovered from microspheres fabricated with Igepal CA-630 or Triton X-100, but not PVA. In addition, SDS-PAGE indicated no change to the backbone integrity. Therefore, the loss of biological activity could be accountable to conformational changes, which were especially prevalent during emulsification with PVA. In summary, PVA should not necessarily be the 'first choice' as the primary w/o emulsion stabiliser for protein encapsulation. Instead, non-ionic surfactants should be considered, particularly for the maintenance of biological activity of conformationally labile proteins during encapsulation.

Chapter 4

Visualisation of the release of encapsulated protein and concomitant morphological changes

4.1 Introduction

The utility of PLGA microspheres has been built over characteristics such as low toxicity, biodegradability, good drug compatibility (Kitchell & Wise 1985; Mathiowitz *et al.* 1997). Over the years, therapeutic compounds have been formulated via microencapsulation as listed in Chapter 1 Table 1.1 (Cleland *et al.* 1997; Perez *et al.* 2002). Although advantages were offered by PLGA encapsulation, the difficulty of controlling drug release was repeatedly reported. In fact, only a few studies have been fully dedicated to this problem, despite it being central to drug release systems. This likely reflects the complexity in understanding the mechanisms behind water penetration and drug diffusion in microspheres. In particular, the burst release phenomenon still remains to be investigated conclusively. However, rapid release is appropriate for some delivery systems; examples are listed in Table 4.1. In general, the

burst release phenomenon is undesirable and its attenuation has been sought. The most promising techniques involve either applying the physico-chemical characteristics of the polymer, or physical hindrance through surface pores via surface coating (Lee *et al.* 2002). With regards to the former, modifications of the polymer backbone have been used to alter the matrix structure, drug distribution, polymer degradation and drug/polymer interaction (Pistel *et al.* 2001).

Situations conducive to burst release from microspheres	Situations inappropriate for burst release from microspheres
♦Wound treatment (immediate relief followed by a diminishing need for drug)	♦Local, systemic toxicity or irritation arising from high drug concentrations
♦ Pulsatile delivery in vaccination	♦Elimination of drugs with a short half-life *in vivo*
♦Targeted delivery followed by a triggered burst release	♦Economically and therapeutically wasteful of drug
♦ Encapsulation of flavours (organoleptics in the food industry)	♦Shortened release profile (require more frequent dosing)

Table 4.1. Applications wherein burst release may be advantageous or detrimental (Huang & Brazel 2001).

Unfortunately, existing techniques developed to attenuate burst release include additional costly steps such as polymer grafting, and even then may not ensure a predictable or controllable release (Pistel *et al.* 2001). Consequently, research must aim to properly understand the drug release mechanism. In an attempt to fulfil this objective, new methods of study have here been designed to visually examine the drug release correlated to morphological changes in microspheres. In these investigations, particles were fabricated with the same stabilisers and methodology as described in the previous chapter. Briefly, FIII9'-10 with and without PVA, BSA, Pluronic F68, Tween 20, Tween 80, Triton X-100, Igepal CA-630, was added to the primary emulsion, and after homogenisation transferred to a hardening tank containing PVA (secondary emulsion). Particles were harvested and lyophilised as before. Microspheres were subjected to cryo-fracture SEM in order to visualise their internal morphology.

Microsphere external morphology was also observed by normal SEM following incubation in aqueous buffer over time. The external and internal morphologies were correlated to the protein release, visualised in real time using CLSM for microspheres loaded with FITC-labelled FIII9'-10 (without surfactant) at 37°C.

4.2 Methods

4.2.1 Internal morphology by cryo-fracture SEM

A cup-shaped sample holder was filled with a suspension of microspheres in distilled water and covered by a thin rectangular sheet of scratched aluminium. The sample holder aperture was sealed by anchoring each end of the aluminium rectangle to a piece of sticky carbon adhesive disc. The whole apparatus was turned upside down to avoid the microspheres sinking to the bottom of the sample holder, and then plunged into slushy nitrogen. As quickly as possible, the sample holder was introduced into the cryo-preparation chamber attached to the SEM (JEOL JSM6310 SEM). The cryo-preparation chamber maintained the sample under vacuum at a low temperature (-165°C). The scratched aluminium rectangle was then removed with a cooled blade causing fracturing of the ice at the sample surface. The sample was then transferred into the SEM chamber and onto a cold stage at -170°C. The sample was observed at low kV while the stage temperature was raised to -80°C to allow the ice to slowly sublime and the fractured microspheres to be revealed. Transferred back into the preparation chamber, the microsphere sample was sputter coated with a thin layer of gold for 3 min and finally returned to the SEM chamber where images were obtained at 10 kV.

4.2.2 Real time observation using CLSM and microwells

Microspheres with FITC-labelled FIII9'-10 without surfactant in the primary emulsion were fabricated as described in section 2.3.1. The microspheres were immobilised in microwells for real time observation by CLSM. Microwells were micromachined, as shown in Fig. 4.1, into a 10 mm square polycarbonate ('Cobex') piece at the Laser Micromachining Centre, Institute of Bioelectronics & Molecular Microsystems, University of Wales, Bangor, UK. Three cubic wells of 150 μm square were maintained in sink conditions by inlet and outlet channels on either side of each well.

A single microsphere (ca. 100-150 μm diameter) was placed manually in each of the three wells, covered and sealed with a coverslip and plasticine. The microchannels were connected to a needle and a peristaltic pump, and fed with fresh PBS buffer, warmed to 37°C. CLSM imaging was performed as described in section 2.3.3.1. The polycarbonate device was left in a solution of 50% ethanol for five minutes between each use in order to wash away any residual protein or particulates.

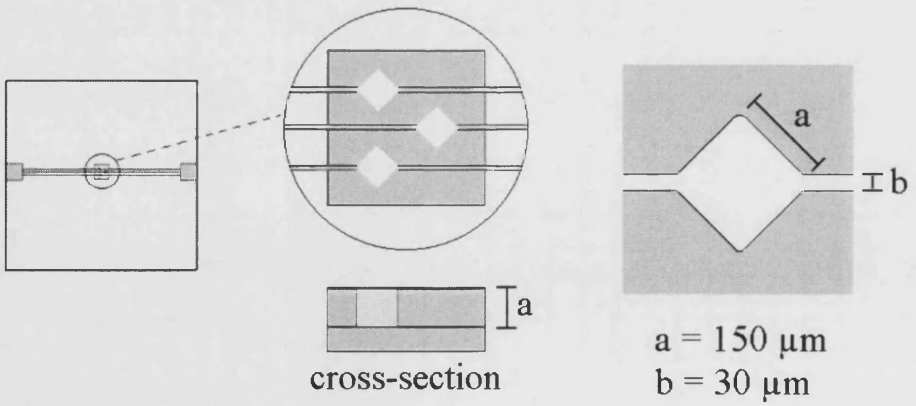

Figure 4.1. Sketches of the polycarbonate piece where each of the three cubic microwells are connected to microchannels on either side. The channel's depth is equivalent to the cube's side (a=150 μm).

4.3 Results and discussion

4.3.1 Examination of the internal morphology of microspheres

Sandor *et al.* demonstrated that the internal structure of the microparticles influences the release mechanism for microspheres with high loadings wherein protein diffusion follows the high density of interconnecting channels (Sandor *et al.* 2001). Other workers have used this hypothesis as a means to explain the release profiles they observed in their study (Blanco & Alonso 1998; Kim & Park 2004a). It is indeed reasonable to believe that a dense inner labyrinth of cavities and channels will enhance the time necessary for the drug to reach an exit hole, whereas few big cavities are more likely to provide an easy and fast access to outer pores. According to Florence *et al.*, the internal morphology is dependent on the stability of the primary emulsion of the w/o/w solvent extraction method (Florence & Whitehill 1981). Three categories of internal structure have been defined as microsphere, multivesicular structure, and microcapsule as illustrated in Fig. 4.2.

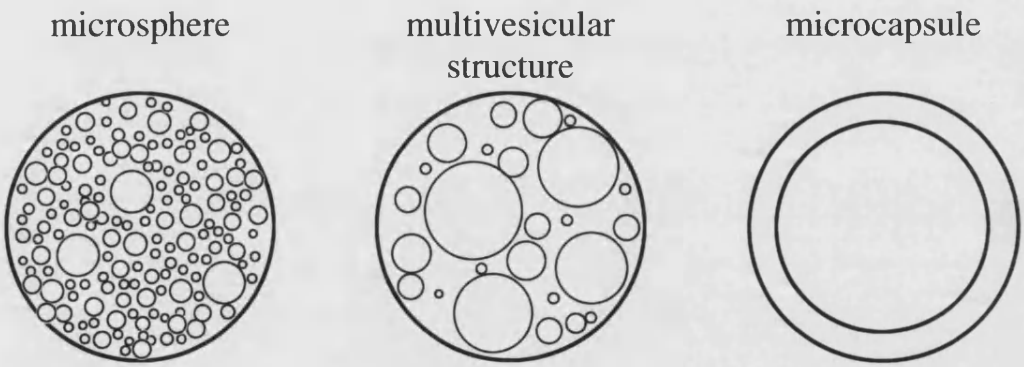

Figure 4.2. Illustration of the three main types of internal structure for particles fabricated via w/o/w solvent extraction method (Florence & Whitehill 1981).

'Microspheres' may be defined by numerous internal cavities interconnected or not (Fig. 4.2). In this case, a highly stable primary emulsion is necessary to retain its conformation and resist the mechanical stresses applied throughout the secondary emulsification. If a less stable primary emulsion is used, the weaker interface promotes the coalescence of the inner water droplets. A non uniform size distribution of inner cavities is evidence of poor primary emulsion stability. This typically defines the structure as 'multivesicular'. Finally, very unstable primary emulsions lead to complete coalescence of water droplets, forming a single large cavity occupying the full space of the particle called 'microcapsule'.

Since the internal morphology may affect drug release, all microparticles (blank, FIII9'-10-loaded with and without stabilisers) were subjected to cryo-SEM. This novel method enables arbitrary fracture of particles embedded in ice and was found to be highly efficient with respect to microtome sectioning. Representative images of fractured particles are shown in Fig. 4.3. For each formulation, the microparticles were sorted in Fig. 4.4 according to the classification proposed by Florence *et al.* (1981). Table 4.2 compiles the classification from Fig. 4.4 since a couple of formulations have led to the development of more than one type of inner structure.

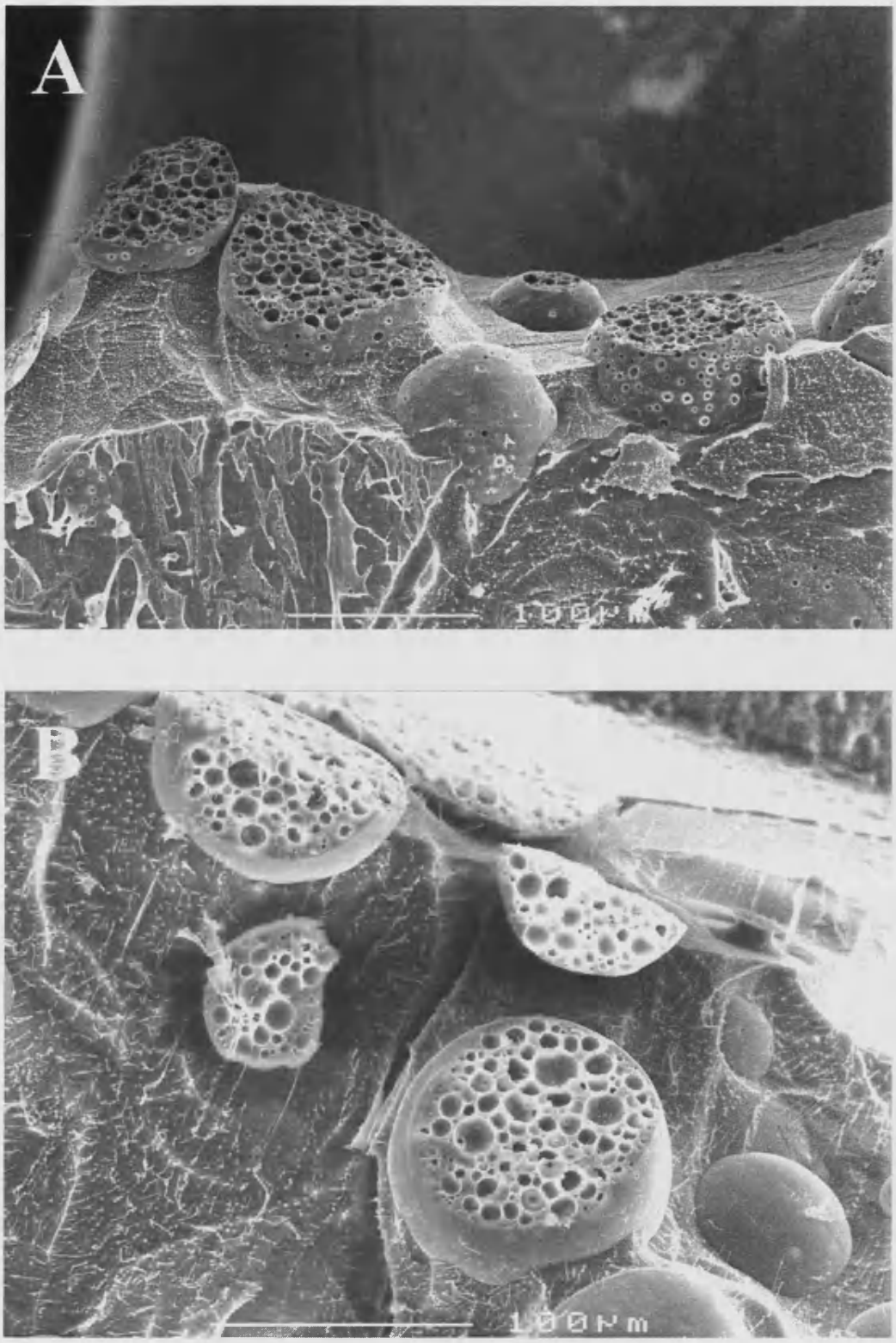

Figure 4.3. Images of cryo-fractured microspheres containing FIII9'-10 with BSA (A), and FIII9'-10 with Triton X-100 (B). The random fracture provides an exceptional

collection of sections of the particles offering to sight apex, latitudinal and equatorial regions. Note that the internal morphology can be clearly distinguished from the ice.

The cryo-SEM analysis suggested that the stability of the primary emulsion varied with surfactant type added. However, defining a trend between the physico-chemical parameters of the surfactants added and microsphere internal morphology was complicated by the use of non-ionic surfactants and triblock copolymers. For instance, microparticles made with either Pluronic F68 or Igepal CA-630 exhibited a multivesicular structure even though Pluronic F68 has a much higher HLB value (>25) than Igepal CA-630 (~13).

The internal morphologies observed contrasted against the trend suggested in Chapter 3 Table 3.4 where surface rugosity was reported to enhance with a decrease in surfactant HLB values. This could be due to the heterogeneous mechanism of solvent extraction. In effect, during the secondary emulsification, the surface of the microparticles is formed instantly, whereas the internal structure materialises at the pace of solvent extraction-evaporation. The slow precipitation of internal regions allows for coalescence to take place if the stability of the inner water droplets can not be sustained. Subsequently, the external morphology may represent polymer imprinting by the stabiliser or surfactant, whereas the internal morphology may reflect interfacial stability within the time frame allocated by the PLGA hardening process.

HLB values should not be relied upon for the selection of non-ionic surfactants for use in microencapsulation. This factor may help in predicting the stability of more simple emulsions, but it has been proven to be irrelevant in this case. A recent study by Mohamed *et al.* shows additional evidence of contradiction between emulsion stability and inner morphology (Mohamed & van der Walle 2006). It is also suggested that results are likely to be specific to the formulation parameters, and therefore, differences are to be expected from one formulation to another even when subtle changes are made.

Microparticles formulation (primary emulsion)	Inner structure classification (Fig. 4.4)
Blank microspheres	microsphere
FIII9'-10	microsphere
FIII9'-10 & PVA	microsphere
FIII9'-10 & BSA	microsphere
FIII9'-10 & Pluronic F68	multivesicular structure
FIII9'-10 & Tween 20	microsphere, multivesicular structure, microcapsule
FIII9'-10 & Tween 80	microsphere, microcapsule
FIII9'-10 & Triton X-100	microsphere
FIII9'-10 & Igepal CA-630	multivesicular structure

Table 4.2. Variety of internal morphologies obtained with respect to the primary emulsion formulation, and analysed by cryo-SEM images from Fig. 4.4.

Finally, the internal morphologies were compared against the *in vitro* release data presented in Chapter 3 (Fig 3.4). It was found that none of the three types of structure could be correlated to a particular release profile. In addition, a burst release was observed for all particles regardless of their inner morphology. These findings would appear to contradict previous data by Sandor *et al.* suggesting a delay or attenuation of burst release with differing internal morphologies. For the microspheres fabricated here, the internal structure was not the predominant factor controlling drug release. However, it is important to note that the size and drug encapsulated between this and other studies are very different, highlighting the important of a case-by-case analysis and not applying 'universal' rules.

Microsphere		
	Blank microspheres	FIII9'-10
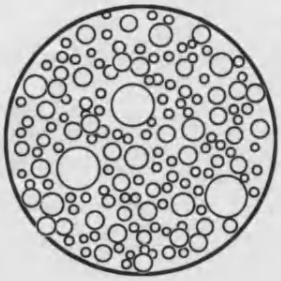	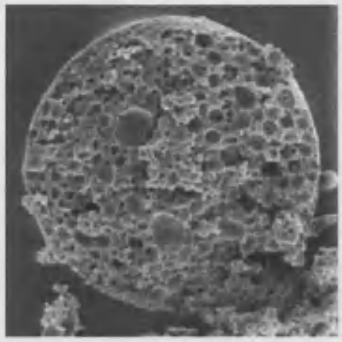	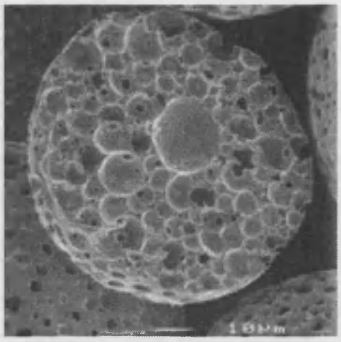
FIII9'-10 & PVA	FIII9'-10 & BSA	FIII9'-10 & Tween 20
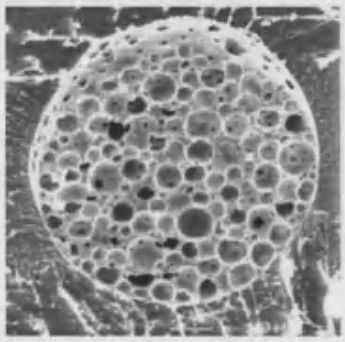		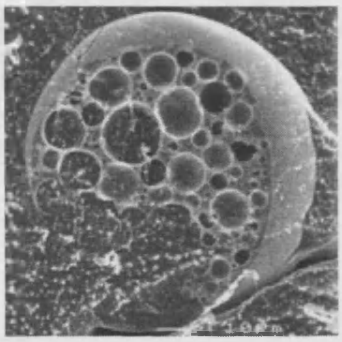
FIII9'-10 & Tween 80	FIII9'-10 & Triton X-100	
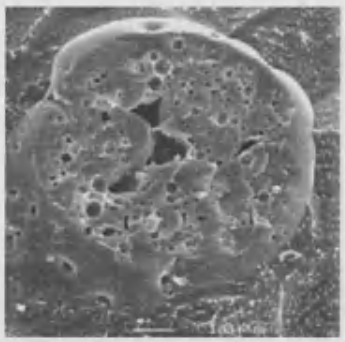	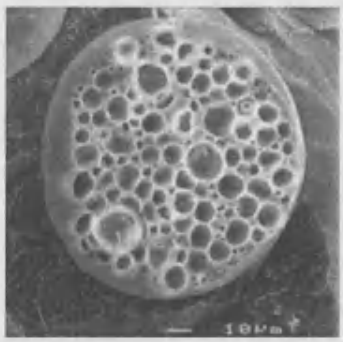	

Multivesicular structure

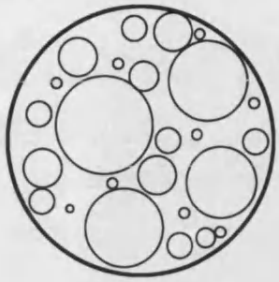

FIII9'-10 & Pluronic F68

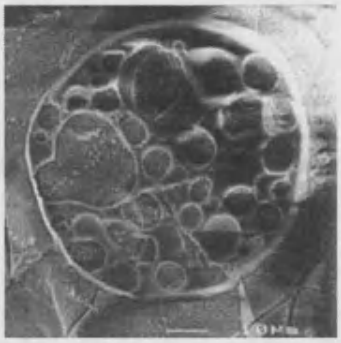

FIII9'-10 & Tween 20

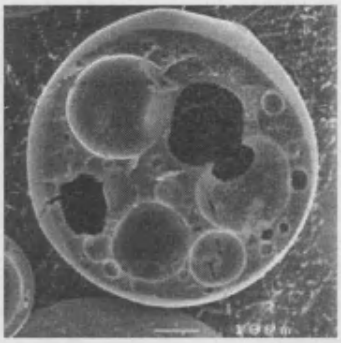

FIII9'-10 & Igepal CA-630

Microcapsule

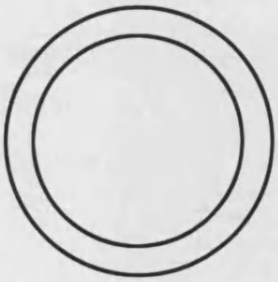

FIII9'-10 & Tween 20

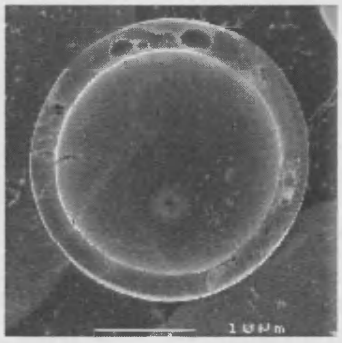

FIII9'-10 & Tween 80

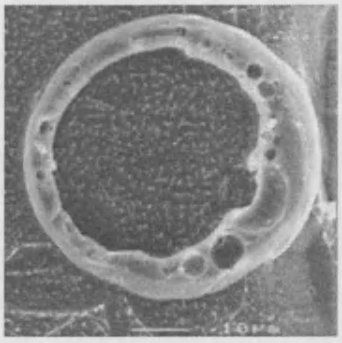

Figure 4.4. Fractured particles imaged by cryo-SEM and grouped by type of internal morphology in accordance with the classification proposed by Florence et al.: microsphere, multivesicular structure, and microcapsule (bar: 10 μm).

4.3.2 Transformation of surface morphology during incubation

Considering the passivity of the internal structure upon protein release, it was considered that the external surface may play a central role in the drug release profile. In order to reproduce the chain of events that presumably influence the particle surface, microspheres fabricated with FIII9'-10 (but without surfactant) were incubated as described during an *in vitro* release protocol (Chapter 2.3.5.3). After removal at the predetermined time points, the microspheres were air-dried and imaged by SEM. The change to microsphere surface morphology could then be monitored with time, as shown in Fig. 4.5.

A transformation of the surface structure persistently took place over time, with a particular emphasis within the first hour of incubation. The ridges covering the entire surface of the dried microspheres disappeared within 30 minutes of incubation (Fig. 4.5). This surface smoothing has been previously described and suggested to be due to the swelling of the PLGA matrix upon hydration (Schlapp & Friess 2003). While water penetrated the channels of the polymeric matrix, chain elasticity presumably counterbalanced the pressure created by the rapid intake of water. Inherent flexibility may accommodate stretching of the outer surface eventually erasing surface ridges within a surprisingly short time. The magnitude of the response could have been predicted due to the additional effects of elevated temperature and plasticization of water. Temperatures above the glass transition temperature of the amorphous polymer are known to greatly enhance the polymer chain mobility (*Tg* of PLGA microspheres fabricated was 29.9°C < 37°C). Also, the plasticizing action of water will facilitate PLGA hydrolysis and further decrease the microspheres' *Tg* as the polymer chains shorten.

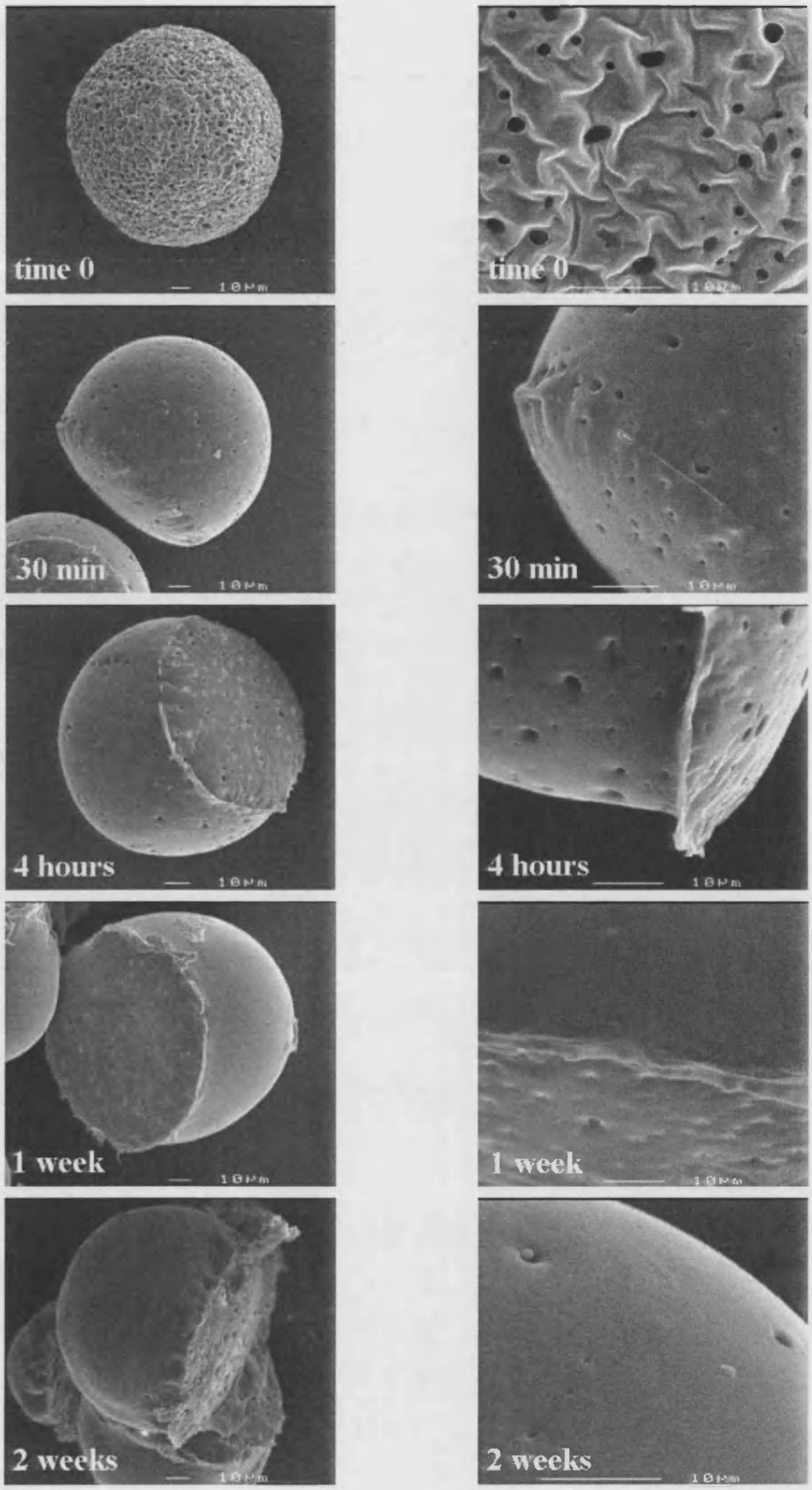

Figure 4.5. Visual examination of the surface changes over time for microspheres containing FIII9'-10 alone and maintained under typical in vitro release conditions. The pictures on the left show an overview of the spheres' morphology. The images on

the right reveal details of the surface. The times indicated on the bottom-left corners correspond to the duration of incubation. 'Time 0' microspheres were imaged immediately after lyophilisation.

Surface remodelling was most evident for those particles which floated in the aqueous buffer and presented the particularity of having one portion exposed to the air, and a second exposed to the water. In effect, surface alteration was localised to region directly in contact with water. The 'cap' emerging from the water could be easily distinguished from the lower section of the particles as it would conserve the original surface morphology of lyophilised microspheres.

From the submerged region of the microsphere, the surface displayed a smoothing effect with a progressive diminution in size and presence of external pores. This may have been due to surface swelling and PLGA chain mobility. However, near complete closure of the pores was decisive between four hours and one week incubation (Fig 4.5). At the same time, a film linking the floating particles developed at the air/liquid interface, as shown in Fig 4.6. It is difficult to unambiguously characterise the nature of this film by visual examination only. It was thought that the film could consist of either surface protein or polymeric residues homogeneously bridging the 'caps' of the floating microparticles. In the latter case, the film would be indicative of a high degree of molecular mobility among polymeric fragments and external PLGA chains. During this process, exit holes may have been remodelled to near disappearance.

This assumption is not incompatible with that by Wang *et al.*, who observed a similar closure and loss of external pores within the first 24 hours of incubation (Wang *et al.* 2002). They suggested that the pores were obstructed from within by PLGA fragments from polymeric degradation. This would require free diffusion of degradation products immediately after immersion. However, numerous studies investigating the mechanisms of polymer degradation and erosion demonstrate that PLGA microspheres degrade via bulk erosion (Burkersroda *et al.* 2002; Husmann *et al.* 2002). This phenomenon is characterised by a delay in mass loss, which would contradict the interpretation by Wang *et al.*

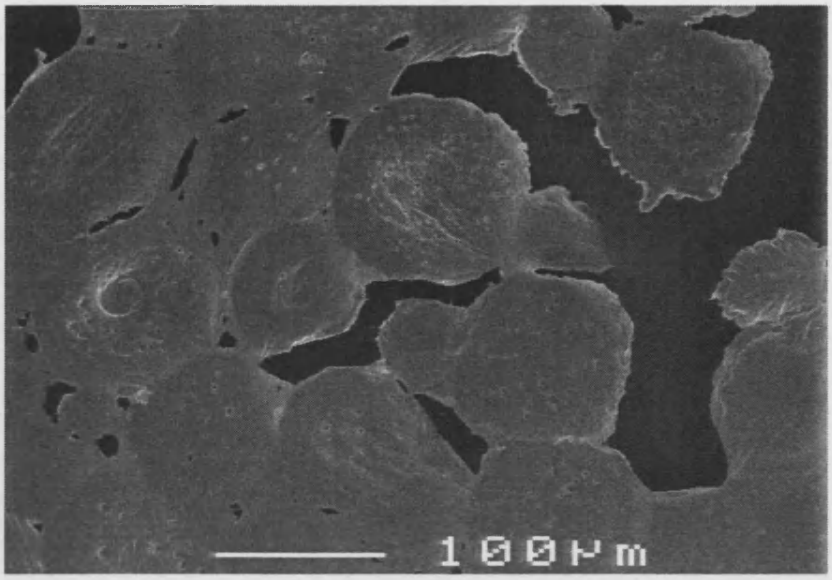

Figure 4.6. View from above of the polymeric film linking the 'caps' of floating microspheres containing FIII9'-10 alone after one week of incubation.

It is important to note that surface remodelling never led to complete disappearance of external pores. Therefore, diffusion of water/drug between the bulk microspheres interior would still be possible, although physically restricted. In order to evaluate the corresponding water and drug mobility during microsphere immersion, the SEM images were compared against the protein release as shown in Fig. 4.7. A complicating consideration here was that it was difficult to undoubtedly correlate the reduction of number of exit holes with a decrease in protein release since the encapsulated drug reservoir was itself lost during release. However, it seems reasonable to believe that the quantity of exit pores should determine the protein diffusion rate.

This assumption has been recently examined by Ethezazi *et al.* who demonstrated via computational simulation that limited access contributed in obtaining a first order release rate (Ehtezazi *et al.* 2000). Following on from this model, the microspheres formulated here with Tween 20, Tween 80, Triton X-100, and Igepal CA-630 should have experienced a longer and slower protein release, since these microspheres exhibited small or few external pores (Chapter 3, Fig. 3.2). However, all of these formulations displayed a burst release profile (Chapter 3, Fig. 3.4). In order to understand the survival of the burst release, microsphere surface analysis was conducted after 30 minute incubation. The images compiled in Fig 4.8 showed that all

surfaces were perforated. In the case of the particles fabricated with Tween 20, Tween 80, Triton X-100, and Igepal CA-630, this porosity would appear to have been sufficient to allow for the initial burst release to proceed. A more thorough understanding of the release mechanism versus control by external porosity was therefore sought and real time observation of protein release was conducted.

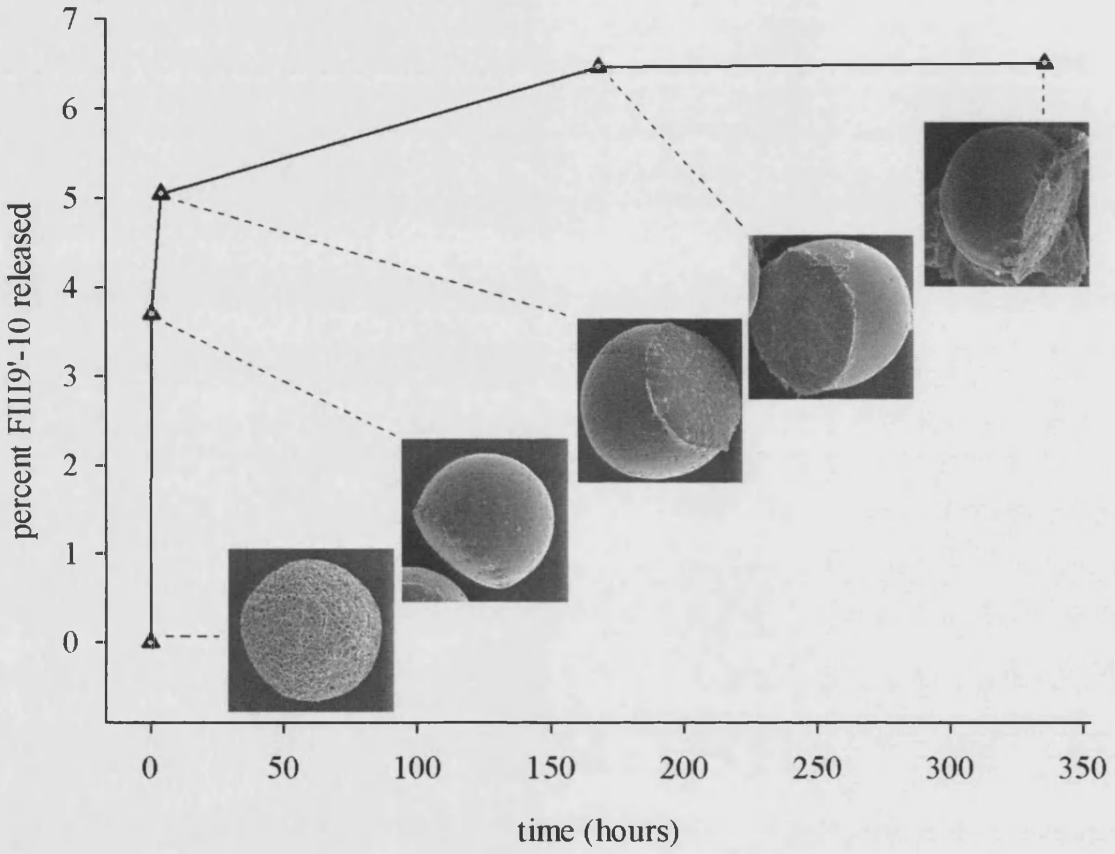

Figure 4.7. Evolution of the protein release with respect to the external morphology of microspheres containing FIII9'-10 without surfactant and maintained under similar in vitro release conditions.

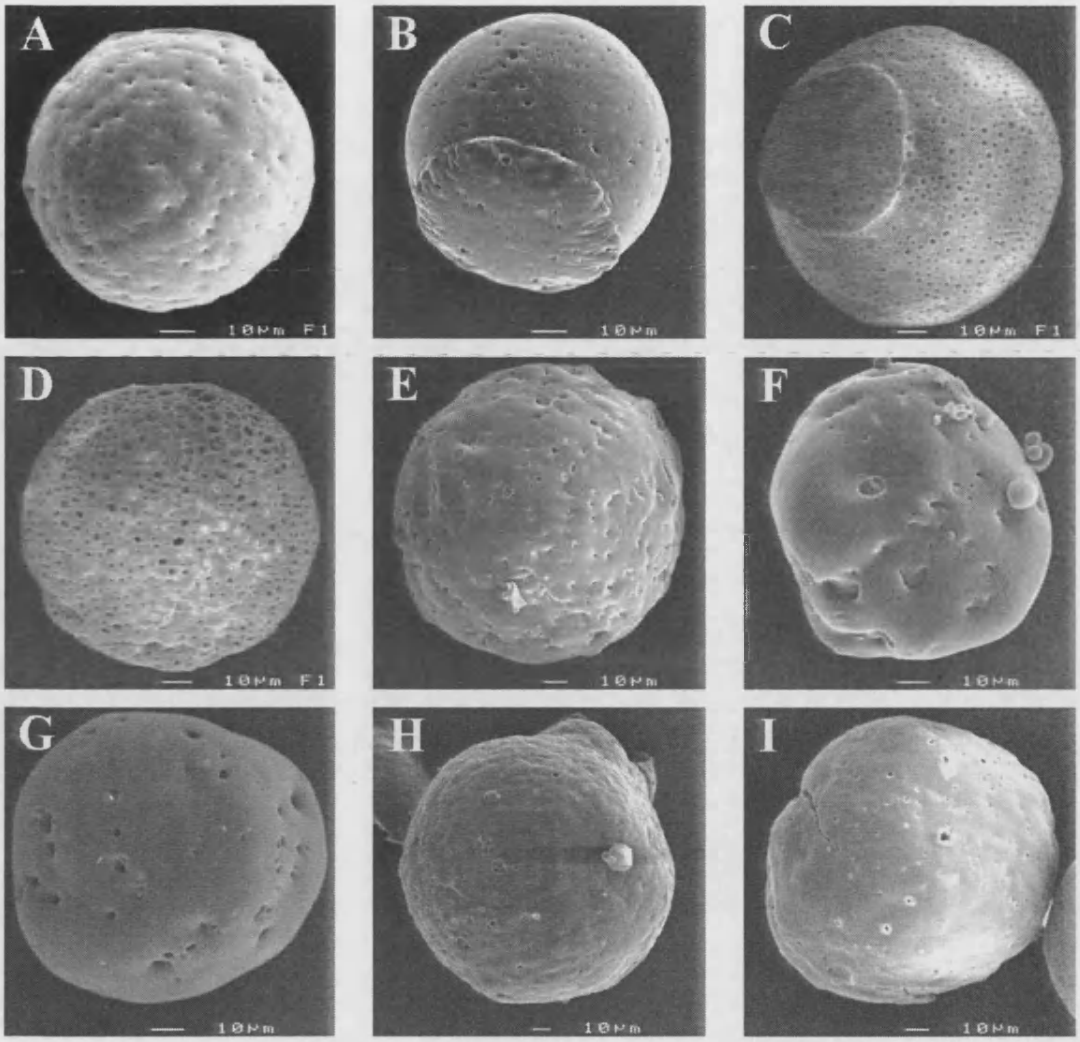

Figure 4.8. External morphology of all microspheres after 30 minute incubation at 37°C. All microparticles were loaded with FIII9'-10 unless blank (A). Surfactant or stabiliser were added to the primary emulsion as indicated: B, no additional surfactant; C, PVA; D, BSA; E, Pluronic F68; F, Tween 20; G, Tween 80; H, Triton X-100; I, Igepal CA-630.

4.3.3 Real time observation of protein release

Studies of protein release are generally based on the analysis of the solution of incubation. In order to build a more accurate picture of the release phenomenon, real time observation was operated via CLSM imaging for microspheres immobilised in microwells and loaded FITC-labelled protein. This novel device was designed to

ensure sink conditions during continuous imaging. Although this technique was useful for the observation of release of a small organic compound in a study led by Messaritaki *et al.*, it appeared that the nature of the drug loaded played an important role in the quality of the pictures obtained (Messaritaki *et al.* 2005). In the present work, the main difficulty consisted in the fluorescence generated on the walls of the wells. It was thought that tagged proteins had adsorbed to the polycarbonate walls of the wells during release, thereby complicating image analysis as demonstrated in Fig. 4.9. Clear visualisation of protein release failed even with prior wash of the microwells in ethanol. In addition, a mirroring effect from the walls impeded distinction between proteins still encapsulated and protein released.

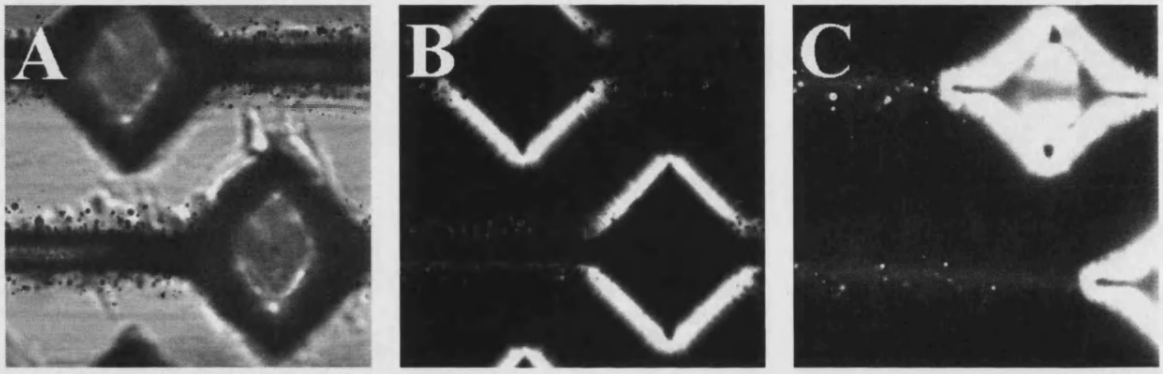

Figure 4.9. Representative microscopic view of the microwells (A), and comparative confocal imaging of empty wells (B) with wells occupied by a single microsphere loaded with FITC-labelled FIII9'-10 (C). Images interpretations were complicated due to the fluorescence generated on the walls of the empty wells (B) added with the walls' mirroring effect (C).

An alternative technique was therefore used where a few microspheres were sprinkled onto a normal glass slide which was then mounted on a thermo-sensed slide holder generating a constant temperature of 37°C. The microspheres were then submerged in PBS warmed to 37°C. The addition of PBS was designated as time zero for the experiment. In order to keep the microspheres immobilised in one place for imaging, no buffer was added or removed during imaging. Therefore ideal sink conditions could not be maintained and may have influenced the data. Nevertheless, protein release was recorded over 65 minutes; Fig. 4.10 showing cross-section images

(1 μm thick slices) of the apical (a), latitudinal (b) and equatorial (c) regions of the same microsphere over time.

Time 0

a b c

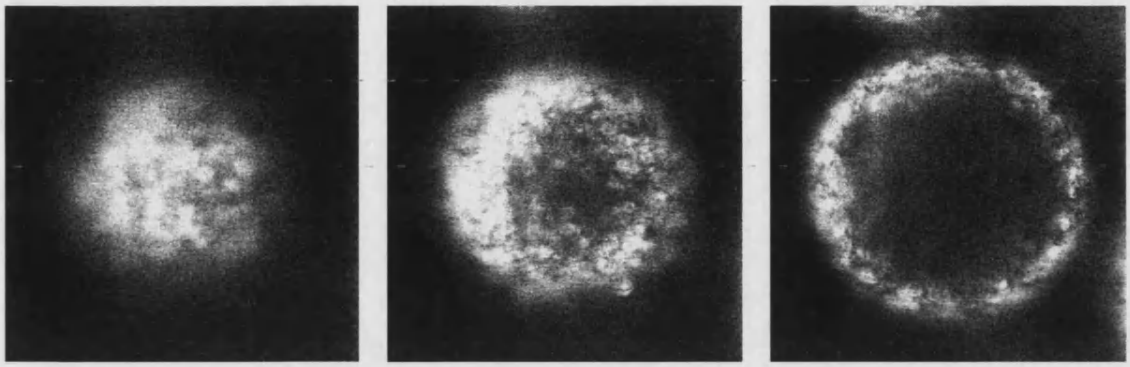

After 5 minutes

a b c

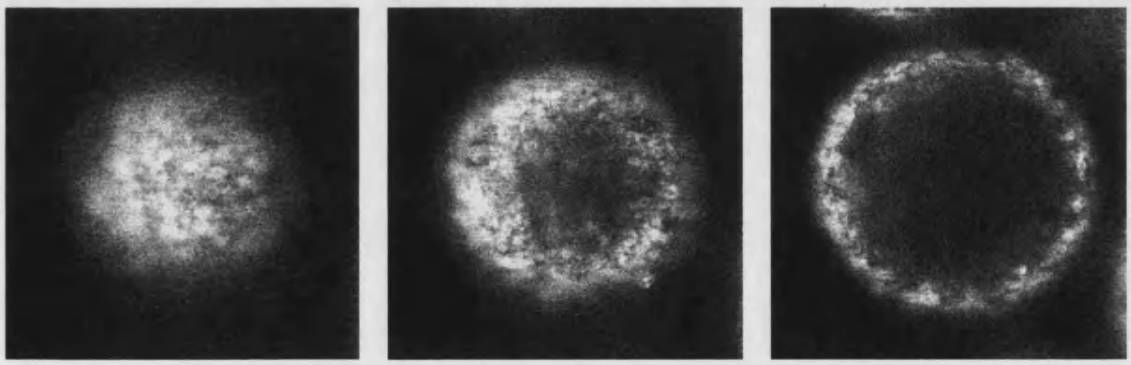

After 10 minutes

a b c

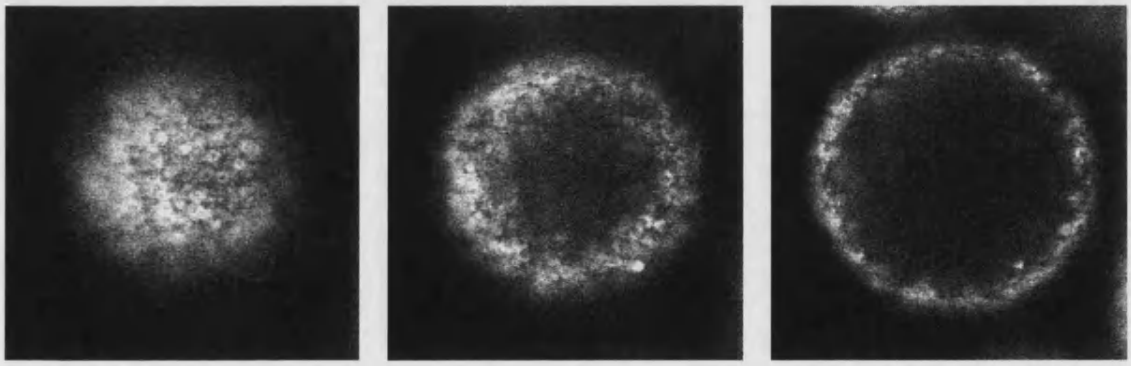

After 20 minutes

a b c

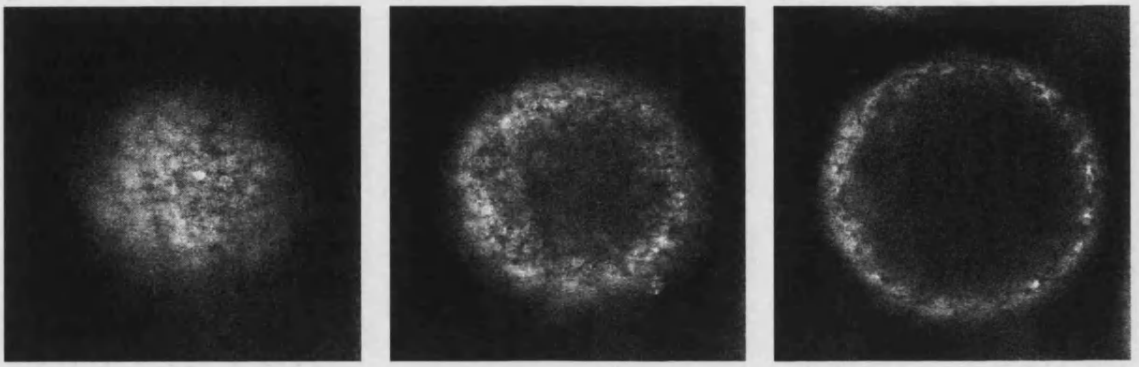

After 30 minutes

a b c

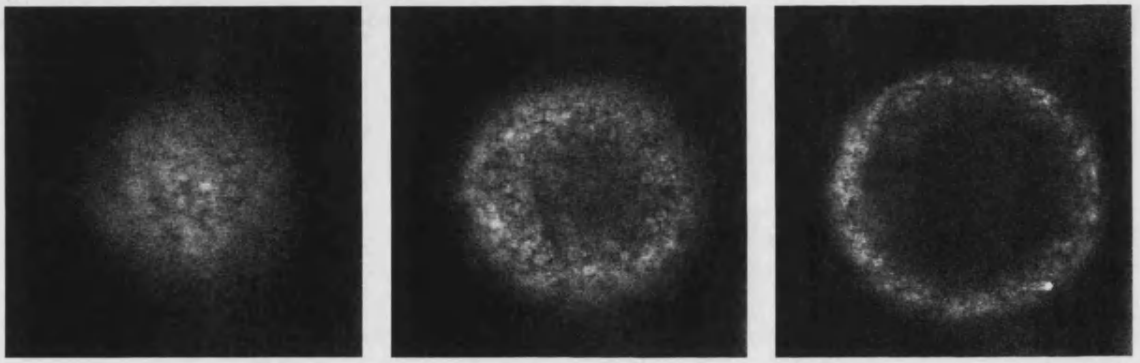

After 40 minutes

a b c

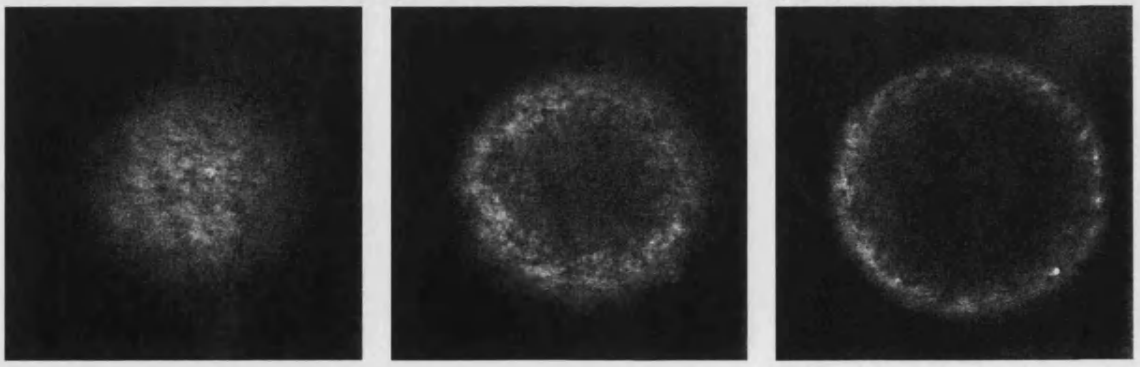

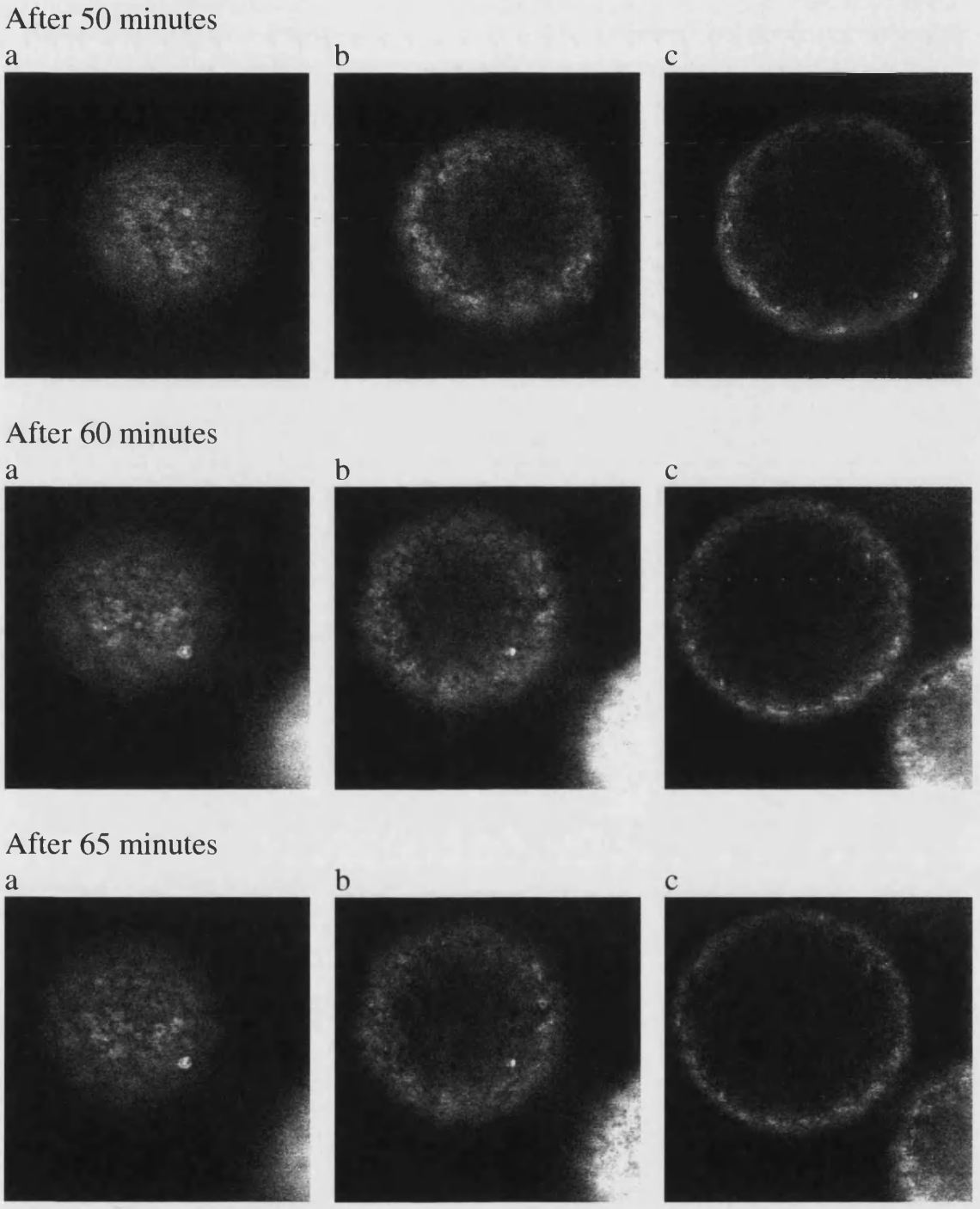

Figure 4.10. Real time observation of FITC-labelled FIII9'-10 release during incubation in PBS at 37°C over 65 minutes (a: apical section; b: latitudinal section; c: equatorial section).

Initial images (time zero) showed a heterogeneous distribution of protein. Regions of higher fluorescence intensity may indicate higher protein concentrations, although this technique is only semi-quantitative and calibration was not performed. Nevertheless, over the 65 minute incubation, the fluorescence faded considerably suggesting loss of encapsulated protein. The protein loss seen over this period may represent the burst release seen *in vitro*, this protein fraction being soluble and noticeably mobile. Clearly, a degree of fluorescence remained following 65 minute incubation and may either correspond to protein entrapped in the internal pores, or within the PLGA matrix, or insoluble (aggregated protein). To distinguish between either three of the possibilities would have required extension of observation to around 4 hours, when the release plateau is observed *in vitro*. Unfortunately, this was not practicable. Also, considering the static nature of the immersion here, a more rapid release profile may be anticipated *in vivo* wherein clearance of released drug would maintain sink conditions.

4.4 Conclusions

Visualisation of microsphere morphology was used to gain further understanding concerning the mechanisms of protein release, particularly the initial burst release. The internal morphology analysed by cryo-SEM contrasted against *in vitro* release profiles obtained previously in Chapter 3 such that no correlation could be discerned. Internal morphology did not influence the burst release phenomenon. However, SEM and cryo-SEM imaging did show the influence of emulsion stabilisers upon microsphere morphology. A decrease in the emulsion stability of the primary emulsion yielded a shift from 'microsphere', to 'multivesicular structure', to 'microcapsule' classification of the interior. Unfortunately, the HLB values of the surfactants could not predict the integrity of the primary emulsions during hardening. Probably, the secondary emulsification of the w/o/w technique comprises additional stresses which may affect considerably the stability of the emulsions.

Although the internal structure could not circumvent the initial burst release, real-time confocal imaging showed that burst release was due to drug mobility and

accessibility to the release medium, and therefore controlled by the external porosity. Unfortunately, while protein release declined following the first hours of incubation, this could not be correlated unambiguously to closure of the external pores observed via SEM imaging. The disappearance of exit pores was accompanied by an overall smoothing of the microsphere surface. Surface remodelling was probably a result of PLGA chain mobility induced by temperature elevated above the *Tg* of the microspheres, and the plasticization effect of water. The molecular rearrangement did not however lead to total collapse of the spherical structure. This fundamental property of amorphous PLGA polymer could be exploited as a means to reduce surface porosity without additional costly steps often necessary to prevent the initial burst release.

Chapter 5

The influence of surfactant on PLGA microsphere glass transition and water sorption

5.1 Introduction

The addition of surfactant to the primary emulsion of the w/o/w solvent extraction process has proved in some cases to have beneficial effects (van de Weert *et al.* 2000b) but in others to be detrimental, or have no effect (Deng *et al.* 1999). There is a paucity of research dedicated to dissecting the underlying molecular interactions between surfactant and drug/PLGA in microsphere formulations. One reason may be the difficulty in elaborating appropriate protocols when working at a sub-micron scale. However, it is possible to assess the overall physical properties of PLGA microspheres and indirectly determine the effects of the surfactant.

The mobility of the PLGA chains in their glassy state (Li *et al.* 1995) will depend on how any additive, either drug or surfactant, interacts with the polymer during solvent evaporation and following lyophilisation. In order to characterise the

amorphous nature of the polymer and to investigate its physical properties, the glass transition temperature, *Tg*, becomes a critical parameter. The examination of the mechanical stability of microspheres at increasing relative humidity is also important in the assessment of shelf-life storage times. Since water is known as a plasticizer for amorphous polymers such as PLGA, the result of storage at high relative humidity may directly influence microsphere morphology. The ability to controllably reduce the number of exit pores at the microspheres surface would be of considerable interest with respect to control of drug release. Wang *et al.* also showed that after 24 hours immersion in water, a 'skin' may envelope the outer surface of the microspheres (Wang *et al.* 2002). The concomitant loss of external pores was suggested to result in the subsequent termination of the period of burst release. In a similar manner, it seems reasonable that the closure of surface pores will attenuate drug release. Shaping the microsphere surface subsequent to fabrication-lyophilisation, however, may provide a more novel route.

In this study, FIII9'-10 was encapsulated with PVA and Triton X-100 as stabilisers of the primary emulsion. The objective was to investigate the influence of water vapour and surfactant molecules on the mechanical integrity of amorphous PLGA microspheres. The storage stability of microspheres was challenged through exposure at ambient humidity and 75% relative humidity, and the parameters influenced by the residual amount of surfactant determined. Vapour sorption was utilised to investigate and demonstrate the hydrophilic nature of each particle formulation. The physical and mechanical stability of the polymer were subsequently tested to reveal PLGA chain mobility using DSC. Surface modifications caused by chain flexibility were expected and pore reduction was examined by atomic force microscopy (AFM). Topographical imaging of the surface of microspheres maintained at increasing relative humidity provided an insight into the plastic nature of the PLGA. Protein location and distribution within microspheres exposed to high humidity was verified with CLSM. Finally, the potential of surface remodelling with respect to controlling burst release was investigated and discussed.

5.2 Methods

5.2.1 Storage at selected humidity

Samples of microspheres were exposed to humidity following the protocol detailed in section 2.3.4.1. The saturated salt solutions were selected to obtain relative humidities of 75% and 93% when left at room temperature. Sodium chloride and potassium nitrate were used to prepare the saturated salt solutions of 75% and 93% relative humidity, respectively (O'Brien 1948).

5.2.2 Atomic force microscopy (AFM) imaging under controlled environmental condition

Atomic Force Microscopy surface topographical images were recorded in TappingMode™ operation as described in section 2.3.2.2. In order to maintain the sample at required humidity, the optical head was sealed off from the ambient environment. Controlled partial vapour pressures were introduced into the chamber through an in-let tubing while a humidity probe deeply inserted recorded the relative humidity during scanning. It was ensured that neither tubing nor probe would interfere with the piezoelectric tube or the reflected laser beam. The starting relative humidity was set to 20% and increased progressively to 40%, 55% and 70% relative humidity while imaging surface remodelling. At each step, the particles were allowed to equilibrate for 4 h, although real-time recording enabled to determine that surface transformations would cease after the first 20 minutes.

5.2.3 Visualisation by CLSM of protein distribution in microspheres exposed to high humidity

FITC-labelled protein was encapsulated without surfactant in PLGA microspheres as detailed in section 2.3.3.1. Immediately after lyophilisation, a few microspheres were evenly sprinkled onto glass slides, and the initial distribution of the labelled protein was observed with confocal microscopy as described in section 2.3.3.1. The same slides were then kept at 93% relative humidity for 1 and 24 hours, and the protein was again localised by confocal imaging. The even spreading of the polymeric particles was necessary to avoid irreversible microsphere aggregation, which would render visualisation difficult.

5.3 Results and discussion

5.3.1 Sizes of microspheres

The mode diameter of the microspheres ranged from 97.0 μm to 125.3 μm diameter as presented in Table 5.1. As already noted in Chapter 3, the addition of Triton X-100 in the internal water phase led to the formation of larger microspheres. Possibly, this change resulted in a high viscosity of the primary emulsion, and therefore larger droplet size, as previously reported in the literature (Yang *et al.* 2001).

Microsphere formulations	Mode diameter (μm)
Blank microspheres	97.0 ± 14.2
FIII9'-10 alone	112.9 ± 6.2
FIII9'-10 and PVA	109.3 ± 11.7
FIII9'-10 and Triton X-100	125.3 ± 6.3

Table 5.1. Size distribution measurements of microspheres (± standard deviation).

5.3.2 Evolution of microspheres hydrophilic properties

The change in mass of a sample upon water uptake is a highly sensitive way of investigating the hydrophilic nature of materials as well as the type of water vapour-material interaction (Buckton & Darcy 1996). Moisture sorption profiles for microspheres containing FIII9'-10 with and without surfactant in the primary emulsion are shown in Fig. 5.1. The profiles in Fig. 5.1 show no discernable differences between blank microspheres and microspheres containing FIII9'-10 alone over all relative humidities tested. The water sorption-desorption profile for microspheres containing PVA and FIII9'-10 was poorly discernable from blank and FIII9'-10-containing microspheres until a relative humidity of 95% was reached. On the other hand, the profile for microspheres containing Triton X-100 and FIII9'-10 was noticeably different above a relative humidity of 45%. Considering that the diameter size of all particles did not vary significantly, the hydration capacity could not be correlated to surface area. This suggested that microspheres containing Triton X-100, and to a lesser extent PVA, within the PLGA matrix were as a consequence more hydrophilic and readily hydrated.

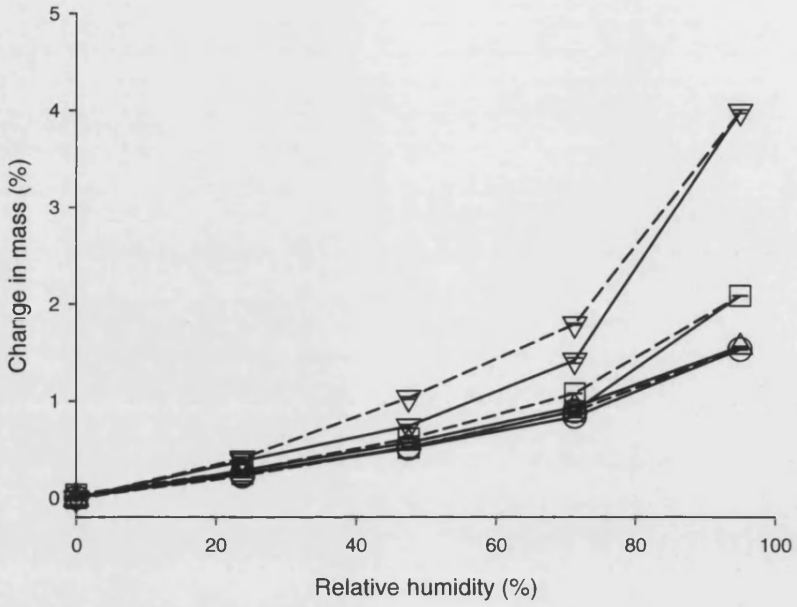

Figure 5.1. Change in mass of microspheres over increasing relative humidity. The water uptake was recorded during sorption (solid lines), and the water loss was inversely sampled during desorption (dotted lines). Symbols: microspheres containing PBS (circles), FIII9'-10 (up triangles), FIII9'-10 and PVA (squares) and FIII9'-10 and Triton X-100 (down triangles). Error bars (smaller than symbols) represent the standard deviation.

It is known that stabilisers, when used in the continuous phase of the secondary emulsion, adsorbs on to the microsphere surface or diffuses in the microparticles (Coombes *et al.* 1998; Shakesheff *et al.* 1997). Despite washing prior to lyophilisation, it is very difficult to completely remove the PVA coating (Sahoo *et al.* 2002). In the case of PVA added to the internal aqueous phase, it is reasonable to expect that PVA also coats the inner cavities and/or pore exits within the polymer matrix. Other groups have also suggested that PVA chains penetrate the PLGA matrix (Boury *et al.* 1995). This will be discussed further in relation to DSC data. While DVS data cannot predict the extent of PVA penetration throughout the PLGA matrix, a homogenous distribution of PVA within PLGA seemed unlikely given their respective physical properties. Ultimately, the total amount of PVA remaining on/in the microspheres only increased water uptake at high relative humidities.

In contrast, Triton X-100 appeared to increase the hydrophilicity of the microspheres more readily, with a change in mass for these microspheres being around

4% at 95% relative humidity (cf. the corresponding percent change in mass for microspheres containing PVA and FIII9'-10, FIII9'-10, and blank microspheres, of 2, 1.5, and 1.5%, respectively). The small molecular size of Triton X-100 (625 Da) compared to PVA may enable its greater infiltration of the PLGA network. Moreover, the PEO headgroup of Triton X-100 is known to be miscible with PLGA (Chung *et al.* 2002). It would not be surprising then that the washing steps did not completely remove the surfactant.

The mode of water vapour-microsphere interaction was revealed by the hysteresis for loss of mass in response to decreasing relative humidity. Microspheres containing no surfactant showed almost no hysteresis (Fig. 5.1 and Table 5.2). It can be argued that water diffusion and mobility in the amorphous PLGA is dependent on the water-PLGA interaction. At low humidity, the water-PLGA interaction is expected to be high, hence a low mobility of the water molecules. As humidity increases, the water affinity towards the amorphous PLGA decreases, eventually changing to a water-vapour interaction favouring water mobility. At this point, the hydration limit of the polymer is reached (Lechuga-Ballesteros *et al.* 2003; Oksanen & Zografi 1993). The subsequent water vapour-microsphere interaction is accompanied with hysteresis as visualised by the difference between the sorption and desorption cycles. The data showed that the hydration limit stood between 47% and 71% relative humidity for microspheres containing PVA and FIII9'-10, and between 23% and 47% relative humidity for microspheres containing Triton X-100 and FIII9'-10.

Percentage relative humidity	Percentage difference in gain and loss of mass			
	Blank microspheres	FIII9'-10 microspheres	FIII9'-10 & PVA microspheres	FIII9'-10 & Triton X-100 microspheres
0.00	0.02	0.02	-0.07	-0.01
23.80	0.02	0.00	-0.03	-0.03
47.50	-0.02	0.00	-0.09	-0.29
71.30	-0.06	0.00	-0.18	-0.37
95.00	0.00	0.00	0.00	0.00

Table 5.2. Difference between the gain and the loss of mass for the microsphere formulations during sorption and desorption cycles.

Finally, upon exposure to 95% relative humidity, SEM micrographs showed irreversible aggregation of the microspheres (Fig. 5.2). Particle cluster could result from binding of surface protein or the formation of interparticulate bridges. The latter case would imply a high degree of molecular mobility of the PLGA chains. Presumably, a high adsorbance of water at the microspheres surface caused the PLGA chains of neighbouring particles to aggregate. The resulting clusters were not free-flowing, as necessary for pharmaceutical criteria or intravenous administration. Therefore, the relative humidity for controlled surface remodelling without microsphere aggregation was thought to be around 75%.

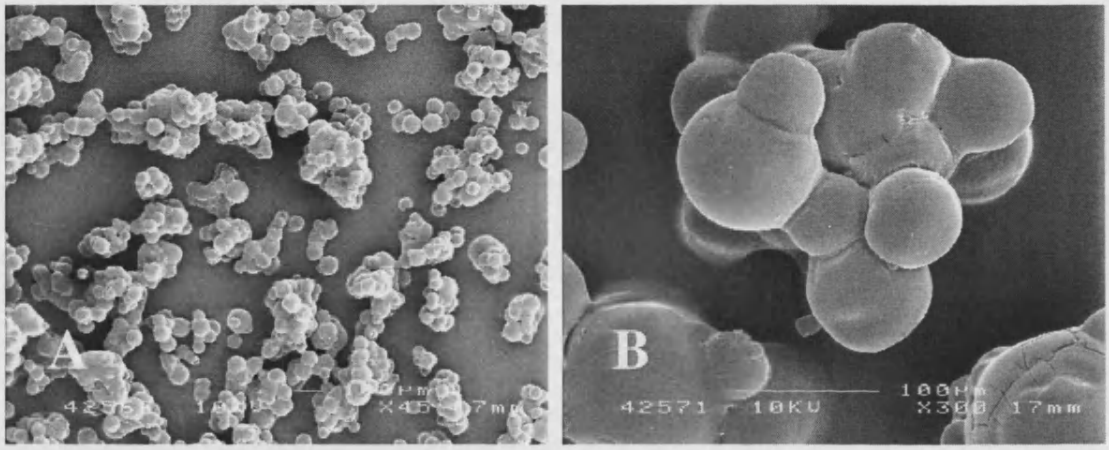

Figure 5.2. SEM images of microspheres containing FIII9'-10 and Triton X-100 at magnification of 45× (A) and 300× (B) upon storing at 93% relative humidity for 24 hours.

5.3.3 Thermal characteristics of the microspheres

The thermal properties of amorphous microspheres reflect the mobility among PLGA chains (Hancock *et al.* 1997; Pozuelo & Baselga 2002). As a result of solvent removal and lyophilisation, the polymeric chains are immobilised while trying to reach equilibrium (Sertsou *et al.* 2003). A glassy state is entered when the molecular mobility is so slow that the material is kinetically unable to fully relax (Hancock & Zografi 1997). Nevertheless, depending on the formulation and the storage conditions,

ageing may occur where the physical properties continue to change slowly with time as the polymer tends to thermal equilibrium with its surroundings (De & Robinson 2004; Van den Mooter *et al.* 1999). Any modification in the structure could therefore be detected and characterised using DSC (Mandal *et al.* 2002a; Mandal *et al.* 2002b; Royall *et al.* 1998). The period of storage used in these studies was 2 weeks, guided by the rapid absorbance of water vapour observed by DVS.

The effect of the storage history on the *Tg* and glass transition profile of the microspheres upon ambient and 75% relative humidity are shown in Fig. 5.3 and summarised in Table 5.3. All *Tg* values are relative to the experimental conditions used here and every precaution was taken during sample preparation to minimise variation in sample weight and heating rate. As expected, a difference was measured between blank and protein- or surfactant-loaded microspheres. Clearly, addition of protein or surfactant altered the glassy state of the PLGA chains.

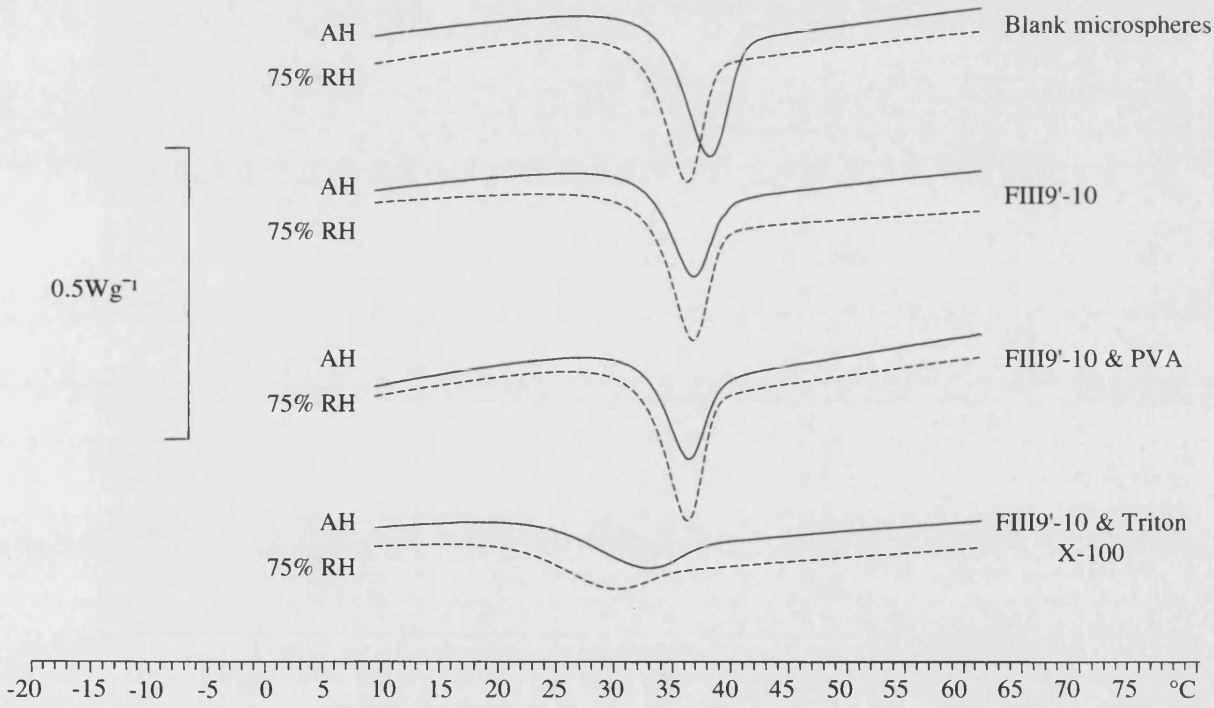

Figure 5.3. Total DSC heating thermograms over the glass transition region for microspheres, with and without protein and surfactant, stored for 2 weeks at ambient humidity (AH) (solid lines), and at 75% relative humidity (RH) (dotted lines).

Alone, the FIII9'-10 protein acted as an antiplasticizing agent, raising the *Tg* of the polymer (cf. the respective Tg_0 values in Table 5.3). This result may in itself be surprising given the weight ratio of protein to PLGA. A tentative explanation of the data may involve unfolded and folded fractions of the protein. During emulsification, the protein is likely to be denatured, unfolded and aggregated as reported in numerous studies (Perez *et al.* 2002; Sah 1999a). The unfolded protein fraction is left insoluble, non-covalently aggregated within the polymeric matrix, whereas the folded protein fraction, being soluble, leaves the microsphere during the burst release phase since it is only loosely associated with the inner cavities of the microsphere. It is possible that PLGA preferentially interacts with one protein form over an other. The protein fraction interacting with the PLGA was therefore likely to be the already exposed unfolded fraction. Thus, PLGA may interact with the unfolded protein fraction via van der Waals forces, reducing polymer chain mobility. This interpretation is consistent with other related work (Sanchez 1992; Yamakawa *et al.* 1992), though further validation and the underlying mechanism regarding the antiplastic activity of the protein remains to be determined.

Microsphere formulations	Time 0 Tg_0 (°C)	Ambient humidity		75% relative humidity	
		24 hours $\Delta Tg_1 = Tg_{24h} - Tg_0$	2 weeks $\Delta Tg_2 = Tg_{2w} - Tg_0$	24 hours $\Delta Tg_1 = Tg_{24h} - Tg_0$	2 weeks $\Delta Tg_2 = Tg_{2w} - Tg_0$
Blank microspheres	27.6	+0.8	+1.4	+1.1	+0.2
FIII9'-10	29.9	-1.7	-1.0	-1.5	-1.9
FIII9'-10 & PVA	29.2	-0.1	+0.9	-1.0	-0.0
FIII9'-10 & Triton X-100	20.1	+5.7	+4.3	+2.8	+1.4

Table 5.3. Evolution of the (onset) Tg of microspheres stored at ambient humidity and 75% relative humidity over time. Microspheres analysed immediately after lyophilisation served as references (Tg_0) against measurements obtained after 24 hours (Tg_1) and 2 weeks (Tg_2) – shown as the change to the Tg.

The DSC data showed that addition of PVA to the primary emulsion raised the *Tg* of the resultant microspheres, whereas Triton X-100 dramatically reduced the *Tg* (cf. the respective Tg_0 values in Table 5.3). It would be difficult to unambiguously define the intermolecular interactions occurring between the surfactants and PLGA (Shamblin *et al.* 1996). However, the role of surfactant penetration within the PLGA matrix was likely to be involved given the known miscibility of the PEO headgroup of Triton X-100 with PLGA (Chung *et al.* 2002). This was consistent with the noticeable broadening of the FIII9'-10 and Triton X-100 curve in the region of the glass transition as illustrated in Fig. 5.3. Consequently, Triton X-100 may have increased the free volume within the entangled PLGA chains, facilitating diffusion of water and PLGA molecular mobility, acting as a plasticizer. Conversely, PVA appeared to only weakly influence the molecular mobility (or free volume) of the PLGA. The PVA molecules tended towards an antiplasticizing effect since small increases to the *Tg* values were observed between microspheres encapsulating FIII9'-10 and microspheres encapsulating FIII9'-10 with PVA.

The change in *Tg* upon storage at ambient and elevated humidity revealed interesting behaviour. For blank microspheres stored at ambient humidity, the *Tg* increased rapidly within the first 24 hours, with relatively little change thereafter (Table 5.3). The increase in the *Tg* may have been a result of local molecular rearrangements (β-relaxations) occurring in any free spaces available as the polymer tended toward thermal equilibrium. The increased density would give rise to mechanical loss, which, under these circumstances, is known as physical ageing. This phenomenon is commonly seen for glasses frozen in non-equilibrium conformation due to reduced mobility upon vitrification (Chartoff 1997; Cowie & Ferguson 1986). Concomitant with the increase in *Tg* is the "overheating peak" (enthalpy relaxation) observed at the glass transition. This point will be addressed in the following section.

For blank microspheres stored at 75% relative humidity, a similar ageing was observed within the first 24 hours; but after 2 weeks the *Tg* had almost returned to its initial value. This could be expected given the uptake of water vapour at the higher humidity and the resultant plasticization effect on the PLGA. For microspheres containing PVA, the decrease in the *Tg* at 75% relative humidity versus ambient humidity was also consistent with the plasticizing effect of adsorbed water which increased the molecular mobility of PLGA (Hancock & Zografi 1994; Oksanen &

Zografi 1990). The drop in the *Tg* for microspheres containing only protein and stored at high humidity was only apparent after 2 weeks. This suggested that protein was a poor mediator of water uptake in comparison to surfactant, which was borne out in the DVS data. These analyses showed that the *Tg* of the microspheres was dependent upon the balance between the kinetics of physical ageing versus water-induced plasticization.

5.3.4 Analyses of the Enthalpy Relaxation

As expected, when the microspheres were quench cooled following the first heating cycle and their thermal behaviour analysed over a second identical cycle, the overheating peak almost disappeared given the minimal potential for relaxation (Fig. 5.4). The overheating peak superposed on the *Tg* may be confused with an endotherm corresponding to the fusion temperature but, crucially, the distinguishing feature is that the baseline does not return to its original level. Comparative DSC data for poly lactic acid microspheres showing ageing of poly lactic acid microspheres is provided by Passerini and Craig (Passerini & Craig 2001).

The examination of the enthalpy relaxation areas over time confirmed the existence of the physical ageing phenomenon suggested previously. Although the differences in enthalpy relaxation values are very small, a trend showing the increasing magnitude of the relaxation endotherms with increasing storage time can be clearly seen in Fig. 5.5 where first heat runs of blank microspheres kept under ambient humidity over time are superposed. This variation characterises the progression of physical ageing undergone by the copolymer. Such typical evolution was observed in the endotherms of all microspheres studied, suggesting that all were ageing over time, as Figure 5.6 illustrates.

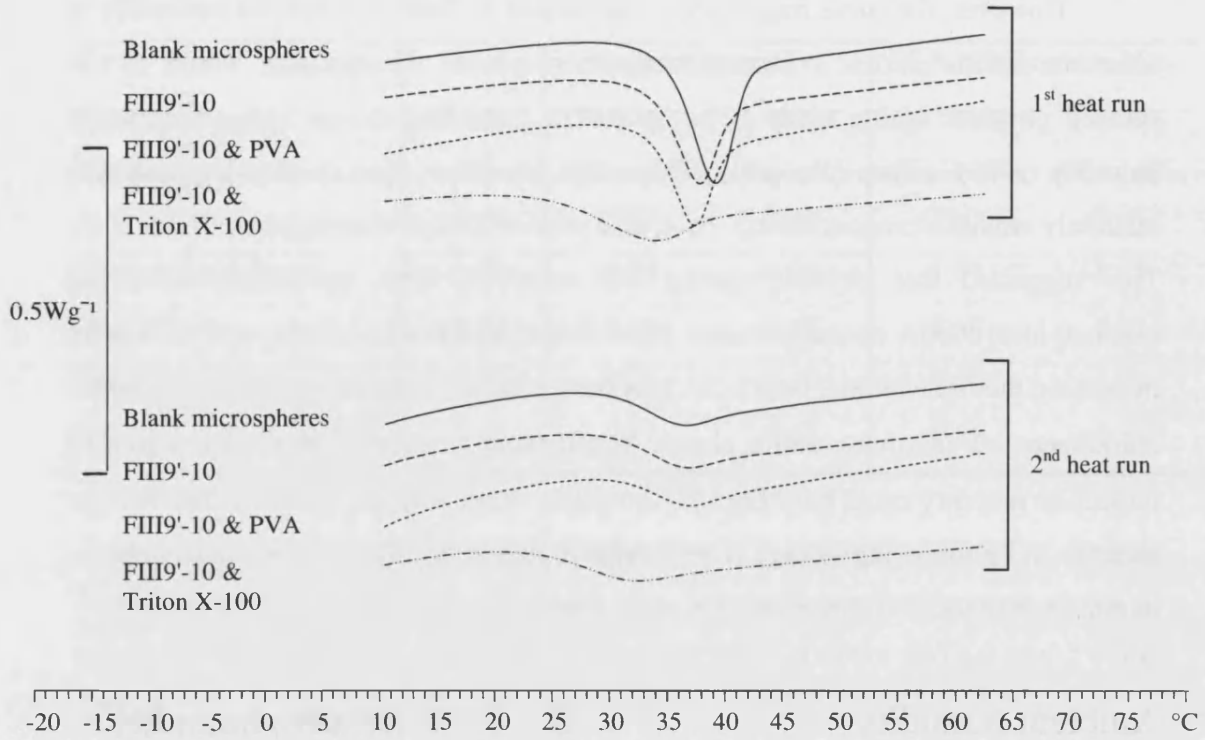

Figure 5.4. Thermograms of microspheres kept at ambient humidity for 2 weeks illustrating the thermal response of the polymer before (1st heat run) and after (2nd heat run) quench cooling.

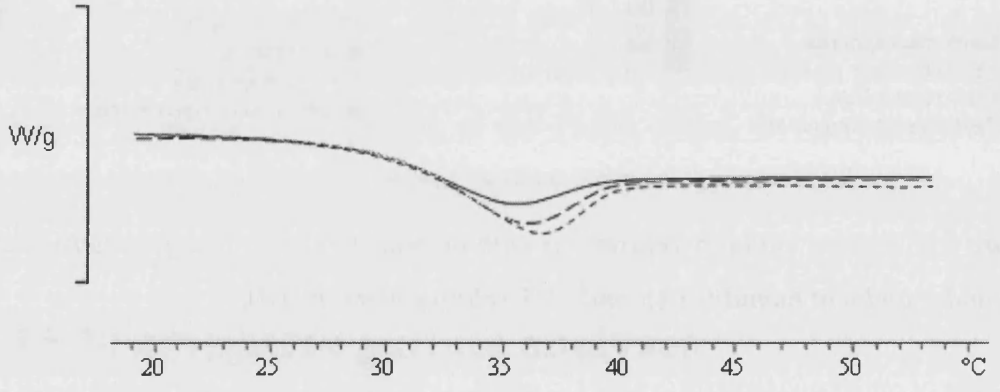

Figure 5.5. Evolution of the enthalpy relaxation of blank microspheres left at ambient humidity with increasing storage time for freshly made microspheres (solid line), and microspheres stored for 24 hours (long dashed line), and 2 weeks (short dashed line).

However, the curve magnitudes summarised in Table 5.4 differed noticeably in accordance with particle's formulations. Microspheres incorporating Triton X-100 showed physical ageing, with a rise in the *Tg* following storage either at ambient humidity or 75% relative humidity (Table 5.3). However, their overheating peak was relatively small in comparison to PVA and protein-loaded microspheres (Table 5.4). This suggested that physical ageing was relatively little, presumably involving minimal local PLGA rearrangements. Since Triton X-100 was strongly plasticizing by increasing the free volume, the PLGA may have instead tended toward large molecular rearrangements involving entire chains (α-relaxations). Further, this high degree of molecular mobility could have been facilitated by water sorption (cf. DVS data and the increase in *Tg* following storage at 75% relative humidity). The resultant plasticization dominated the thermal characteristics of the microspheres containing Triton X-100.

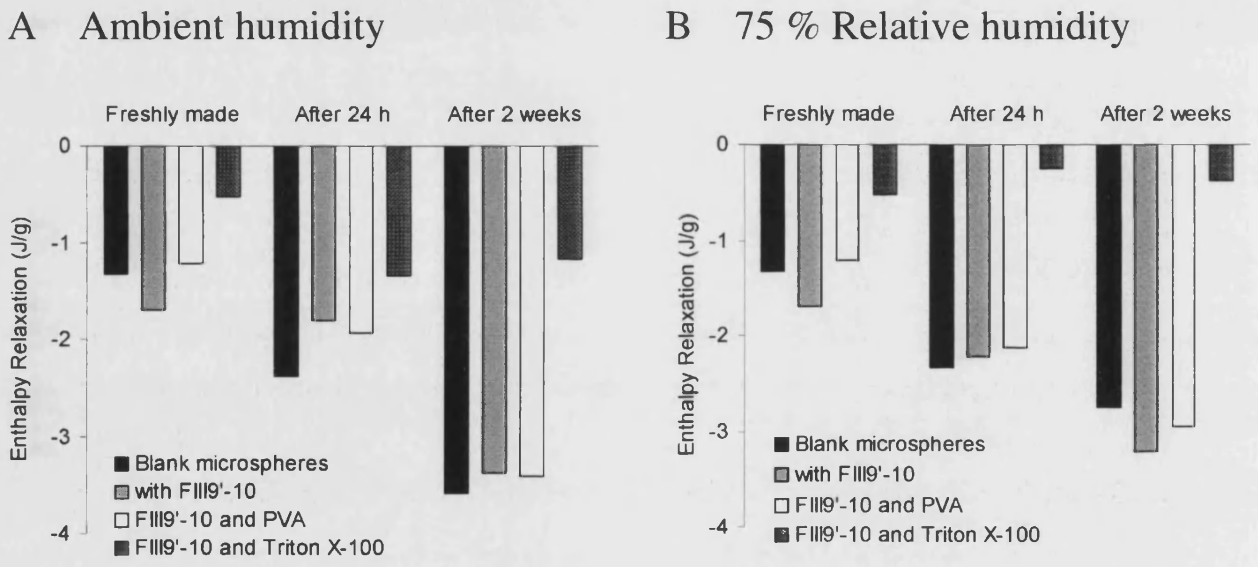

Figure 5.6. Raising enthalpy relaxations with increasing ageing time for microspheres kept under ambient humidity (A), and 75% relative humidity (B).

Microsphere formulations	Time 0 ΔH_0 (J/g)	Ambient humidity 24 hours $\Delta H_{24h} - \Delta H_0$ (J/g)	Ambient humidity 2 weeks $\Delta H_{2w} - \Delta H_0$ (J/g)	75 % relative humidity 24 hours $\Delta H_{24h} - \Delta H_0$ (J/g)	75 % relative humidity 2 weeks $\Delta H_{2w} - \Delta H_0$ (J/g)
Blank microspheres	-1.33	-1.05	-2.26	-1.01	-1.43
FIII9'-10	-1.69	-0.11	-1.68	-0.54	-1.53
FIII9'-10 & PVA	-1.22	-0.71	-2.19	-0.90	-1.74
FIII9'-10 & Triton X-100	-0.53	-0.81	-0.63	+0.28	+0.14

Table 5.4. Progression of the enthalpy relaxation of microspheres stored at ambient humidity and 75% relative humidity over time. Microspheres freshly made served as references (ΔH_0) against measurements obtained after 24 hours (ΔH_{24h}) and 2 weeks (ΔH_{2w}).

It is likely that the plasticization experienced by all other microspheres subjected to elevated humidity competed with ageing. For all microspheres maintained at 75% relative humidity, the relaxation endotherms progressed to a lesser degree than for samples stored at ambient humidity after 2 ageing weeks. Unlike microspheres formulated with Triton X-100, it was not possible to determine clearly which of the plasticizing or the ageing effect was predominant. However, considering that the enthalpy relaxations as well as the *Tg* of the microspheres evolved to higher values, the PLGA may have tended toward ageing more than plasticizing. Given the evidence for significant molecular rearrangement of the PLGA chains, it was anticipated that associated changes to the microspheres' surface morphology may be observed.

5.3.5 Microsphere surface analyses

SEM analysis of the microspheres before and after exposure to 75% relative humidity showed a general smoothing of the microsphere surface (Fig. 5.7). To further investigate the effects of moisture on the morphological properties of the microspheres, AFM was used with a resolution far beyond the capacity of an SEM.

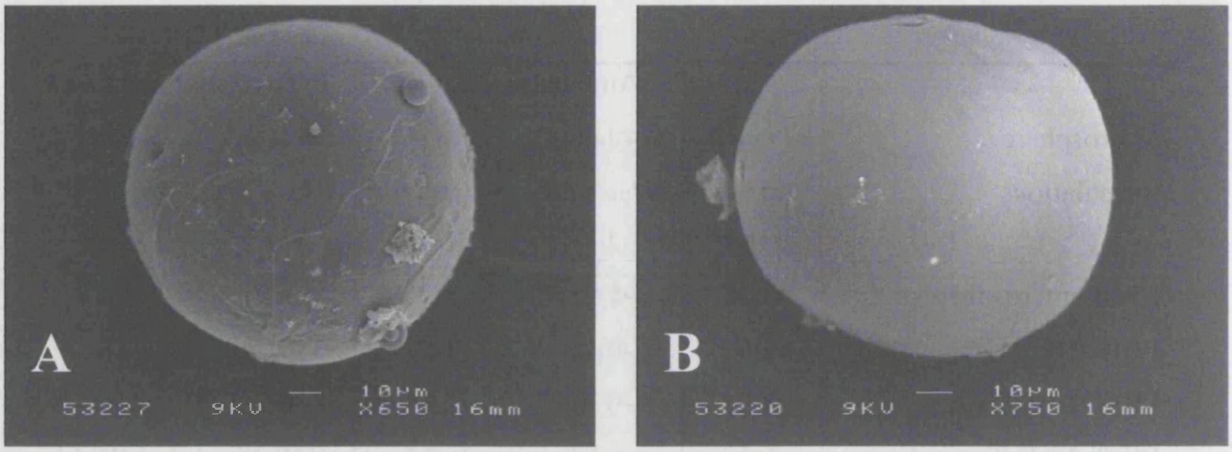

Figure 5.7. SEM images of microspheres containing FIII9'-10 and Triton X-100, immediately after lyophilisation (A), and stored for 24 hours at 75% relative humidity (B).

A representative AFM image of the porous structure of a microsphere (containing FIII9'-10 and PVA) at ambient humidity is shown in Fig. 5.8. The topographical image highlights the significant variance in the size and diameters of the pores of the microspheres which were not observable via SEM imaging.

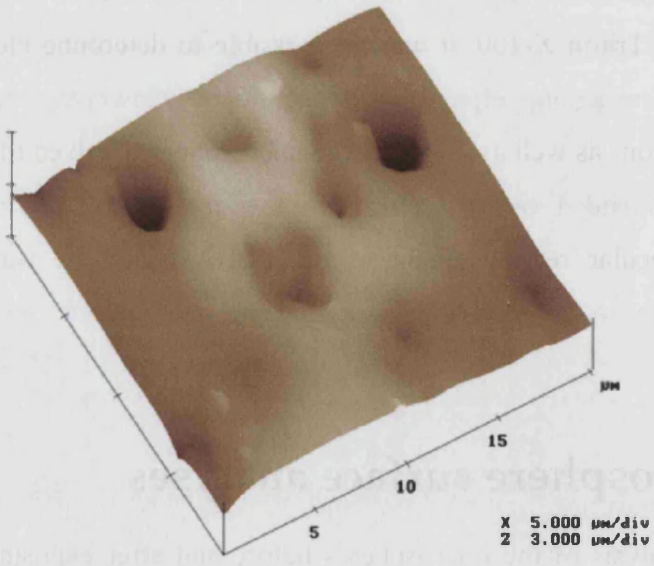

Figure 5.8. Representative topography of the surface of a microsphere containing FIII9'-10 and PVA, recorded using the AFM contact mode at ambient humidity.

In order to examine the direct influence of increasing relative humidity on pore stability, individual pores of the microparticles were directly imaged while varying the relative humidity. The high resolution AFM images showed subtle remodelling to the pore structure of all microspheres (Fig. 5.9), but only microspheres containing FIII9'-10 and Triton X-100 showed alteration of the pore depth as seen in Fig. 5.10. Cross-sectional analysis of the external dimensions of the selected pore in Fig. 5.10 for increasing relative humidity is summarised in Table 5.5. It is immediately clear that pore depth was markedly reduced as the relative humidity was increased from 55% to 75%. The modification of this pore's structure may be related to the increased chain mobility of the polymeric matrix associated with the decrease in the *Tg*, as suggested by the DSC data. Thus, as the relative humidity increased, the plasticizing effect of the water vapour facilitated chain mobility (the *Tg* tending towards the experimental, room, temperature). However, plasticization of the PLGA matrix was clearly not sufficient for complete structural collapse of the microsphere's surface.

A

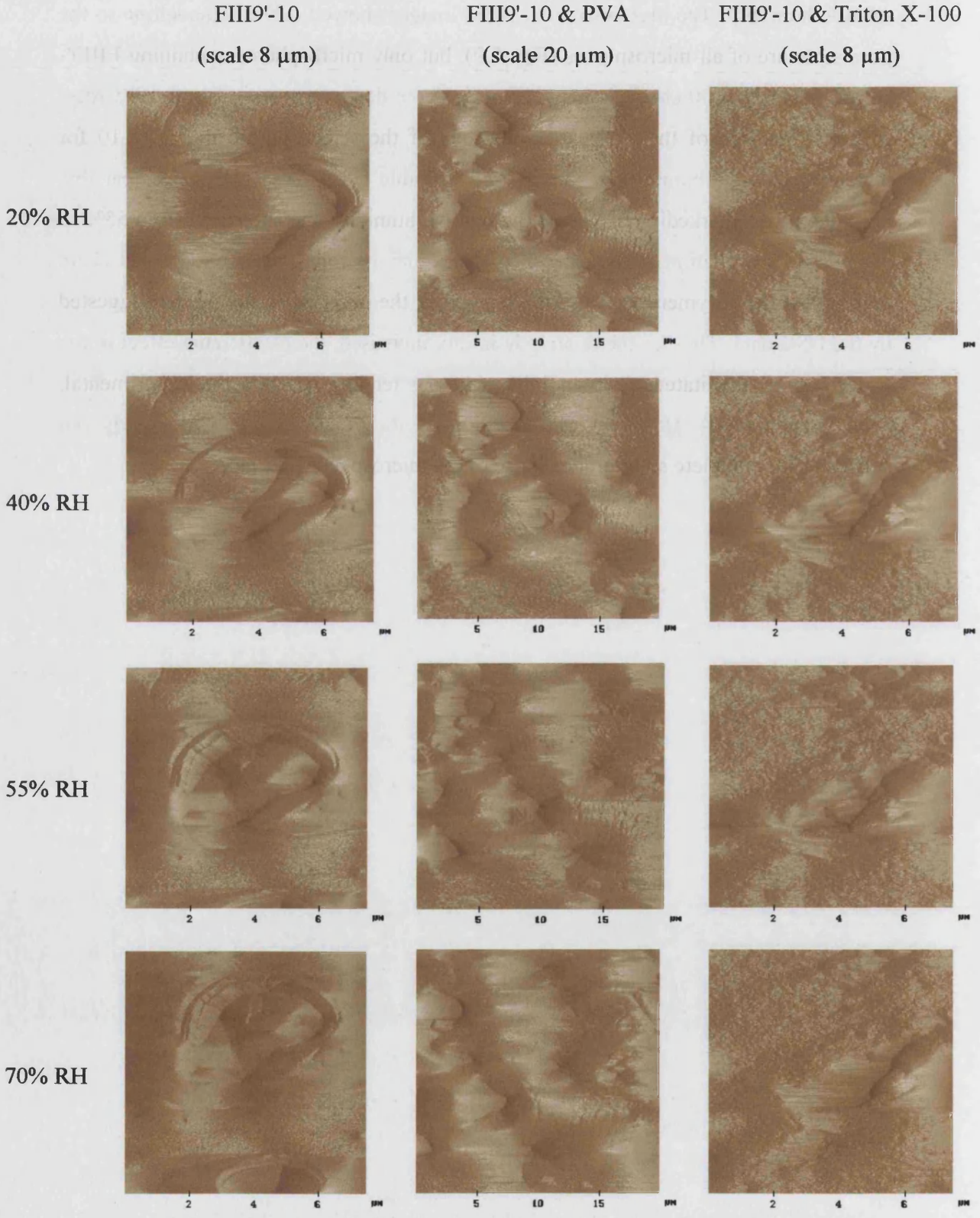
FIII9'-10
(scale 8 μm)
FIII9'-10 & PVA
(scale 20 μm)
FIII9'-10 & Triton X-100
(scale 8 μm)
20% RH
40% RH
55% RH
70% RH

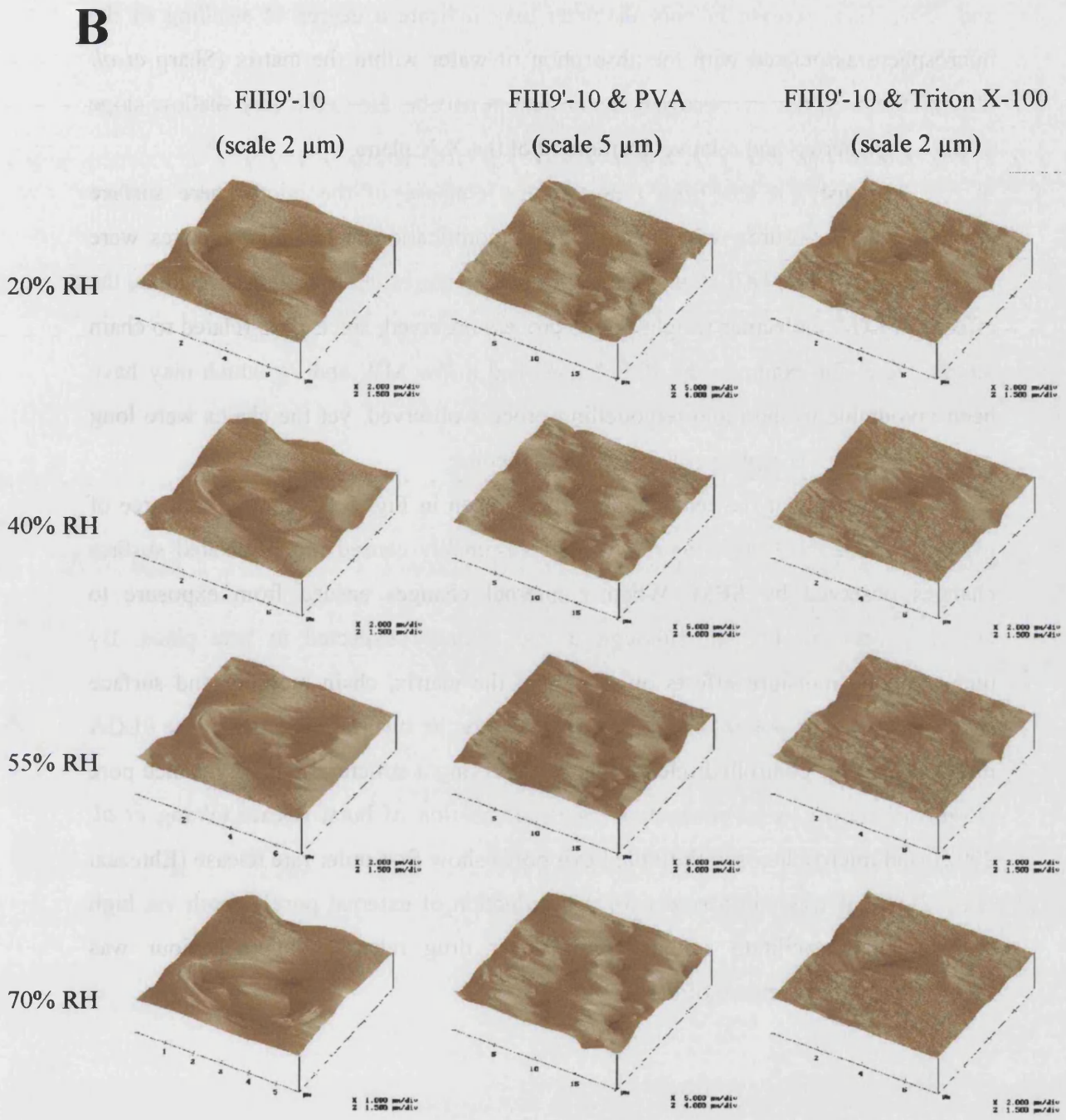

Figure 5.9. Evolution of the surface topography view from above (A), and from an angle of 45° (B) for microspheres containing FIII9'-10 alone, or with PVA and Triton X-100 as indicated. The particles were exposed to relative humidity increasing in steps from 20%, to 40%, 55% and 70% relative humidity (RH).

Further analysis of the pore's profile (Fig. 5.10) also showed a progressive increase in the diameter of the pore upon increasing the relative humidity between 25%

and 75%. This increase in pore diameter may indicate a degree of swelling of the microsphere associated with the absorption of water within the matrix (Sharp *et al.* 2001). However, the increasing diameter may in part be due to the very shallow slope at ca. 4.5 μm across and relative positioning of the X-Y plane.

Previously, it has been reported that collapse of the microsphere surface (complete pore closure) was due to internal modifications when microspheres were incubated in solution (Ali *et al.* 1993). It would be interesting to further investigate the effect of PLGA molecular weight on the process observed, since *Tg* is related to chain length. Here, for example, the PLGA used had a low MW and *Tg* which may have been favourable to the rapid remodelling process observed, yet the chains were long enough to resist a complete collapse of the structure.

It is clear that the remodelling process seen in Fig. 5.10 required a degree of plasticity from the PLGA matrix, which presumably caused the associated surface changes observed by SEM. Whether internal changes ensued from exposure to humidity was not known, although it was strongly expected to take place. By understanding moisture effects on the *Tg* of the matrix, chain mobility and surface structure, it may be possible to controllably modify the surface properties of the PLGA microspheres for controlled release while conserving a structural integrity. Since pore closure is known to be concomitant with attenuation of burst release (Wang *et al.* 2002), and microspheres with limited exit pores show first order rate release (Ehtezazi *et al.* 2000), it was considered here that reduction of external pore's depth via high humidity may facilitate similar control over drug release. This behaviour was investigated for the release of FIII9'-10.

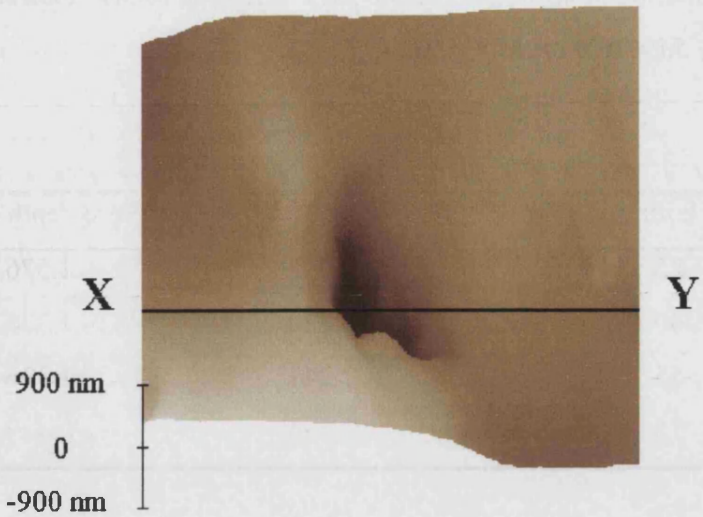

A 25% RH

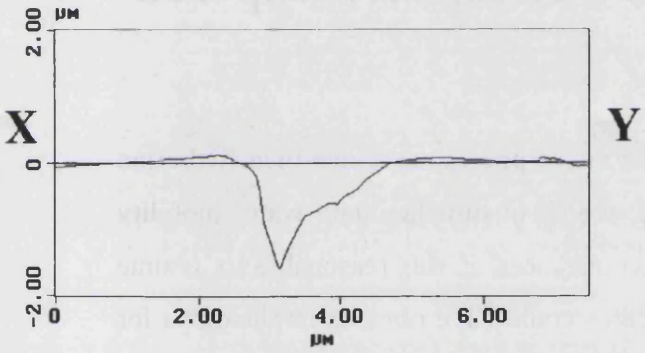

B 40% RH

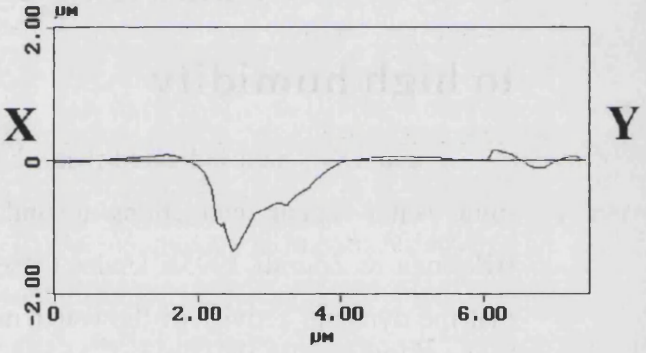

C 55% RH

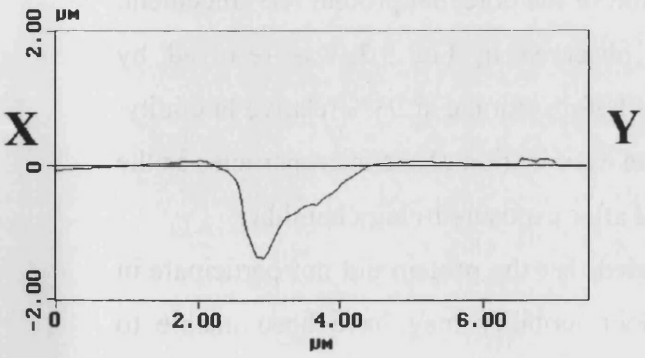

D 75% RH

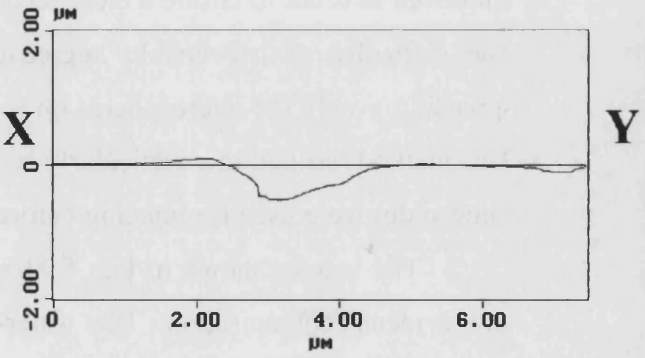

Figure 5.10. AFM topography of a surface pore for a microsphere containing FIII9'-10 and Triton X-100 under ambient humidity at 20°C. A cross-section along the line

marked X-Y revealed the modification of the pore's profile under relative humidity of 25% (A), 40% (B), 55% (C), and 75% (D).

Relative humidity (%)	Pore diameter (μm)	Pore depth (μm)
25	2.095	1.576
40	2.139	1.376
55	2.241	1.336
75	2.256	0.479

Table 5.5. Diameter and depth of the surface pore imaged in Figure 5.10.

5.3.6 Protein distribution in microspheres exposed to high humidity

The DVS data indicated that when the microspheres are above their hydration limit, water-vapour interactions are induced, which in turn facilitate water mobility (Oksanen & Zografi 1993). Under these circumstances, it was reasonable to assume that the dynamic activity of the water molecules could have obvious implications for protein redistribution within the microspheres. Following this concern, FITC-labelled protein was encapsulated and the microspheres were examined by CLSM after exposure to 93% relative humidity for 1 and 24 hours. Such high humidity was employed in order to ensure a clear recognition of the potential protein rearrangement. The difficulty of irreversible aggregation observed in Fig 5.2 was resolved by spreading evenly the microspheres on a slide before storage at 93% relative humidity. This method resulted in a particularly accurate examination of the microparticles as the same slides were used for imaging before and after exposure to high humidity.

The images shown in Fig. 5.11 revealed that the protein did not participate in any evident reorganisation. The water-vapour mobility may have been unable to support the circulation of the protein around the cavities or outside the microsphere as liquid water can do. In the latter case, water is known to be responsible for drug flow which inevitably leads to drug extraction due to osmotic pressure. While a continuous

environment such as liquid water or buffer imposes osmotic differences, it is most probable that air nearly saturated with water-vapour molecules could not maintain conditions consistent enough to properly generate osmotic pressure. The absence of osmotic differences apparently confined the proteins to their original position.

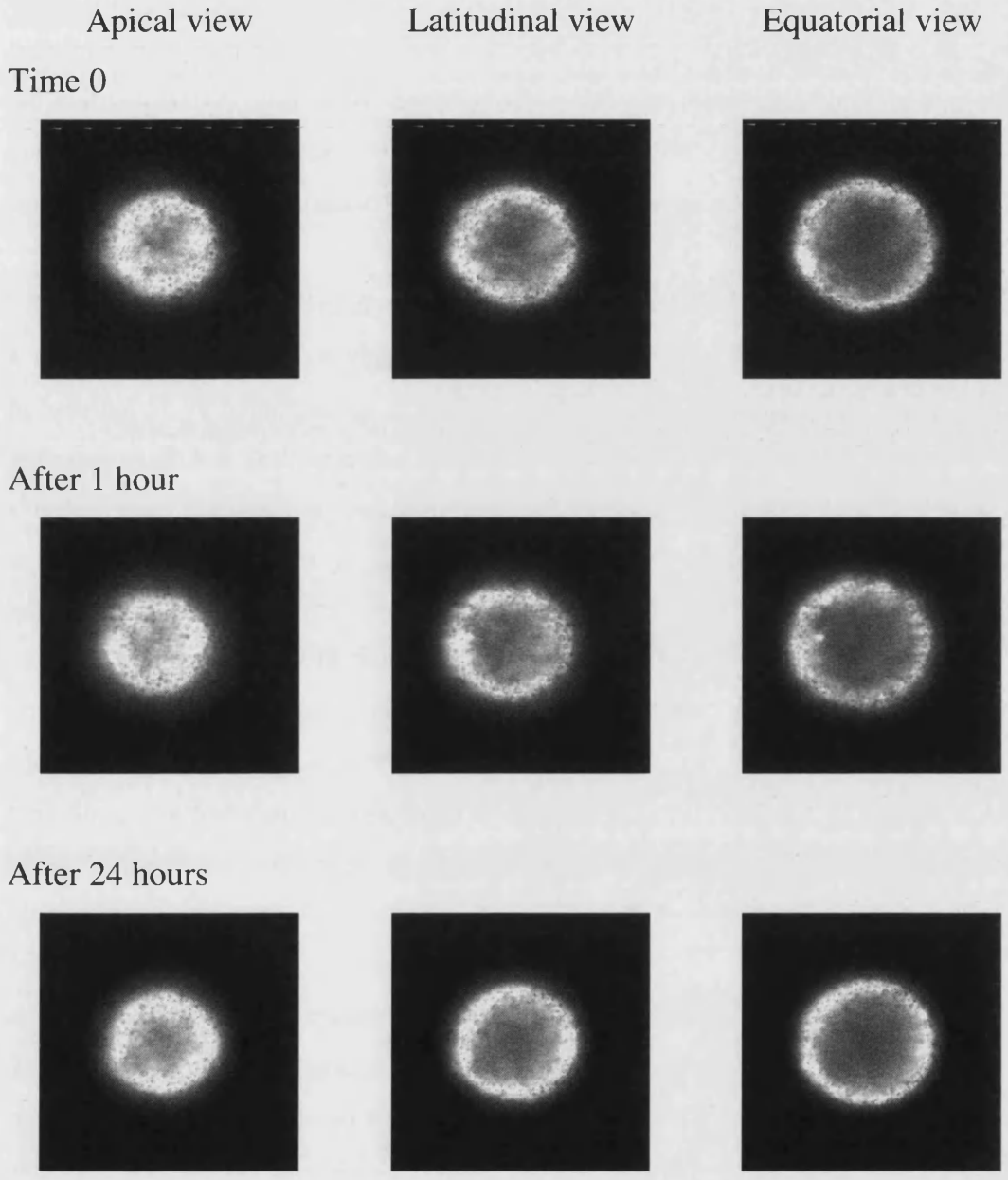

Figure 5.11. Representative images of FITC-labelled FIII9'-10 distributed throughout microspheres (~100 µm diameter) after fabrication (Time 0), and after 1 and 24 hours storage at 93% relative humidity.

5.3.7 *In vitro* protein release

Microspheres formulated with FIII9'-10 alone and with PVA or Triton X-100 were stored for 24 h at 75% relative humidity before incubation as this humidity would allow for surface remodelling while conserving the free-flowability of the particles. The primary emulsion was found to be best stabilised with Triton X-100 yielding the highest encapsulation efficiencies for the FIII9'-10. Accordingly, the absolute concentrations of protein released *in vitro* over the 12 weeks period was greatest for microspheres prepared with Triton X-100 (Table 5.6).

For all the microsphere formulations, it is interesting to note that, for incubation at 37°C, the PLGA matrix of the microspheres will have existed in a rubbery state (the *Tg* being < 37°C, Table 5.3). This is accompanied by an increase in chain mobility, facilitating the diffusivity of both the escaping drug and the penetrating water (Friess & Schlapp 2002). The *in vitro* protein release profiles of all microspheres showed a typical burst release (Fig. 5.12 A-C), with at least 30% of the protein encapsulated released within the first hour. However, the extent of release within the first hour was dependent on the formulation and, especially, the storage at ambient humidity or high humidity prior to immersion in aqueous buffer. At ambient humidity, for microspheres prepared with either FIII9'-10, or FIII9'-10 and Triton X-100 in the primary emulsion, above 80% of the encapsulated protein was released within the first hour with comparatively little subsequent release. For the same microsphere formulations stored at 75% relative humidity, the burst release was significantly attenuated and a large proportion of the protein was released in a secondary phase occurring at the 4-8 week period. This was particularly noticeable for the microspheres prepared with Triton X-100, which were observed to undergo pore reduction at 75% relative humidity. The strong attenuation of the burst release is very likely to be related to surface pore modification, although a first order release was not observed as may have been expected from a previous study (Ehtezazi *et al.* 2000). The reason for this may have been that the number of pores in this study remained the same, albeit partially closed, whereas Ehtezazi *et al.* prepared microspheres with minimal numbers of surface pores (Ehtezazi *et al.* 2000).

Also, in the case of microspheres containing FIII9'-10 and Triton X-100, the second burst recorded after 8 weeks was equivalent in terms of protein release to the primary release phase (Fig. 5.12 B). Occurrence of a secondary release phase at around 8-weeks is accountable to erosion of the PLGA matrix. However, the secondary release phase seen here is unusually rapid (given the logarithmic scale) and, remodelling of the internal pores upon exposure to high humidity was suspected. Remodelling of the internal matrix could be expected because the movement of a water molecule within PLGA matrix is rapid (Batycky *et al.* 1997), and would be enhanced by the hydrophilic nature of Triton X-100. This large secondary release may have been due to 'temporary storage' of protein within the remodelled microsphere which otherwise have escaped, under ambient humidity, in the burst release (Fig. 5.12 B). In effect, protein reservoirs were entrapped within the microsphere, with little protein actually entangled with the PLGA matrix.

These release data also corroborate the strong plasticizing effect induced by Triton X-100, and the smaller attenuation of the burst release for microspheres containing no surfactant in the primary emulsion suggested minimal PLGA plasticization. This was further consistent with the observation that addition of the antiplasticizer (PVA) to the primary emulsion did not attenuate the burst release following exposure of the microspheres at high humidities (Fig. 5.12 C).

Storage conditions	FIII9'-10 released from surfactant-free microspheres (μg/ml)	FIII9'-10 released from microspheres fabricated with PVA (μg/ml)	FIII9'-10 released from microspheres fabricated with Triton X-100 (μg/ml)
Ambient humidity	21.91	13.64	38.44
75% relative humidity	18.35	17.60	33.85
Encapsulation efficiencies (± S.D.)	13.2% (± 4.5%)	23.0% (± 12.9%)	48.2% (± 17.2%)

Table 5.6. Encapsulation efficiency and total protein concentrations released from microspheres with prior storage at ambient humidity and 75% relative humidity for 24 hours.

A

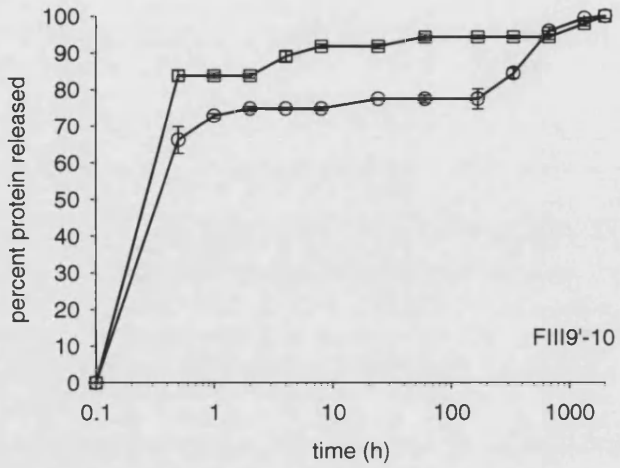
percent protein released
100
90
80
70
60
50
40
30
20
10
0
0.1
1
10
100
1000
time (h)
FIII9'-10

B

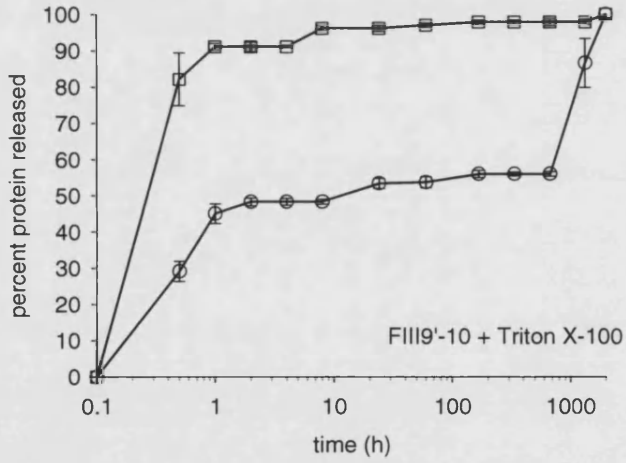
percent protein released
100
90
80
70
60
50
40
30
20
10
0
0.1
1
10
100
1000
time (h)
FIII9'-10 + Triton X-100

C

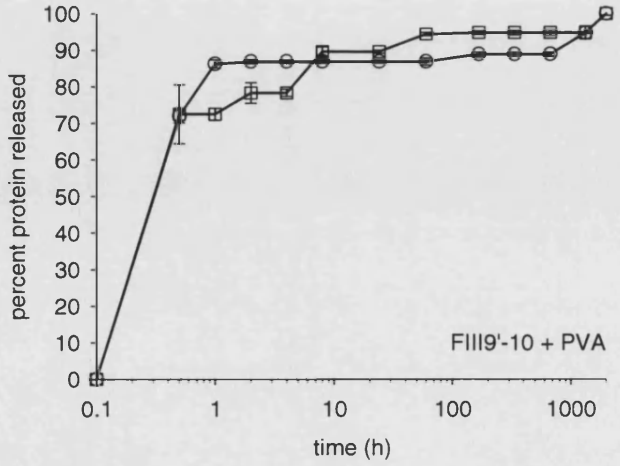
percent protein released
100
90
80
70
60
50
40
30
20
10
0
0.1
1
10
100
1000
time (h)
FIII9'-10 + PVA

Figure 5.12. In vitro FIII9'-10 release from microspheres first maintained at ambient humidity (□) or at 75% relative humidity (○) for 24 hours, and then immersed in PBS over 12 weeks, at 37°C. The data are normalised to the cumulative protein concentration at 12 weeks. A, microspheres prepared without surfactant in the primary emulsion; B, microspheres prepared with Triton X-100 added to the primary emulsion; C, microspheres prepared with PVA in the primary emulsion.

5.4 Conclusions

Residual PVA and Triton X-100 were found to increase the hydrophilicity of the resultant microspheres. Triton X-100 had a strong plasticizing effect on the PLGA matrix with an associated increase in the free volume. In contrast, PVA and encapsulated protein acted as antiplasticizing agents. The mechanical properties of surfactant free microspheres were influenced by the environmental humidity. At ambient humidity, PLGA chain reorganization resulted in a denser matrix and increased the *Tg*, whereas at 75% relative humidity, the plasticizing effect of water vapour was observed by depression of the *Tg*. AFM imaging demonstrated that the PLGA surface is amenable to remodelling upon exposure to elevated conditions of relative humidity (> 75% RH), with a tendency towards surface smoothing and pore closure. This is consistent with previous work by Wang *et al.* showing complete pore closure upon microsphere immersion in aqueous buffer (Wang *et al.* 2002). Despite the reduction in pore depth facilitated by water vapour-induced plasticization, complete pore collapse was not observed. Remodelling of pores in this manner for microspheres containing FIII9'-10 with Triton X-100 halved the burst release. The accompanying secondary release being of equal magnitude and rate, suggested remodelling of the internal porous matrix. Therefore, depending on the stability of the drug encapsulated, brief exposure of PLGA microspheres to high humidities may prove to be an effective and novel method to attenuate the initial burst release.

Chapter 6

Examination of the mechanical properties of PLGA microspheres

6.1 Introduction

Recent thermodynamic analysis of PLGA microparticles has yielded important information concerning their mechanical properties and how they may be related to stability during storage, drug encapsulation and release (Friess & Schlapp 2002; Zhang *et al.* 2003). Ideally, the mechanical state of the polymeric microspheres should remain stable and facilitate an appropriate drug release.

The work here aimed to characterise the material properties of the PLGA microparticles by thermodynamic measurements using DSC. Two different chain lengths of PLGA were selected to fabricate microparticles, and their mechanical integrity was evaluated under various conditions. The influence of protein size and structure, as well as the effect of freeze-drying versus drying under a stream of dry nitrogen gas on PLGA microspheres was assessed. Finally, the polymeric particles were exposed to different storage conditions over three months and their physical state

was subsequently evaluated. Unfortunately, further investigation of PLGA mechanical properties could not be pursued due to time limitations.

6.2 Methods

6.2.1 Lysozyme microencapsulation

Lysozyme was loaded without surfactant into PLGA microspheres following the emulsion evaporation process described previously (Chapter 2.3.1). Briefly, an inner aqueous phase of 95 µl of lysozyme at 20 mg/ml in PBS was incorporated to 950 µl of DCM with PLGA (5% w/v), and homogenised at 22000 rpm for 15 seconds (IKA Ultra Turrax T18). This primary emulsion was transferred into 40 ml of water with PVA (0.5% w/v) and stirred at 500 rpm for 2 h at room temperature to allow for solvent evaporation and capsides hardening. The particles were collected, dried and stored as described in Chapter 2.3.1.

6.2.2 Fabrication and drying of microspheres

Blank microspheres were fabricated with low molecular weight PLGA (15,000 g/mol), or high molecular weight PLGA (135,000 g/mol). Microspheres were dried following either the freeze-drying process described in section 2.3.1, or the drying process using nitrogen gas during thermogravimetric (TGA) analysis. For the latter, microspheres suspended in a minimal volume of water were placed in an aluminium pan and positioned on a sensitive microbalance assembly (TGA/SDT A822e, Mettler Toledo). Dry nitrogen gas circulated over the pan while maintaining a temperature of 25°C. Under these conditions, water evaporated from the sample causing a change in mass which was recorded by the TGA apparatus. The sample was considered to be fully dried when no further change in mass was observed. The physical properties were quantified by DSC immediately after completion of drying, and the data were analysed against the unprocessed PLGA of respective molecular weight.

6.2.3 Storage of the microspheres over three months

The effects of storage over three months were studied on blank microspheres, microspheres made with FIII9'-10 and PVA or Triton X-100, and microspheres made without FIII9'-10 but containing the same fraction of PVA or Triton X-100 (5 μl) added to the inner water phase of the primary emulsion. The latter particles were termed as 'blank and PVA' and 'blank and Triton X-100'. Low and high molecular weight PLGAs were used to fabricate each type of microparticle.

Microspheres were first analysed immediately after lyophilisation by DSC. Then, each batch of microspheres was divided into two Eppendorf tubes, sealed tightly with Parafilm, and placed under different storage conditions for three months. One batch was kept under ambient conditions, that is, at ambient temperature (~20°C) and ambient humidity (~23% relative humidity). The other was placed in a sealed box with fresh silica gel (replaced as necessary) and stored in a fridge (~4°C). After three months, the microspheres were analysed by DSC.

6.3 Results and discussion

6.3.1 Influence of the nature of the encapsulated drug

Lysozyme is a small globular protein (ca. 14 kDa) with four disulphide bonds and therefore relatively rigid. This is in contrast to FIII9'-10 which is a β-sandwich domain pair (ca. 20 kDa) with no disulphide bonds. The two proteins were encapsulated in low molecular weight PLGA (ca. 15000 MW) without addition of surfactant to the primary emulsion. The microspheres' thermodynamic characteristics were measured after freeze-drying and compared to blank microparticles. The *Tg* and

enthalpy relaxation measurements of blank microspheres and microspheres loaded with FIII9'-10 and lysozyme are summarised in Table 6.1.

While FIII9'-10 acted as an antiplasticizer increasing the *Tg*, lysozyme did not cause any change to the *Tg* compared to blank microspheres. Enthalpy relaxation values suggested that the ageing of PLGA was more pronounced for encapsulation of lysozyme, although additional experimentation should be pursued to confirm the variations. Differences between the *Tg* and enthalpy relaxation values for FIII9'-10 and lysozyme may reflect protein specific interactions with the PLGA chains. While this could be accounted to the different secondary and tertiary structures, these data do not provide unambiguous evidence for this.

Microspheres formulation	*Tg* (°C)	*ΔH* (J/g)
Blank microspheres	27.6	-1.3
Microspheres with FIII9'-10	29.7	-1.7
Microspheres with lysozyme	27.5	-2.4

Table 6.1. Measurements of the Tg and enthalpy relaxation of microspheres containing either FIII9'-10 or lysozyme, and compared against blank microspheres.

Van der Waals forces have been identified as the main form of interaction between protein and polymer, in some cases retaining the protein within the structure during *in vitro* release (Jiang *et al.* 2002). The extent of the protein/polymer interactions is also known to depend on electrostatic, double layer forces. A study by Blanco and Alonso demonstrated that lysozyme (pKa 9.2 and therefore basic) exhibited particularly high interactions with the acidic PLGA chains (pKa 3.8), whereas BSA (pKa 5.6) had a much lower affinity towards the polymer (Blanco & Alonso 1998). Presumably, lysozyme and FIII9'-10 lodged within the polymeric microspheres here were both subjected to these intermolecular forces.

Proteins are known to unfold and aggregate during encapsulation, and it has been previously suggested the same for FIII9'-10. It would have been interesting to compare what predominantly acts for folded/unfolded protein fractions and how they may affect *Tg* and polymer ageing. However, time limitations and the anticipated complexity of such experiment prevented further study.

6.3.2 Effects of the drying process on the stability of PLGA

Two drying techniques were selected and tested on blank microspheres in order to evaluate the effects of removal of bulk water on PLGA stability. Freeze-drying, which generally eliminates bulk and bound water, was chosen and compared to drying using dry nitrogen gas at 25°C with monitoring of drying by thermogravimetric (TGA) analysis. The *Tg* and enthalpy relaxation of raw polymers and dried microspheres were computed and summarised below.

	Low MW PLGA		High MW PLGA	
	Tg (°C)	*ΔH* (J/g)	*Tg* (°C)	*ΔH* (J/g)
Unprocessed PLGA	30.2	-3.8	43.2	-5.7
Blank microspheres freeze-dried	27.6	-1.3	38.4	-4.2
Blank microspheres air-dried	28.0	-1.3	40.6	-5.4

Table 6.2. Physical properties of freeze-dried and nitrogen-dried microspheres compared against unprocessed polymer. Low and high molecular weight PLGA were used to manufacture blank microspheres.

As expected, the *Tg* for the high molecular weight PLGA was greater than for the low molecular weight PLGA and corresponded to the manufacturing data (Birmingham polymers, UK). It was also noted that unprocessed PLGA of both low and high molecular weights had higher *Tg* values than the corresponding microspheres. It follows that PLGA chains in the microsphere have a greater degree of disorder than the unprocessed PLGA. This observation is in accordance with work published by Sandor *et al.*, showing that rapid PLGA precipitation during solvent extraction immobilised the polymeric chains into a highly dispersed configuration (Sandor *et al.* 2002).

For low molecular weight PLGA, no significant change of *Tg* was observed when comparing the two different drying techniques, whereas high molecular weight

PLGA microspheres dried by lyophilisation had a lower *Tg* than when air-dried. The latter could be attributed to more complete removal of bulk water. In effect, Passerini *et al.* examined oil-in-water microparticles and found incomplete water removal after lyophilisation (Passerini & Craig 2001). It follows that the content of residual water was greater for the lyophilisation process than air-drying. However, it seemed unlikely that the plasticization from residual water would cause such a decrease in *Tg* and enthalpy relaxation of the freeze-dried particles made with high molecular weight PLGA. It may be the case that lyophilisation physically changed the PLGA matrix. Kim *et al.* reported that upon snap-freezing, the volume fraction of ice expands such that voids were left behind once the water had been sublimed (Kim & Park 2004b). The gain in free-volume would logically facilitate chain mobility, and so lower the *Tg* of the lyophilised microparticles, beyond that seen by air-drying.

6.3.3 Stability over different storage conditions for 3 months

Drug delivery vehicles must preserve the therapeutic activity of the encapsulated drug during storage. To achieve this, the integrity of the carrier is important. For amorphous polymers such as PLGA, physical ageing is associated with minor chain relaxation (side-group rotations) (Ford & Timmins 1989). Storage at temperatures near the polymer *Tg* value are expected to increase the rate of ageing, this being of particular consideration for low molecular weight PLGA (*Tg* ~ room temperature). Furthermore, surfactant and drug encapsulated may act as plasticizers. Since glassy and rubbery states affect drug release and PLGA degradation, it is important to characterise the change in *Tg* and enthalpy relaxation during microsphere storage.

Data for microspheres stored three months under ambient or cold and dry conditions are presented in Table 6.3. The glass transition of blank microspheres increased over three months regardless of storage conditions and was associated with greater ageing. Microspheres formulated with high molecular weight PLGA and with FIII9'-10 and Triton X-100 showed a large decrease in three months storage irrespective of storage condition. It is interesting to note that this is in contrast with the

same formulation but with low molecular weight PLGA where large rises in *Tg* were observed. The difference is difficult to explain, but may reflect the different extent of influence from Triton X-100 (plasticizing) and FIII9'-10 (antiplasticizing) on high and low molecular weight PLGA during storage. Overall, the majority of the microspheres demonstrated typical profiles of physical ageing. However, noticeable differences distinguished microparticles made either with low or high molecular weight PLGA.

Microspheres formulation	Low MW PLGA			High MW PLGA		
	Freshly made	3 months under ambient conditions	3 months under cold and dry conditions	Freshly made	3 months under ambient conditions	3 months under cold and dry conditions
	Tg_0 (°C)	$\Delta Tg_{AC} = Tg_{AC} - Tg_0$	$\Delta Tg_{CD} = Tg_{CD} - Tg_0$	Tg_0 (°C)	$\Delta Tg_{AC} = Tg_{AC} - Tg_0$	$\Delta Tg_{CD} = Tg_{CD} - Tg_0$
Blank microspheres	27.6	+2.0	+1.8	38.4	+3.2	+4.3
Blank & PVA	27.2	+2.4	+2.9	37.8	+3.9	+5.3
FIII9'-10 & PVA	29.2	+1.4	-0.4	39.6	+0.7	+1.4
Blank & Triton X-100	26.4	-2.1	+1.5	33.5	+2.1	+3.5
FIII9'-10 & Triton X-100	20.1	+6.8	+11.8	41.8	-4.5	-4.8

Table 6.3. Evolution of the (onset) Tg of microspheres made with low and high molecular weight PLGA and stored for three months under ambient or cold and dry conditions. Tg values for microspheres analysed immediately after lyophilisation (Tg_0) served as reference for values obtained after three months under ambient conditions (Tg_{AC}) and cold and dry conditions (Tg_{CD}). Values are shown as the change to the Tg.

The *Tg* of microspheres fabricated with high molecular weight PLGA varied in accordance with the particle formulation, as was expected. However, no significant difference was observed with respect to the storage conditions. Only microparticles formulated with FIII9'-10 and Triton X-100 had their *Tg* lowered after three months storage, yet again the decrease was identical whether kept under ambient or cold conditions. The consistency of the polymer mechanical evolution suggested that microspheres made with high molecular weight PLGA could ignore the stresses applied by storage parameters. Presumably, the long chains' need for equilibrium

would overcome the environmental conditions and initiate small chain relaxations, characteristic of physical ageing. The differences of ageing progressions between batches may originate in varying formulation parameters.

Microspheres fabricated with low molecular weight PLGA demonstrated stronger fluctuations within batches and storage conditions, although in some cases the changes may have been within the margin of sensitivity of the DSC (for example, microspheres containing FIII9'-10 and PVA). For example, particles fabricated with Triton X-100 alone showed an increase in the *Tg* when kept under cold and dry conditions, but under ambient conditions showed a decrease in the *Tg*. These variations suggested that the mechanical integrity of short PLGA chains was harder to maintain and to predict over time. Influenced by the environment and the formulation parameters, short polymeric chains may not be able to sustain the phenomenon of physical ageing in a consistent manner.

It is also interesting to note that the plasticizing and antiplasticizing natures of Triton X-100 and PVA, respectively, were revealed mostly when FIII9'-10 was encapsulated together with the surfactants. This may be caused by the protein/surfactant interaction which might hinder the extraction of surfactant molecules during the wash. Greater residual amounts of surfactant within the structure would then alter more severely the conversion of the polymeric chains from free rotation, when dissolved into the solvent, to inactivity when precipitated.

6.4 Conclusions

PLGA microspheres were analysed under different conditions in order to understand what modulates the polymer mechanical integrity and ideally, what could improve it. Protein/polymer interactions were found to alter the polymer chains in microspheres made with low molecular weight PLGA. However, supplementary work would be necessary to determine which of the folded or unfolded protein fraction is more susceptible to induce structural perturbations. Drying under nitrogen gas was found to be a more acceptable drying technique as it allowed for a greater repossession of the PLGA thermo-equilibrium than lyophilisation. Besides, air-drying does not

require detrimental steps such as snap-freezing. The difference between lyophilising and air-drying was particularly evident for microspheres made with high molecular weight PLGA which also differed from low molecular weight PLGA during storage. After three months storage, all microspheres made with high molecular weight PLGA had consistently aged regardless of the formulation parameters. On the contrary, the mechanical activity of microspheres containing low molecular weight PLGA was dependent on the formulations parameters. It follows that long PLGA chains are more consistent over time than short polymer chains which are more easily influenced and their mechanical changes are more unpredictable.

Conclusions

General conclusions

This thesis focused on the encapsulation of FIII9'-10 in PLGA microspheres fabricated with non-ionic surfactants added to the primary emulsion of the w/o/w emulsion-evaporation technique. Pluronic F68, Tween 20, Tween 80, Triton X-100 and Igepal CA-630, were selected as alternatives to model stabilisers such as PVA and BSA. Innovative analytical devices and techniques were designed in order to assess the viability of the novel microspheres and to gain an insight into protein and particles characteristics.

The integrity and level of biological activity of the integrin-binding FIII9'-10 were tested on protein released from incubated microspheres. SDS-PAGE analysis showed that the protein backbone was consistently preserved throughout microsphere fabrication. More importantly, FIII9'-10 released after 3 hour incubation promoted cell attachment in a concentration-dependent manner, as desired. Therefore, the biological activity of FIII9'-10 was proven unaltered, and the microencapsulation of a conformationally labile protein, an encouraging prospect. Meanwhile, the evaluation of the protein's vehicle indicated that several features of the microspheres had been affected by the emulsifiers added to the primary emulsion. These features listed below are fundamental to drug delivery systems:

- encapsulation efficiency
- protein release profile
- size of the particles
- surface roughness

- surface porosity
- internal morphology
- hydrophilic properties of the microspheres
- thermodynamic properties of PLGA

The performance variations among batches were assigned to the underlying molecular interactions between surfactant and drug/PLGA. Unfortunately, it was not possible to unambiguously define the nature of these molecular interactions, and only their impact on the particles could be determined accurately. In some cases, these interactions were detrimental to the drug delivery system. For example, a multivesicular structure or a microcapsule would be formed with Pluronic F68, Tween 20, Tween 80, or Igepal CA-630. These results implied that these surfactants were unable to resist stresses such as solvent extraction or polymer precipitation during the secondary emulsification. Also, the encapsulation efficiency was overall not significantly improved, unless Triton X-100 or Igepal CA-630 was used. However, the common feature shared by all microspheres was the initial burst release which was further inspected.

Real-time CLSM helped to visualise the liberation of soluble and mobile protein through exit pores of microspheres in static immersion. Meanwhile, cryo-fracture SEM revealing the particles' internal structure indicated that the initial burst release mechanism was unrelated to the inner matrix morphology. Therefore, it was concluded that the accessibility to the release medium was the predominant factor inducing burst release. However, despite the small number and size of pores on surface of particles made with Pluronic F68, Tween 20, Tween 80, Triton X-100 or Igepal CA-630, the porosity appeared to be still sufficient to allow for the initial burst release to proceed. It follows that further reduction in external porosity is necessary to attain an ideal zero-order drug release. In order to fulfil this objective, a new approach based on the mechanical properties of amorphous PLGA was studied and discussed.

The potential of PLGA molecular rearrangement was originally revealed by SEM images of incubated microspheres showing surface smoothing and external pore disappearance. The persistent and rapid changes of the particles' external morphology were attributed to the high molecular mobility initiated and sustained by the elevated temperature as well as the plasticizing effect of water. Surface remodelling via molecular rearrangement was therefore considered as a prospective method to reduce

surface porosity of selected microparticles. Microspheres made with FIII9'-10 and Triton X-100 were chosen for their high encapsulation efficiency and initial low surface porosity. Microspheres made with FIII9'-10 and PVA were used as a reference. The hydrophilic properties of the particles were first examined by DVS. It was found that the residual amount of Triton X-100 greatly enhanced the microspheres' hydrophilicity. Effectively, the small size of Triton X-100 molecules and their known miscibility with PLGA allowed for their infiltration in between PLGA chains. Therefore, additional free-volume was created and made available not only for water-vapour penetration, but also for side-group rotations of PLGA chains. Residual Triton X-100 molecules were also attributed the plasticizing effect responsible for reducing the *Tg* of the amorphous microspheres. This plasticization was advantageously used to further the molecular mobility in PLGA microspheres exposed to 75% relative humidity. It was anticipated that high level of molecular motion would promote surface remodelling to the point of pore closure which, ultimately, would be a major obstacle for protein release. In effect, not only the initial burst was significantly attenuated, but a second burst was also recorded after 8 weeks incubation probably as a result of internal remodelling.

Finally, further evaluation of the polymeric chain stability conducted over three months confirmed the stronger consistency of long PLGA chains over shorter ones. Also, it was found that the weaker mechanical integrity of short PLGA chains would benefit from less detrimental formulation parameters such as air-drying as opposed to freeze-drying. However, further research is necessary to offer a consistent understanding of PLGA mechanical behaviour.

Suggested future work

Over the course of this thesis, the role of PLGA mechanical properties was emphasised. Exposure to 75% relative humidity was proven an effective method to reduce the initial burst release. In order to conclusively verify this method, the integrity of the protein should be assessed again. As the initial burst release was influenced by the thermodynamic characteristics of the PLGA matrix, it is reasonable

to wonder if the rate of protein release is also dependent on the mechanical state of PLGA chains. The answer to that question could be deduced from a comparative analysis of the molecular mobility of particles made with low and high molecular weight PLGA against the drug release profile. If molecular activity and drug release increase concurrently, it may be the case that drug mobility is facilitated by side-group rotations of adjacent PLGA chains. In fact, the same could apply to the extraction of polymeric degradation products during polymer erosion. Additional analysis of microspheres' *Tg* and enthalpy relaxation over incubation time should be compared against mass and molecular weight loss of the polymeric microspheres.

Also, the molecular interactions between surfactant and drug/PLGA should be carefully examined as they have been proven to change the local environment of the drug. Although these interactions might affect the PLGA, more importantly they are generally detrimental to the protein. In effect, the protein conformation is often disturbed due to protein adsorption at the water/oil interface, even in the presence of stabilisers. It is important to understand the reasons why stabilisers may fail to protect the protein from irreversible damage. Causes such as competitive adsorption between drug and stabiliser at the water/oil interface should be expected and examined along with electrostatic interactions. Ideally, a thorough understanding of the molecular interactions between surfactant and drug/PLGA may help in explaining the relative easiness of microencapsulation of certain drugs over others.

Finally, extended work could focus on external and internal morphologies of particles in order to clearly determine the correlation between external porosity and initial burst release. Batches of microspheres characterised by a range of external porosity should be examined and their release profiles recorded. Analysis of the specific surface area and the average pore radius might also bring additional information. Ultimately, it would be interesting to analyse the internal morphology of microspheres during *in vitro* testing. Given the results obtained on microspheres exposed to high humidity, it would be advantageous to determine the link between internal structure remodelling and the possibility of a second burst release.

References

Adams, J. C. & F. M. Watt: Fibronectin Inhibits the Terminal Differentiation of Human Keratinocytes. *Nature* 1989, **340,** 307-309.

Akhtar, S. & K. J. Lewis: Antisense oligonucleotide delivery to cultured macrophages is improved by incorporation into sustained-release biodegradable polymer microspheres. *International Journal of Pharmaceutics* 1997, **151,** 57-67.

Ali, S. A. M., P. J. Doherty & D. F. Williams: Mechanism of polymer degradation in implantable devices. 2. Poly(DL-lactic acid). *Journal of Biomedical Materials Research* 1993, **27,** 1409-1418.

Altroff, H.: The role of FIII domains of Human Fibronectin in cell adhesion. In: *Nuffield department of obstrectics and gynaecology, University of Oxford.* University of Oxford, Oxford, 1999.

Altroff, H., L. Choulier & H. J. Mardon: Synergistic activity of the ninth and tenth FIII domains of human fibronectin depends upon structural stability. *Journal of Biological Chemistry* 2003, **278,** 491-497.

Altroff, H., C. F. van der Walle, J. Asselin, R. Fairless, I. D. Campbell & H. J. Mardon: The Eighth FIII Domain of Human Fibronectin Promotes Integrin Binding via Stabilization of the Ninth FIII Domain. *The Journal of Biological Chemistry* 2001, **276,** 38885-38892.

An, S. S. A., J. Jimenezbarbero, T. E. Petersen & M. Llinas: The 2 polypeptide-chains in fibronectin are joined in antiparallel fashion - NMR structural characterization. *Biochemistry* 1992, **31,** 9927-9933.

Andreozzi, L., M. Faetti, M. Giordano & D. Palazzuoli: Enthalpy relaxation of low molecular weight PMMA: a strategy to evaluate the Tool-Narayanaswamy-Moynihan model paramaters. *Journal of Physics: Condensed Matter* 2003, **15,** S1215-S1226.

Aplin, J. D., T. Haigh, C. J. P. Jones, H. J. Church & L. Vicovac: Development of cytotrophoblast columns from explanted first-trimester human placental villi: Role of fibronectin and integrin [alpha]5[beta]1. *Biology of Reproduction* 1999, **60,** 828-838.

Aso, Y., Y. Sumie, A. L. W. Po & T. Tadao: Effect of temperature on mechanisms of drug release and matrix degradation of poly(lactide) microspheres. *Journal of Controlled Release* 1994, **31,** 33-39.

Atkins, T. W., S. J. Peacock & D. J. Yates: Incorporation and release of vancomycin from poly(D,L-lactide-co-glycolide) microspheres. *Journal of Microencapsulation* 1998, **15,** 31-44.

Bailey, N. A., M. Sandor, M. Kreitz & E. Mathiowitz: Comparison of the enthalpic relaxation of poly(lactide-co-glycolide) 50:50 nanospheres and raw polymer. *Journal of Applied Polymer Science* 2002, **86,** 1868-1872.

Batycky, R. P., J. Hanes, R. Langer & D. A. Edwards: A theoretical model of erosion and macromolecular drug release from biodegrading microspheres. *Journal of Pharmaceutical Sciences* 1997, **86,** 1464-1477.

Beckerle, M. C.: Cell Adhesion. Ed.: B. D. H. a. D. M. Glover. Oxford University Press, 2001.

Beumer, G. J., C. A. van Blitterswijk & M. Ponec: Degradative behaviour of polymeric matrices in (sub)dermal and muscle tissue of the rat: a quantitative study. *Biomaterials* 1994, **15,** 551-559.

Bivas-Benita, M., S. Romeijn, H. E. Junginger & G. Borchard: PLGA-PEI nanoparticles for gene delivery to pulmonary epithelium. *European Journal of Pharmaceutics and Biopharmaceutics* 2004, **58,** 1-6.

Blanco, D. & M. J. Alonso: Protein encapsulation and release from poly(lactide-co-glycolide) microspheres: effect of the protein and polymer properties and of the co-encapsulation of surfactants. *European Journal of Pharmaceutics and Biopharmaceutics* 1998, **45,** 285-94.

Blanco-Prieto, M. J., K. Besseghir, P. Orsolini, F. Heimgartner, C. Deuschel, H. P. Merkle, H. Nam-Tran & B. Gander: Importance of the test medium for the release kinetics of a somatostatin analogue from poly(-lactide-co-glycolide) microspheres. *International Journal of Pharmaceutics* 1999, **184,** 243-250.

Bleich, J., B. W. Muller & W. Wassmus: Aerosol Solvent-Extraction System - a New Microparticle Production Technique. *International Journal of Pharmaceutics* 1993, **97,** 111-117.

Bouissou, C., U. Potter, H. Altroff, H. Mardon & C. van der Walle: Controlled release of the fibronectin central cell binding domain from polymeric microspheres. *Journal of Controlled Release* 2004, **95,** 557-566.

Boury, F., T. Ivanova, I. Panaiotov, J. E. Proust, A. Bois & J. Richou: Dynamic Properties of Poly(DL-lactide) and Polyvinyl Alcohol Monolayers at the Air/Water and Dichloromethane/Water Interfaces. *Journal of Colloid and Interface Science* 1995, **169,** 380-392.

Buckton, G. & P. Darcy: Water mobility in amorphous lactose below and close to the glass transition temperature. *International Journal of Pharmaceutics* 1996, **136,** 141-146.

Burkersroda, F. v., L. Schedl & A. Gopferich: Why degradable polymers undergo surface erosion or bulk erosion. *Biomaterials* 2002, **23,** 4221-4231.

Campbell, N. A. & J. B. Reece: Biology. Pearson/Benjamin Cummings, 1947.

Capan, Y., B. H. Woo, S. Gebrekidan, S. Ahmed & P. P. DeLuca: Influence of formulation parameters on the characteristics of poly(lactide-co-glycolide) microspheres containing poly(lysine) complexed plasmid DNA. *Journal of Controlled Release* 1999, **60,** 279-286.

Castellanos, I. J. & K. Griebenow: Improved -Chymotrypsin Stability Upon Encapsulation in PLGA Microspheres by Solvent Replacement. *Pharmaceutical Research* 2003, **20,** 1873-1880(8).

Chartoff, R. P.: Thermoplastic polymers. In: *Thermal Characterization of Polymeric Materials*. Ed.: E. A. Turi. Academic Press, San Diego, 1997, pp. 551-554.

Chew, N. Y. K. & H. K. Chan: Influence of particle size, air flow, and inhaler device on the dispersion of mannitol powders as aerosols. *Pharmaceutical Research* 1999, **16,** 1098-1103.

Chew, N. Y. K. & H. K. Chan: Use of solid corrugated particles to enhance powder aerosol performance. *Pharmaceutical Research* 2001, **18,** 1570-1577.

Chung, Y. M., K. L. Simmons, A. Gutowska & B. Jeong: Sol-gel transition temperature of PLGA-g-PEG aqueous solutions. *Biomacromolecules* 2002, **3,** 511-516.

Clark, E. A. & J. S. Brugge: Integrins and signal-transduction pathways - the road taken. *Science* 1995, **268,** 233-239.

Cleland, J. L.: Protein Delivery from Biodegradable Microspheres. In: *Pharmaceutical Biotechnology*, 1997, pp. 1-43.

Cleland, J. L., A. Lim, L. Barron, E. T. Duenas & M. F. Powell: Development of a single-shot subunit vaccine for HIV-1 .4. Optimizing microencapsulation and pulsatile release of MN rgp120 from biodegradable microspheres. *Journal of Controlled Release* 1997, **47,** 135-150.

Cohen, S., T. Yoshioka, M. Lucarelli, L. H. Hwang & R. Langer: Controlled Delivery Systems for Proteins Based on Poly(Lactic/Glycolic Acid) Microspheres. *Pharmaceutical Research* 1991, **8,** 713-720(8).

Coombes, A. G. A., M. K. Yeh, E. C. Lavelle & S. S. Davis: The control of protein release from poly(DL-lactide co-glycolide) microparticles by variation of the external aqueous phase surfactant in the water-in oil-in water method. *Journal of Controlled Release* 1998, **52,** 311-320.

Cowie, J. M. G. & R. Ferguson: The Ageing of Poly(vinyl methyl ether) as Determined from Enthalpy Relaxation Measurements. *Polymer Communications* 1986, **27,** 258-260.

Crotts, G. & T. G. Park: Preparation of porous and nonporous biodegradable polymeric hollow microspheres. *Journal of Controlled Release* 1995, **35,** 91-105.

Crotts, G., H. Sah & T. G. Park: Adsorption determines *in-vitro* protein release rate from biodegradable microspheres: quantitative analysis of surface area during degradation. *Journal of Controlled Release* 1997, **47,** 101-111.

Cutler, S. M. & A. J. Garcia: Engineering cell adhesive surfaces that direct integrin [alpha]5[beta]1 binding using a recombinant fragment of fibronectin. *Biomaterials* 2003, **24,** 1759-1770.

De, S. & D. H. Robinson: Particle size and temperature effect on the physical stability of PLGA nanospheres and microspheres containing Bodipy. *AAPS PharmSciTech.* 2004, **13,** 1-7.

Deng, M. & K. E. Uhrich: Effects of in vitro degradation on properties of poly(DL-lactide-co-glycolide) pertinent to its biological performance. *Journal of Materials Science: Materials in Medicine* 2002, **13,** 1091-1096(6).

Deng, X. M., X. H. Li, M. L. Yuan, C. D. Xiong, Z. T. Huang, W. X. Jia & Y. H. Zhang: Optimization of preparative conditions for poly-DL-lactide-polyethylene glycol microspheres with entrapped *Vibrio Cholera* antigens. *Journal of Controlled Release* 1999, **58,** 123-131.

Desai, M. P., V. Labhasetwar, E. Walter, R. J. Levy & G. L. Amidon: The mechanism of uptake of biodegradable microparticles in Caco-2 cells is size dependent. *Pharmaceutical Research* 1997, **14,** 1568-1573(6).

Dobry, A. & F. Boyer-Kawenoki: Phase separation in polymer solution. *Journal of Polymer Science* 1947, **2,** 90-100.

Dunn, R. L., G. L. Yewey, S. M. Fujita, K. R. Josephs, S. L. Whitman, G. L. Southard, W. S. Dernell, R. C. Straw, S. J. Withrow & B. E. Powers: Sustained release of cisplatin in dogs from an injectable implant delivery system. *Journal of Bioactive and Compatible Polymers* 1996, **11,** 286-300.

Eckert, C. A., B. L. Knutson & P. G. Debenedetti: Supercritical fluids as solvents for chemical and materials processing. *Nature* 1996, **383,** 313-318.

Ehtezazi, T., C. Washington & C. D. Melia: First order release rate from porous PLA microspheres with limited exit holes on the exterior surface. *Journal of Controlled Release* 2000, **66,** 27-38.

Florence, A. T.: The Oral Absorption of Micro- and Nanoparticulates: Neither Exceptional Nor Unusual. *Pharmaceutical Research* 1997, **14,** 259-266(8).

Florence, A. T. & D. Whitehill: Some Features of Breakdown in Water-in-Oil-in-Water Multiple Emulsions. *Journal of Colloid and Interface Science* 1981, **79,** 243-256.

Ford, J. L. & P. Timmins: Pharmaceutical Thermal Analysis (Techniques and Applications). Ellis Horwood, 1989.

Freitas, S., H. P. Merkle & B. Gander: Microencapsulation by solvent extraction/evaporation: reviewing the state of the art of microsphere preparation process technology. *Journal of Controlled Release* 2005, **102,** 313-332.

Friess, W. & M. Schlapp: Release mechanisms from gentamicin loaded poly(lactic-co-glycolic acid) (PLGA) microparticles. *Journal of Pharmaceutical Sciences* 2002, **91,** 845-855.

Fu, K., D. W. Pack, A. M. Klibanov & R. Langer: Visual Evidence of Acidic Environment Within Degrading Poly(lactic-co-glycolic acid) (PLGA) Microspheres. *Pharmaceutical Research* 2000, **17,** 100-106(7).

Fu, Y. J., F. L. Mi, T. B. Wong & S. S. Shyu: Characteristic and controlled release of anticancer drug loaded poly (D,L-lactide) microparticles prepared by spray drying technique. *Journal of Microencapsulation* 2001, **18,** 733-747.

Gavini, E., P. Chetoni, M. Cossu, M. G. Alvarez, M. F. Saettone & P. Giunchedi: PLGA microspheres for the ocular delivery of a peptide drug, vancomycin using emulsification/spray-drying as the preparation method: *in vitro/in vivo* studies. *European Journal of Pharmaceutics and Biopharmaceutics* 2004, **57,** 207-212.

Giancotti, F. G. & E. Ruoslahti: Transduction - Integrin signaling. *Science* 1999, **285,** 1028-1032.

Gopferich, A.: Mechanisms of polymer degradation and erosion. *Biomaterials* 1996, **17,** 103-114.

Göpferich, A.: Polymer Bulk Erosion. *Macromolecules* 1997, **30,** 2598-2604.

Gopferich, A. & R. Langer: Modeling monomer release from bioerodible polymers. *Journal of Controlled Release* 1995, **33,** 55-69.

Grant, R. P., H. Altroff, H. J. Mardon, C. Spitzfaden & I. D. Campbell: Structural requirements for biological activity of the ninth and tenth FIII domains of human fibronectin. *Journal of Biological Chemistry* 1997, **272,** 6159-6166.

Hancock, B. C., S. L. Shamblin & G. Zografi: Molecular Mobility of Amorphous Pharmaceutical Solids Below Their Glass-Transition Temperatures. *Pharmaceutical Research* 1995, **12,** 799-806.

Hancock, B. C., P. York & R. C. Rowe: The use of solubility parameters in pharmaceutical dosage form design. *International Journal of Pharmaceutics* 1997, **148,** 1-21.

Hancock, B. C. & G. Zografi: The Relationship Between the Glass Transition Temperature and the Water Content of Amorphous Pharmaceutical Solids. *Pharmaceutical Research* 1994, **11,** 471-477(7).

Hancock, B. C. & G. Zografi: Characteristics and significance of the amorphous state in pharmaceutical systems. *Journal of Pharmaceutical Sciences* 1997, **86,** 1-12.

Hannigan, G. E., C. LeungHagesteijn, L. FitzGibbon, M. G. Coppolino, G. Radeva, J. Filmus, J. C. Bell & S. Dedhar: Regulation of cell adhesion and anchorage-dependent growth by a new beta(1)-integrin-linked protein kinase. *Nature* 1996, **379,** 91-96.

Hatefi, A. & B. Amsden: Biodegradable injectable in situ forming drug delivery systems. *Journal of Controlled Release* 2002, **80,** 9-28.

Hibbs, M. L., S. Jakes, S. A. Stacker, R. W. Wallace & T. A. Springer: The Cytoplasmic Domain of the Integrin Lymphocyte Function-Associated Antigen-1 Beta-Subunit - Sites Required for Binding to Intercellular-Adhesion Molecule-1 and the Phorbol Ester Stimulated Phosphorylation Site. *Journal of Experimental Medicine* 1991, **174,** 1227-1238.

Hodge, I.: Enthalpy relaxation and recovery in aorphous mterials. *Journal of Non-Crystalline Solids* 1994, **169,** 211-266.

Homayoun, P., T. Mandal, D. Landry & H. Komiskey: Controlled release of anti-cocaine catalytic antibody from biodegradable polymer microspheres. *J Pharm Pharmacol.* 2003, **55,** 933-8.

Hora, H. S., R. K. Rana, J. H. Nunberg, T. R. Tice, R. M. Gilley & M. E. Hudson: Release of human serum albumin from poly(latice-co-glycolide) microspheres. *Pharm. Res.* 1990, **7,** 1190-1194.

Huang, X. & C. S. Brazel: On the importance and mechanisms of burst release in matrix-controlled drug delivery systems. *Journal of Controlled Release* 2001, **73,** 121-136.

Humphries, M. J., P. A. McEwan, S. J. Barton, P. A. Buckley, J. Bella & A. P. Mould: Integrin structure: heady advances in ligand binding, but activation still makes the knees wobble. *Trends in Biochemical Sciences* 2003, **28,** 313-320.

Hunter, J. R., R. G. Carbonell & P. K. Kilpatrick: Coadsorption and exchange of Lysozyme/β-Casein mixtures at the air/water interface. *Journal of Colloid and Interface Science* 1991, **143,** 37-53.

Hunter, J. R., P. K. Kilpatrick & R. G. Carbonell: Lysozyme adsorption at the air/water interface. *Journal of Colloid and Interface Science* 1990, **137,** 462-482.

Husmann, M., S. Schenderlein, M. Luck, H. Lindner & P. Kleinebudde: Polymer erosion in PLGA microparticles produced by phase separation method. *International Journal of Pharmaceutics* 2002, **242,** 277-280.

Jain, R. A.: The manufacturing techniques of various drug loaded biodegradable poly(lactide-co-glycolide) (PLGA) devices. *Biomaterials* 2000, **21,** 2475-2490.

Jeffery, H., S. S. Davis & D. T. O'hagan: The Preparation and Characterization of Poly(Lactide-Co-Glycolide) Microparticles .1. Oil-in-Water Emulsion Solvent Evaporation. *International Journal of Pharmaceutics* 1991, **77,** 169-175.

Jeffery, H., S. S. Davis & D. T. O'Hagan: The preparation and characterization of poly(lactide-co-glycolide) microparticles. II. The entrapment of a model protein using a (water-in-oil)-in-water emulsion solvent evaporation technique. *Pharm Res* 1993, **10,** 362-8.

Jeong, J. H., D. W. Lim, D. K. Han & T. G. Park: Synthesis, Characterization, and Protein Adsorption Behaviors of PLGA/PEG Di-block Copolymer Blend Films. *Colloids and Surfaces B: Biointerfaces* 2000, **18,** 371-379.

Jeyanthi, R., B. C. Thanoo, R. C. Metha & P. P. Deluca: Effect of solvent removal technique on the matrix characteristics of polylactide/glycolide microspheres for peptide delivery. *Journal of Controlled Release* 1996, **38,** 235-244.

Jiang, G., B. H. Woo, F. Kang, J. Singh & P. P. DeLuca: Assessment of protein release kinetics, stability and protein polymer interaction of lysozyme encapsulated poly(lactide-co-glycolide) microspheres. *Journal of Controlled Release* 2002, **79,** 137-145.

Johansen, P., Y. Men, H. P. Merkle & B. Gander: Revisiting PLA/PLGA microspheres: an analysis of their potential in parenteral vaccination. *European Journal of Pharmaceutics and Biopharmaceutics* 2000, **50,** 129-146.

Johnson, K. E., T. Darribere & J. C. Boucaut: Ambystoma-maculatum gastrulae have an oriented fibronectin-containing extracellular-matrix. *Journal of Experimental Zoology* 1992, **261,** 458-471.

Johnson, K. J., H. Sage, G. Briscoe & H. P. Erickson: The compact conformation of fibronectin is determined by intramolecular ionic interactions. *Journal of Biological Chemistry* 1999, **274,** 15473-15479.

Johnson, O. L. & M. A. Tracy: Peptides and proteins drug delivery. In: *Encyclopedia of Controlled Drug Delivery.* Ed.: E. Mathiowitz. Wiley, New York, 1999, pp. 823-826.

Kang, F. R., G. Jiang, A. Hinderliter, P. P. DeLuca & J. Singh: Lysozyme stability in primary emulsion for PLGA microsphere preparation: Effect of recovery methods and stabilizing excipients. *Pharmaceutical Research* 2002, **19,** 629-633.

Kauzmann, W.: The nature of the glassy state and the behaviour of liquids at low temperatures. *Chem Rev* 1948, **43,** 219-256.

Kelly, T., L. Molony & K. Burridge: Purification of 2 smooth-muscle glycoproteins related to integrin - distribution in cultured chicken-embryo fibroblasts. *Journal of Biological Chemistry* 1987, **262,** 17189-17199.

Kim, H. K. & T. G. Park: Microencapsulation of human growth hormone within biodegradable polyester microspheres: Protein aggregation stability and incomplete release mechanism. *Biotechnology and Bioengineering* 1999, **65,** 659-667.

Kim, H. K. & T. G. Park: Comparative study on sustained release of human growth hormone from semi-crystalline poly(lactic acid) and amorphous poly(lactic-co-glycolic acid) microspheres: morphological effect on protein release. *Journal of Controlled Release* 2004a, **98,** 115-125.

Kim, T. H. & T. G. Park: Critical effect of freezing/freeze-drying on sustained release of FITC-dextran encapsulated within PLGA microspheres. *International Journal of Pharmaceutics* 2004b, **271,** 207-214.

Kitchell, J. & D. Wise: Poly(lactic/glycolic acid) biodegradable drug-polymer matrix systems. *Methods Enzymol.* 1985, **112,** 436-48.

Kranz, H., N. Ubrich, P. Maincent & R. Bodmeier: Physicomechanical properties of biodegradable poly(D,L-lactide) and poly(D,L-lactide-co-glycolide) films in the dry and wet states. *Journal of Pharmaceutical Sciences* 2000, **89,** 1558-1566.

Kreis, T. & R. Vale: Guidebook to the extracellular matrix, anchor, and adhesion proteins. Oxford University Press, 1999.

Kubo, M., M. Kan, M. Isemura, I. Yamane & H. Tagami: Effects of Extracellular Matrices on Human Keratinocyte Adhesion and Growth and on Its Secretion and Deposition of Fibronectin in Culture. *Journal of Investigative Dermatology* 1987, **88,** 594-601.

Laemmli, U. K.: Cleavage of structural proteins during assembly of head of bacteriophage-T4. *Nature* 1970, **227,** 680-&.

Laflamme, S. E., L. A. Thomas, S. S. Yamada & K. M. Yamada: Single subunit chimeric integrins as mimics and inhibitors of endogenous integrin functions in receptor localization, cell spreading and migration, and matrix assembly. *Journal of Cell Biology* 1994, **126,** 1287-1298.

Lamarre, L. & C. Sung: Studies of physical aging and molecular motion by azochromophoric labels attached to the main chains of amorphous polymers. *Macromolecules* 1983, **16,** 1729-1736.

Lambert, W. J. & K. D. Peck: Development of an in situ forming biodegradable poly-lactide-coglycolide system for the controlled release of proteins. *Journal of Controlled Release* 1995, **33,** 189-195.

Le Corre, P., V. Gajan, F. Chevanne, R. Le Verge & J. H. Rytting: *In vitro* controlled release kinetics of local anaesthetics from poly(D,L-lactide) and poly(lactide-co-glycolide) microspheres. *Journal of Microencapsulation* 1997, **14,** 243-255.

Leahy, D. J., I. Aukhil & H. P. Erickson: 2.0 angstrom crystal structure of a four-domain segment of human fibronectin encompassing the RGD loop and synergy region. *Cell* 1996, **84,** 155-164.

Lechuga-Ballesteros, D., A. Bakri & D. P. Miller: Microcalorimetric measurement of the interactions between water vapor and amorphous pharmaceutical solids. *Pharmaceutical Research* 2003, **20,** 308-318.

Lee, H. J.: Biopharmaceutical properties and pharmacokinetics of peptide and protein drugs. In: *Peptide-based Drug Design Controlling Transport and Metabolism.* Eds.: M. D. Taylor and G. L. Amidon. American Chemical Society, Washington, 1995, pp. 69-91.

Lee, T. H., J. Wang & C.-H. Wang: Double-walled microspheres for the sustained release of a highly water soluble drug: characterization and irradiation studies. *Journal of Controlled Release* 2002, **83,** 437-452.

Lemaire, V., J. Belair & P. Hildgen: Structural modeling of drug release from biodegradable porous matrices based on a combined diffusion/erosion process. *International Journal of Pharmaceutics* 2003, **258,** 95-107.

Li, W.-I., K. W. Anderson, R. C. Mehta & P. P. Deluca: Prediction of solvent removal profile and effect on properties for peptide-loaded PLGA microspheres prepared by solvent extraction/ evaporation method. *Journal of Controlled Release* 1995, **37,** 199-214.

Lin, R. Y., L. S. Ng & C. H. Wang: In vitro study of anticancer drug doxorubicin in PLGA-based microparticles. *Biomaterials* 2005, **26,** 4476-4485.

Liu, D. Z., W. P. Chen, C. P. Lee, S. L. Wu, Y. C. Wang & T. W. Chung: Effects of alginate coated on PLGA microspheres for delivery tetracycline hydrochloride to periodontal pockets. *Journal of Microencapsulation* 2004, **21,** 643-652.

Mandal, T., L. Bostanian, R. Graves, S. Chapman & I. Womack: Development of biodegradable microcapsules as carrier for oral controlled delivery of amifostine. *Drug Dev Ind Pharm.* 2002a, **28,** 339-44.

Mandal, T. K., L. A. Bostanian, R. A. Graves & S. R. Chapman: Poly(d,l-lactide-co-glycolide) encapsulated poly(vinyl alcohol) hydrogel as a drug delivery system. *Pharmaceutical Research* 2002b, **19,** 1713-1719(7).

Mathiowitz, E., J. S. Jacob, Y. S. Jong, G. P. Carino, D. E. Chickering, P. Chaturvedi, C. A. Santos, K. Vijayaraghavan, S. Montgomery, M. Bassett & C. Morrell: Biologically erodable microspheres as potential oral drug delivery systems. *Nature* 1997, **386,** 410-4.

Mathiowitz, E. & R. S. Langer: Preparation of multiwall polymeric microparticles, US, 1989.

Matschke, C., U. Isele, P. van Hoogevest & A. Fahr: Sustained-release injectables formed in situ and their potential use for veterinary products. *Journal of Controlled Release* 2002, **85,** 1-15.

Mehta, R. C., B. C. Thanoo & P. P. Deluca: Peptide containing microspheres from low molecular weight and hydrophilic poly(d,l-lactide-co-glycolide). *Journal of Controlled Release* 1996, **41,** 249-257.

Messaritaki, A., S. J. Black, C. F. van der Walle & S. P. Rigby: NMR and confocal microscopy studies of the mechanisms of burst drug release from PLGA microspheres. *Journal of Controlled Release* 2005, **108,** 271-281.

Middelberg, A. P. J., C. J. Radke & H. W. Blanch: Peptide interfacial adsorption is kinetically limited by the thermodynamic stability of self association. *Proceedings of the National Academy of Sciences of the United States of America* 2000, **97,** 5054-5059.

Mohamed, F. & C. F. van der Walle: PLGA microcapsules with novel dimpled surfaces for pulmonary delivery of DNA. *International Journal of Pharmaceutics* 2006, **311,** 97-107.

Morlock, M., H. Koll, G. Winter & T. Kissel: Microencapsulation of rh-erythropoietin, using biodegradable poly(lactide-co-glycolide): protein stability and the effects of stabilizing excipients. *European Journal of Pharmaceutics and Biopharmaceutics* 1997, **43,** 29-36.

Mosesson, M. W. & D. L. Amrani: The Structure and Biologic Activities of Plasma Fibronectin. *Blood* 1980, **56,** 145-158.

Nagai, T., N. Yamakawa, S. Aota, S. S. Yamada, S. K. Akiyama, K. Olden & K. M. Yamada: Monoclonal-Antibody Characterization of 2 Distant Sites Required for Function of the Central Cell-Binding Domain of Fibronectin in Cell-Adhesion, Cell-Migration, and Matrix Assembly. *Journal of Cell Biology* 1991, **114,** 1295-1305.

Nam, Y. S. & T. Park Protein loaded biodegradable microspheres based on PLGA-protein bioconjugates. *Journal of Macroencapsulation* 1999, **16,** 625-637.

Nihant, N., C. Schugens, C. Grandfils, R. Jerome & P. Teyssie: Polylactide Microparticles Prepared by Double Emulsion/Evaporation Technique .1. Effect of Primary Emulsion Stability. *Pharmaceutical Research* 1994a, **11,** 1479-1484.

Nihant, N., S. Stassen, C. Grandfils, R. Jerome & P. Teyssie: Microencapsulation by Coacervation of Poly(Lactide-Co-Glycolide) .2. Encapsulation of a Dispersed Aqueous-Phase. *Polymer International* 1993, **32,** 171-176.

Nihant, N., S. Stassen, C. Grandfils, R. Jerome, P. Teyssie & G. Goffinet: Microencapsulation by Coacervation of Poly(Lactide-Co-Glycolide) .3. Characterization of the Final Microspheres. *Polymer International* 1994b, **34,** 289-299.

O'Brien, F. E. M.: The control of humidity by saturated salt solutions-a compilation of data. *J. Sci. Instr* 1948, **25,** 73-76.

Oh, J. E., Y. S. Nam, K. H. Lee & T. G. Park: Conjugation of drug to poly(lactic-co-glycolic acid) for controlled release from biodegradable microspheres. *Journal of Controlled Release* 1999, **57,** 269-280.

Oksanen, C. A. & G. Zografi: The Relationship Between the Glass Transition Temperature and Water Vapor Absorption by Poly(vinylpyrrolidone). *Pharmaceutical Research* 1990, **7,** 654 - 657.

Oksanen, C. A. & G. Zografi: Molecular Mobility in Mixtures of Absorbed Water and Solid Poly(vinylpyrrolidone). *Pharmaceutical Research* 1993, **10,** 791-799(9).

Okumu, F. W., J. L. Cleland & R. T. Borchardt: The effect of size, charge and cyclization of model peptides on their in vitro release from DL-PLGA microspheres. *Journal of Controlled Release* 1997, **49,** 133-140.

Park, T. G.: Degradation of poly(lactic-co-glycolic acid) microspheres: effect of copolymer composition. *Biomaterials* 1995, **16,** 1123-1130.

Park, T. G., W. Lu & G. Crotts: Importance of *in vitro* experimental conditions on protein release kinetics, stability and polymer degradation in protein encapsulated poly (lactic acid-co-glycolic acid) microspheres. *Journal of Controlled Release* 1995, **33,** 211-222.

Passerini, N. & D. Q. M. Craig: An investigation into the effects of residual water on the glass transition temperature of polylactide microspheres using modulated temperature DSC. *Journal of Controlled Release* 2001, **73,** 111-115.

Pekarek, K. J., J. S. Jacob & E. Mathiowitz: Double-walled polymer microspheres for controlled drug release. *Nature* 1994, **367,** 258-260.

Perez, C., P. De Jesus & K. Griebenow: Preservation of lysozyme structure and function upon encapsulation and release from poly(lactic-co-glycolic) acid microspheres prepared by the water-in-oil-in-water method. *International Journal of Pharmaceutics* 2002, **248,** 193-206.

Peyre, M., D. Sesardic, H. P. Merkle, B. Gander & P. Johansen: An experimental divalent vaccine based on biodegradable microspheres induces protective immunity against tetanus and diphteria. *Journal of Pharmaceutical Sciences* 2003, **92,** 957-966.

Pierschbacher, M. D. & E. Ruoslahti: Cell attachment activity of fibronectin can be duplicated by small synthetic fragments of the molecule. *Nature* 1984, **309,** 30-33.

Pistel, K. F., A. Breitenbach, R. Zange-Volland & T. Kissel: Brush-like branched biodegradable polyesters, part III - Protein release from microspheres of poly(vinyl alcohol)-graft- poly(D,L-lactic-co-glycolic acid). *Journal of Controlled Release* 2001, **73,** 7-20.

Pistner, H., D. R. Bendi, J. Mühling & J. F. Reuther: Poly(lactide): a long-term degradation study in vivo. Part III. Analytical characterization. *Biomaterials* 1993, **14,** 291-298.

Pozuelo, J. & J. Baselga: Glass transition temperature of low molecular weight poly(3-aminopropyl methyl siloxane). A molecular dynamics study. *Polymer* 2002, **43,** 6049-6055.

Prabha, S., W. Z. Zhou, J. Panyam & V. Labhasetwar: Size-dependency of nanoparticle-mediated gene transfection: studies with fractionated nanoparticles. *International Journal of Pharmaceutics* 2002, **244,** 105-115.

Radomsky, M. L., G. Brouwer, B. J. Floy, D. J. Loury, F. Chu, A. J. Tipton & L. M. Sanders: The controlled release of ganirelix from the ATRIGEL(TM) injectable implant system. *Proceedings of the Controlled Release Society* 1993, 458-459.

Rafati, H., A. G. A. Coombes, J. Adler, J. Holland & S. S. Davis: Protein-loaded poly(DL-lactide-co-glycolide) microparticles for oral administration: Formulation, structural and release characteristics. *Journal of Controlled Release* 1997, **43,** 89-102.

Randolph, T. W., A. D. Randolph, M. Mebes & S. Yeung: Sub-micrometer-sized biodegradable particles of poly(L-lactic acid) via the gas antisolvent spray precipitation process. *Biotechnology Progress* 1993, **9,** 429-435.

Ravvarapu, H. B., K. L. Moyer & R. L. Dunn: Sustained suppression of pituitary-gonadal axis with an injectable, *in situ* forming implant of leuprolide acetate. *Journal of Pharmaceutical Sciences* 2000, **89,** 732-741.

Rojas, J., H. Pinto-Alphandary, E. Leo, S. Pecquet, P. Couvreur, A. Gulik & E. Fattal: A polysorbate-based non-ionic surfactant can modulate loading and release of beta-lactoglobulin entrapped in multiphase poly(DL-lactide-co-glycolide) microspheres. *Pharmaceutical Research* 1999, **16,** 255-260.

Royall, P. G., D. Q. M. Craig & C. Doherty: Characterisation of the Glass Transition of an Amorphous Drug Using Modulated DSC. *Pharmaceutical Research* 1998, **15,** 1117-1121(5).

Royall, P. G., D. Q. M. Craig & C. Doherty: Characterisation of moisture uptake effects on the glass transitional behaviour of an amorphous drug using modulated temperature DSC. *International Journal of Pharmaceutics* 1999, **192,** 39-46.

Ruiz, J.-M., J.-P. Busnel & J.-P. Benoît: Influence of Average Molecular Weights of Poly(DL-Lactic Acid-Co-Glycolic Acid) Copolymers 50/50 on Phase Separation and in Vitro Drug Release from Microspheres. *Pharmaceutical Research* 1990, **7,** 928 - 934.

Ruoslahti, E.: RGD and other recognition sequences for integrins. *Annual Review of Cell and Developmental Biology* 1996, **12,** 697-715.

Sah, H.: A new strategy to determine the actual protein content of poly(lactide-co-glycolide) microspheres. *J Pharm Sci* 1997, **86,** 1315-8.

Sah, H.: Protein behavior at the water/methylene chloride interface. *J Pharm Sci* 1999a, **88,** 1320-5.

Sah, H.: Stabilization of proteins against methylene chloride/water interface-induced denaturation and aggregation. *J Control Release* 1999b, **58,** 143-51.

Sahoo, S. K., J. Panyam, S. Prabha & V. Labhasetwar: Residual polyvinyl alcohol associated with poly (lactide-co-glycolide) nanoparticles affects their physical properties and cellular uptake. *Journal of Controlled Release* 2002, **82,** 105-114.

Sambrook, J., D. W. Russell & J. Sambrook: Molecular Cloning: A Laboratory Manual. Cold Spring Harbor Laboratory Press, Cold Spring Harbor, 2001, pp. 999.

Sanchez, I. C.: Physics of Polymer Surfaces and Interfaces. Butterworth - Heinemann, 1992.

Sandor, M., N. A. Bailey & E. Mathiowitz: Characterization of polyanhydride microsphere degradation by DSC. *Polymer* 2002, **43,** 279-288.

Sandor, M., D. Enscore, P. Weston & E. Mathiowitz: Effect of protein molecular weight on release from micron-sized PLGA microspheres. *J Control Release* 2001, **76,** 297-311.

Sansdrap, P., J. Fontaine & A. J. Moes: Nifedipine-loaded PLGA microspheres: In vitro/in vivo comparison of drug release and polymer degradation. *S.T.P. Pharma Sciences* 1999, **9,** 443-446.

Schlapp, M. & W. Friess: Collagen/PLGA microparticle composites for local controlled delivery of gentamicin. *Journal of Pharmaceutical Sciences* 2003, **92,** 2145-51.

Schlicher, E. J. A. M., N. S. Postma, J. Zuidema, H. Talsma & W. E. Hennink: Preparation and characterisation of Poly(lactic-co-glycolic acid) microspheres containing desferrioxamine. *International Journal of Pharmaceutics* 1997, **153,** 235-245.

Schugens, C., N. Laruelle, N. Nihant, C. Grandfils, R. Jerome & P. Teyssie: Effect of the Emulsion Stability on the Morphology and Porosity of Semicrystalline Poly L-Lactide Microparticles Prepared by W/O/W Double Emulsion-Evaporation. *Journal of Controlled Release* 1994, **32,** 161-176.

Sertsou, G., J. Butler, J. Hempenstall & T. Rades: Physical stability and enthalpy relaxation of drug-hydroxypropyl methylcellulose phthalate solvent change co-precipitates. *Journal of Pharmacy and Pharmacology* 2003, **55,** 35-41.

Shakesheff, K. M., C. Evora, I. Soriano & R. Langer: The Adsorption of Poly(vinyl alcohol) to Biodegradable Microparticles Studied by X-Ray Photoelectron Spectroscopy (XPS). *Journal of Colloid and Interface Science* 1997, **185,** 538-547.

Shamblin, S. L., B. C. Hancock, Y. Dupuis & M. J. Pikal: Interpretation of relaxation time constants for amorphous pharmaceutical systems. *Journal of Pharmaceutical Sciences* 1999, **89,** 417-427.

Shamblin, S. L., E. Y. Huang & G. Zografi: The effects of co-lyophilized polymeric additives on the glass transition temperature and crystallization of amorphous sucrose. *Journal of Thermal Analysis* 1996, **47,** 1567-1579.

Sharp, J. S., J. A. Forrest & R. A. L. Jones: Swelling of Poly(DL-lactide) and polylactide-co-glycolide in humid environments. *Macromolecules* 2001, **34,** 8752-8760.

Shih, C., N. Waldron & G. M. Zentner: Quantitative analysis of ester linkages in poly(-lactide) and poly(-lactide-co-glycolide). *Journal of Controlled Release* 1996, **38,** 69-73.

Shively, M. L., B. A. Coonts, W. D. Renner, J. L. Southard & A. T. Bennett: Physico-chemical characterization of a polymeric injectable implant delivery system. *Journal of Controlled Release* 1995, **33,** 237-243.

Siepmann, J. & A. Gopferich: Mathematical modeling of bioerodible, polymeric drug delivery systems. *Advanced Drug Delivery Reviews* 2001, **48,** 229-247.

Skorstengaard, K., H. C. Thogersen & T. E. Petersen: Complete Primary Structure of the Collagen-Binding Domain of Bovine Fibronectin. *European Journal of Biochemistry* 1984, **140,** 235-243.

Steendam, R., M. J. van Steenbergen, W. E. Hennink, H. W. Frijlink & C. F. Lerk: Effect of molecular weight and glass transition on relaxation and release behaviour of poly(DL-lactic acid) tablets. *Journal of Controlled Release* 2001, **70,** 71-82.

Stenman, S. & A. Vaheri: Distribution of a Major Connective-Tissue Protein, Fibronectin, in Normal Human Tissues. *Journal of Experimental Medicine* 1978, **147,** 1054-1064.

Suarez, S., P. O'Hara, M. Kazantseva, C. E. Newcomer, R. Hopfer, D. N. McMurray & A. J. Hickey: Respirable PLGA microspheres containing rifampicin for the treatment of tuberculosis: screening in an infectious disease model. *Pharmaceutical Research* 2001, **18,** 1315-1319(5).

Subramaniam, B., R. A. Rajewski & K. Snavely: Pharmaceutical processing with supercritical carbon dioxide. *Journal of Pharmaceutical Sciences* 1997, **86,** 885-890.

Thomasin, C., P. Johansen, R. Alder, R. Bemsel, G. Hottinger, H. Altorfer, A. D. Wright, G. Wehrli, H. P. Merkle & B. Gander: A contribution to overcoming the problem of residual solvents in biodegradable microspheres prepared by coacervation. *European Journal of Pharmaceutics and Biopharmaceutics* 1996, **42,** 16-24.

Thomasin, C., H. P. Merkle & B. Gander: Drug microencapsulation by PLA/PLGA coacervation in the light of thermodynamics. 2. Parameters determining microsphere formation. *Journal of Pharmaceutical Sciences* 1998, **87,** 269-275.

Tice, T. R. & D. R. Cowsar: Biodegradable controlled-release parenteral systems. *Pharm Technol* 1984, **11,** 26-35.

Tsung, M. J. & D. J. Burgess: Preparation and characterization of gelatin surface modified PLGA microspheres. *Aaps Pharmsci* 2001, **3,** art. no.-11.

van de Weert, M., W. E. Hennink & W. Jiskoot: Protein instability in poly(lactic-co-glycolic acid) microparticles. *Pharm Res* 2000a, **17,** 1159-67.

van de Weert, M., J. Hoechstetter, W. E. Hennink & D. J. Crommelin: The effect of a water/organic solvent interface on the structural stability of lysozyme. *J Control Release* 2000b, **68,** 351-9.

van de Weert, M., R. van 't Hof, J. van der Weerd, R. M. A. Heeren, G. Posthuma, W. E. Hennink & D. J. A. Crommelin: Lysozyme distribution and conformation in a biodegradable polymer matrix as determined by FTIR techniques. *Journal of Controlled Release* 2000c, **68,** 31-40.

Van den Mooter, G., P. Augustijns & R. Kinget: Stability prediction of amorphous benzodiazepines by calculation of the mean relaxation time constant using the Williams-Watts decay function. *European Journal of Pharmaceutics and Biopharmaceutics* 1999, **48,** 43-48.

Van der Walle, C. F., H. Altroff & H. J. Mardon: Novel mutant fibronectin FIII 9-10 domain pair with increased conformational stability and biological activity. *Protein Engineering* 2002, **15,** 1021-1024.

van der Walle, C. F., H. Altroff & H. J. Mardon: Novel mutant human fibronectin FIII9-10 domain pair with increased conformational stability and biological activity. *Protein Engineering* 2002, **15,** 1021-1024.

Walter, E., D. Dreher, M. Kok, L. Thiele, S. G. Kiama, P. Gehr & H. P. Merkle: Hydrophilic poly(DL-lactide-co-glycolide) microspheres for the delivery of DNA to human-derived macrophages and dendritic cells. *Journal of Controlled Release* 2001, **76,** 149-168.

Wang, J., B. M. Wang & S. P. Schwendeman: Characterization of the initial burst release of a model peptide from poly(D,L-lactide-co-glycolide) microspheres. *J Control Release* 2002, **82,** 289-307.

Whittlesey, K. J. & L. D. Shea: Delivery systems for small molecule drugs, proteins, and DNA: the neuroscience/biomaterial interface. *Experimental Neurology* 2004, **190,** 1-16.

Witschi, C. & E. Doelker: Influence of the microencapsulation method and peptide loading on poly(lactic acid) and poly(lactic-co-glycolic acid) degradation during in vitro testing. *Journal of Controlled Release* 1998, **51,** 327-341.

Yamakawa, I., K. Ashizawa, T. Tsuda, S. Watanabe, M. Hayashi & S. Awazu: Thermal-characteristics of poly (Dl-lactic acid) microspheres containing neurotensin analog. *Chemical & Pharmaceutical Bulletin* 1992, **40,** 2870-2872.

Yan, C., J. H. Resau, J. Hewetson, M. West, W. L. Rill & M. Kende: Characterization and morphological analysis of protein-loaded poly(lactide-co-glycolide) microparticles prepared by water-in-oil-in-water emulsion technique. *Journal of Controlled Release* 1994, **32,** 231-241.

Yang, Y. Y., H. H. Chia & T. S. Chung: Effect of preparation temperature on the characteristics and release profiles of PLGA microspheres containing protein fabricated by double-emulsion solvent extraction/evaporation method. *Journal of Controlled Release* 2000, **69,** 81-96.

Yang, Y. Y., T. S. Chung & N. P. Ng: Morphology, drug distribution, and in vitro release profiles of biodegradable polymeric microspheres containing protein fabricated by double-emulsion solvent extraction/evaporation method. *Biomaterials* 2001, **22,** 231-41.

Yoo, H. S., K. H. Lee, J. E. Oh & T. G. Park: *In vitro* and *in vivo* anti-tumor activities of nanoparticles based on doxorubicin-PLGA conjugates. *Journal of Controlled Release* 2000, **68,** 419-431.

Yoo, H. S., J. E. Oh, K. H. Lee & T. G. Park: Biodegradable nanoparticles containing doxorubicin-PLGA conjugate for sustained release. *Pharmaceutical Research* 1999, **16,** 1114-1118.

Yuksel, N., T. Tincer & T. Baykara: Interaction between nicardipine hydrochloride and polymeric microspheres for a controlled release system. *International Journal of Pharmaceutics* 1996, **140,** 145-154.

Zauner, W., N. A. Farrow & A. M. R. Haines: *In vitro* uptake of polystyrene microspheres: effect of particle size, cell line and cell density. *Journal of Controlled Release* 2001, **71,** 39-51.

Zhang, M. P., Z. C. Yang, L. L. Chow & C. H. Wang: Simulation of drug release from biodegradable polymeric microspheres with bulk and surface erosions. *Journal of Pharmaceutical Sciences* 2003, **92,** 2040-2056.